Air Force Institute of Technology
AFIT Scholar

3-24-2012

Increasing Reliability of a Small 2-Stroke Internal Combustion Engine for Dynamically Changing Attitudes

Steven C. Crosbie

Follow this and additional works at: https://scholar.afit.edu/etd

Part of the Aerospace Engineering Commons

INCREASING RELIABILITY OF A SMALL 2-STROKE INTERNAL COMBUSTION ENGINE FOR DYNAMICALLY CHANGING ALTITUDES

THESIS

Steven C Crosbie, Captain, USAF

AFIT/GAE/ENY/12-M08

DEPARTMENT OF THE AIR FORCE
AIR UNIVERSITY

AIR FORCE INSTITUTE OF TECHNOLOGY

Wright-Patterson Air Force Base, Ohio

THESIS

Presented to the Faculty

Department of Aeronautics and Astronautics

Graduate School of Engineering and Management

Air Force Institute of Technology

Air University

Air Education and Training Command

In Partial Fulfillment of the Requirements for the

Degree of Master of Science in Aeronautical Engineering

Steven C Crosbie

Captain, USAF

March 2012

AFIT/GAE/ENY/12-M08

**INCREASING RELIABILITY OF A SMALL 2-STROKE INTERNAL
COMBUSION ENGINE FOR DYNAMICALLY CHANGING ALTITUDE**

Steven C Crosbie

Captain, USAF

March 2012

Approved:

_____   _____
Dr. Marc Polanka (Chairman)   date

_____   _____
Dr. Paul King (Member)   date

_____   _____
Lt Col Frederick Harmon (Member)   date

AFIT/GAE/ENY/12-M08

Abstract

Remotely Piloted Aircraft (RPA) typically utilize commercial internal combustion engines (ICE) as their power sources. These engines are designed to run at sea level, but these aircraft are often pressed into service at higher altitudes where the performance characteristics deteriorate. A Brison 95cc two-stroke engine's performance characteristics at altitude are investigated using a test facility that can measure these characteristics over a range of pressures and temperatures. With its stock carburetor at sea level static (SLS) conditions, the engine makes 5.5 peak hp and brake specific fuel consumption (BSFC) ranged from 1.2-4.0 lb/(hp-hr). At 10,000 ft conditions, the peak hp drops 40% while off peak power conditions can see a drop of over 90%. As well, the carburetor makes operating at high altitudes unreliable and unpredictable. In order to increase reliability, a throttle body fuel injection (TBI) system was installed on the engine. The fuel injection system matched carburetor peak power at SLS conditions while increasing power by as much as 90% at low RPM and high altitude operating conditions. BSFC is decreased to a consistent 1.0 to 1.2 lb/(hp-hr) across all operating conditions. Lastly both reliability at high altitude and startup reliability are increased with the TBI system while eliminating the need for the tuning by the end user.

Acknowledgements

Lastly, I would like to thank my parents. Thank you for listening to me vent about being covered in work from classes or my schedule being tight for working in the lab. Thank you for understanding why visits for holidays were shortened so I could get back to Ohio to work on this research. Without your continued support, none of this would be possible.

Table of Contents

List of Figures

List of Tables

List of Symbols

Symbol

ρ_{power}	Power density (hp/lb)
m_a	Mass of air entering cylinder (lb)
m_{engine}	Engine mass (lb)
m_{tr}	Total mass of charge (lb)
m_{tas}	Trapped air mass (lb)
m_{ex}	Mass of escaped intake charge (lb)
m_{ar}	Mass of burned gases retained in cylinder (lb)
SE	Scavenging efficiency (%)
CR_g	Geometric compression ratio
CR_t	Trapped compression ratio
V_d	Displacement volume (in^3)
V_c	Clearance volume (in^3)
V_{ts}	Volume of the cylinder after exhaust port closure (in^3)
D	Diameter of the cylinder, drag for SLUFF calculations (in or lb$_f$)
L_{ts}	Distance the piston moves from BDC to after exhaust port closure (in)
$\dot{m}_f$	Fuel flow rate (cc/min)
P_b	Brake engine power (hp)
T	Engine torque, propeller thrust for SLUF calculations (lb$_f$)
F	Force
b	Distance for torque calculation (ft)
N	Revolutions Per Minute
N_R	Crank revolutions per power stroke
P_a	Manifold pressure (psi)
R_a	Gas constant for air (ft lb$_f$ slug^{-1} °R^{-1})
T_a	Ambient temperature (°F)
N_b	Brake power for Kuroda approximation
P_s	Ambient pressure for Kuroda approximation
P	Power (hp)
φ	Equivalence ratio
F/A	Fuel to air ratio actual
$(F/A)_{St}$	Fuel to air ratio for stoichiometic conditions
A/F	Air to fuel ratio
$(A/F)_{St}$	Air to fuel ratio stoichiometric conditions (14.7 for AVGAS)
λ	Lambda

List of Abbreviations

Abbreviation

AFIT	Air Force Institute of Technology
AFR	Air-to-Fuel ratio
AFRL	Air Force Research Laboratory
AGL	Above ground level
ASTM	American Society for Testing and Materials
ATDC	After top dead center
BDC	Bottom dead center
BMEP	Brake mean effective pressure
BSFC	Brake specific fuel consumption
BTDC	Before top dead center
CDI	Capacitive discharge ignition
COTS	Commercial off the shelf
COV	Coefficient of variation
ECU	Engine computer
FV	Fuel valve
HP	Horsepower
IC	Internal combustion
ICE	Internal combustion engine
KIAS	Knots indicated air speed
MAF	Mass air flow sensor
MSL	Mean sea level
PC	Personal computer
PID	Proportional, Integral, Derivative gain
PT	Pressure transducer
OPR	Overall pressure ratio
QUB	Queen's University of Belfast
RPA	Remotely piloted aircraft
ROC	Rate of climb
SI	Spark ignition
SLS	Sea level static
SLUF	Straight level un-accelerated flight
TBI	Throttle body injection
TDC	Top dead center
TPS	Throttle position sensor
TT	Thermocouple
U.S.	United States
UAS	Unmanned aerial system
UAV	Unmanned aerial vehicle
VAC	Voltage alternating current
VDC	Voltage direct current
VFD	Variable frequency drive
WOT	Wide open throttle

INCREASING RELIABILITY OF A SMALL 2-STROKE INTERNAL COMBUSTION ENGINE FOR DYNAMICALLY CHANGING ALTITUDES

I. Introduction

Unmanned aircraft systems (UAS) and the effects they have on the battle space continue to emerge as one of the most demanded capabilities requested by component commanders. The United States Air Force (USAF) UAS Flight Plant outlines a family of unmanned aircraft including small man portable models that include micro and nano-sided aircraft, medium sized aircraft, large "tanker sized" aircraft, and some aircraft with unique capabilities(1). All of these aircraft require special and unique power systems, but today's systems are forced to make do with commercial off the shelf (COTS) engines. Some of these engines include the multi-cylinder spark ignition Rotax 914 which powers the MQ-1 Predator, mid-sized rotary Wankle type UAV Engines Ltd model 801, to small single cylinder engines like the Fuji B34 and Brison 5.8.

The size and type of engine selected for a particular platform is based upon the mission requirements, range, endurance, performance, geometry constraints, and payload tradeoffs. Figure 1 gives a description of the current UAS systems as well as future systems grouped based upon mission and performance. The general focus of this research is on those systems which fall under Groups 1 and 2 as well as smaller systems from Group 3.

UAS Category	Maximum Gross Takeoff Weight (lbs)	Normal Operating Altitude (ft)	Speed (KIAS)	Current / Future Representative UAS
Group 1	0-20	<1,200 AGL	100 kts	Wasp III, FCS Class I, TACMAV, RQ-14A/B, BUSTER, BATCAM, RQ-11B/C, FPASS, RQ-16A, Pointer, Aqua Terra, Puma
Group 2	21-55	<3,500 AGL	<250	Vehicle Craft Unmanned Aircraft System, ScanEagle, Silver Fox, Aerosonde
Group 3	<1320	<18,000 MSL		RQ-7B, RQ-15, STUAS, XPV-1, XPV-2
Group 4	>1320		Any Airspeed	MQ-5B, MQ-8B, MQ-1A/B/C, A-160
Group 5		>18,000 MSL		MQ-9A, RQ-4, RQ-4N, Global Observer, N-UCAS

Figure 1: Current U.S. Unmanned Aerial Systems Programs (1)

Group 1 and 2 systems have unique power requirements due to their lightweight characteristics and nature of their missions. Due to the nature of small acquisition budgets and quick timelines, commercial off the shelf (COTS) engines are used for the lower power UAVs. Often these engines are sourced from ground power equipment or hobby radio controlled aircraft industries as these are some of the only sources of engines with the appropriate power density required.

Figure 2 shows that higher power densities can be reached by using small high overall pressure ratio (OPR) gas turbine engines, but these engines have a significant disadvantage when it comes to brake specific fuel consumption when compared to internal combustion (IC) engines. While advanced IC engines are making strides yearly in efficiency, they are still unable to match the power density of small turbine engines.

Additionally, the Group 1 and 2 systems utilize the lower power density of two-stroke IC engines which can also suffer from high BSFC and reliability problems.
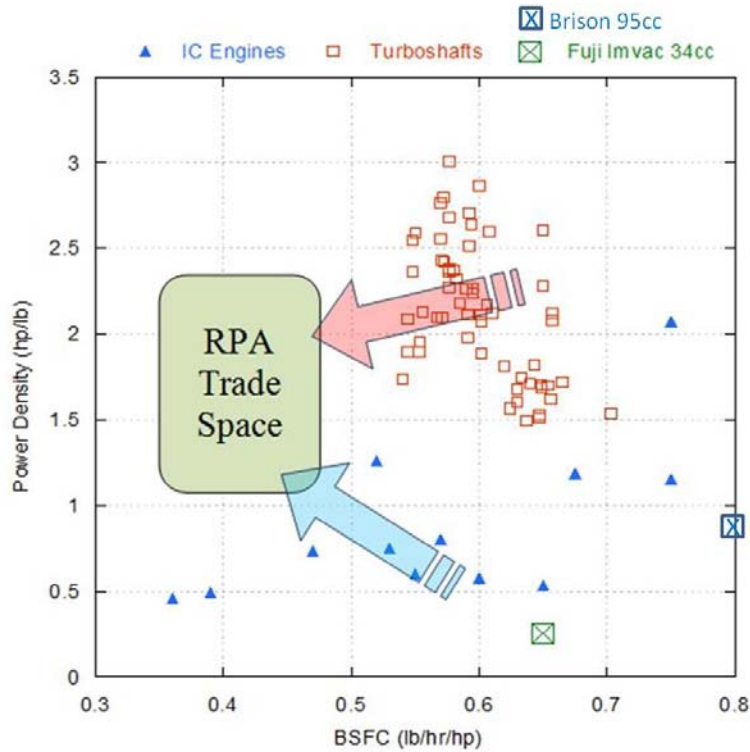
Figure 2: Small internal combustion engine (<750 kW) and turboshaft engine power density vs. brake specific fuel consumption (BSFC) (Adapted from 2)

The COTS engines used in Group 1 and 2 UAS airframes do not normally include the modern day technologies that make a typical IC engine fuel efficient. Technologies such as fuel injection, engine computers, direct injection, capacitive discharge ignition, and forced induction are not used on these engines because any of these subsystems can more than double the cost of these engines or the systems are not perceived reliable enough for aircraft use. Doubling the cost of an RC engine has substantial negative ramifications to a small engine manufacturer while the additional cost to each remotely piloted aircraft (RPA) for DoD use might not be as prohibitive.

The Department of Defense is not in the business of developing a new engine for every UAS platform developed. The number of systems developed that require unique engine specifications would make designing engines extremely expensive and would push acquisition timelines to unrealistic lengths. Scaling modern fuel delivery, injection, and ignition systems down to the sizes needed for these small UAS while maintaining high effectiveness and durability is a difficult feat that not many subsystem manufacturers have solved.

Additionally, the small scale COTS engines see very little research and development establishing performance metrics or improving performance. Notionally, most small COTS engines in use today were originally developed to operate within several hundred vertical feet of where their carburetors were tuned. These engines are intended for use by the hobby RC enthusiast and the expectation is there for hobbyists to understand carburetor tuning and how to accomplish this task.

The requirements demanded of a UAS engine differs in purpose from the COTS engines used today. According to the head of Propulsion Systems Department for Israel Aircraft Industries (4), most of the flight time for a UAS system is performed while flying at loiter speeds, which run at low throttle settings. On the other hand significant flight time is accumulated for training missions requiring numerous takeoffs using maximum power settings for prolonged periods of time. The low and high power requirements mean engines need to be designed, optimized, and tested for both of these conditions. Smaller UAS aircraft manufactures have an even more difficult time selecting engines that have good cruise and takeoff performance characteristics while being reliable, easily maintainable, fuel efficient, and fitting the small size requirements. The

demands placed on these engines by the military have lead to the desire to determine engine performance of their UAS engines over a range of pressure and temperature conditions.

I.1 Objectives

There are several key objectives for the current research project. The main goal of this research was to take the existing altitude chamber test facility and characterize the performance of a representative remotely powered aircraft engine as a function of altitude using AVGAS as the primary fuel. Typical engine operating speeds and load conditions were run at several different operating altitudes in the stock engine configuration to create baseline performance statistics of the engine. These performance metrics are key in determining the appropriate propellers to match with this engine.

After creating the baseline, the second goal was to test the sensitivity of engine performance based upon carburetor settings. The carburetor is tuned manually at the factory and then sent out to the field for operators to use. Adjustments to the carburetor are often inaccurate and crude. These adjustments can cause large variability in the engine performance. Some RPA manufacturers allow for carburetor changes in field while some do not, so providing test data for carburetor maladjustment is essential so users understand how important proper air-to-fuel (AFR) mixture control is to the mission.

Both the RPA community and the recreational hobby aircraft community share similar concerns to engine reliability concerning the supplied carburetors. Therefore, the third objective is to remove the carburetor and install a fuel injection system on the

engine to try and mitigate the need for user adjustments for changing altitudes, engine temperature, or ambient temperature. Increasing startup reliability is a tertiary goal of this step, but not an unimportant one. Startup concerns plague the hobby aircraft industry and this research sets out to solve those problems for the user.

After the conversion to a throttle body injection fuel injection system, performance data was collected at various throttle settings and altitudes in order to provide an engine performance map. This map can be used to select appropriate propeller designs for the performance characteristics of the engine. After collecting throttle settings data, the repeatability of the performance data was analyzed in order to give a better picture of how reliability was increased with the fuel injection system.

The last goal of this research is to determine if published AFR numbers for best brake specific fuel consumption (BSFC) and maximum power are applicable for the Brison 5.8. Understanding what AFR is best for fuel consumption or maximum power are important to the United States military and help in determining how to tune the engine for its specific mission requirements.

Once all of the performance metrics are collected, aircraft manufacturers can then take these performance maps and use them to match the engine with the appropriate propeller. Just like engines produce power at different RPM based on design, propellers too have produce different amounts of torque at different RPMs. Matching the appropriate propeller for the anticipated engine speed based on power needed and BSFC desired is an important element of aircraft power plant design.

I.2   Methodology

The first step towards achieving these research goals was to refine the current test

facility built by Schmick (5). There were several problems with the test facility that

needed to be addressed before reliable data could be derived from the facility. Each

subsystem needed to be isolated and tested for reliability as well as calibrated before

taking test data.

After the test stand was checked out and calibrated, a representative test engine was

placed in the test chamber. The stock engine comes with a carburetor and this carburetor

needed tuning before any test data could be collected. After tuning the carburetor, sea

level performance data was recorded between 3,000 and 7,500 RPM at full throttle. The

altitude chamber was set to 5,000 feet and 10,000 feet operating altitudes and the same

full throttle test data was completed.

After completing this data, investigation of the impact of carburetor settings was

completed by setting the carburetor at a known rich condition and re-running the

performance tests to compare against proper engine tuning. Additionally, the engine was

tuned for both the 5,000 foot and 10,000 foot conditions to try and quantify the best

engine performance possible at those altitudes.

After quantifying performance with the stock carburetor a generic throttle body fuel

injection (TBI) system was purchased for modification and installation on the test engine.

After installing the TBI system, the engine computer (ECU) needed an accurate fuel map

loaded.   The injector pulse width was derived from a throttle position versus engine

RPM table and the load value in this table is derived from engine testing. After building

the table and installing a wide-band oxygen (O_2) sensor, the full throttle performance data

was collected with the fuel injection system. Additionally, 75%, 50%, and 25% throttle setting conditions were tested in order to create engine maps with the TBI system.

After creating engine maps for the Brison, a throttle sensitivity analysis was completed to determine how throttle input changes affect engine performance. The engine was set to 4,000 RPM and the throttle was changed in 5% intervals to determine how engine performance drops as the throttle plate is closed. After the throttle study, a repeatability analysis was completed to determine if the engine performance changes between or during test events.

The final goal was to determine what AFR provides best BSFC and maximum power for the Brison 5.8. Published data gives ranges of where these performance metrics can be maximized or minimized, but no actual data exists for the Brison. Sea level static operating conditions will be used as well as 100% throttle settings. The engine fuel tables were tuned between fuel ratios of 10 to 17 and data was collected for a set RPM. Tuning the entire table over again was not needed due to only testing the 100% throttle condition at one RPM setting. Testing at only one RPM and throttle position allowed for quicker completion of the test matrix. The oxygen sensor was again used to calibrate the tables and closed loop operation was disabled in the ECU. Once all of the collection was completed, the data can be compared to what was collected for an AFR of 13 to see if the published (Figure 14) data holds true for the Brison 5.8.

After collecting all of the Brison engine performance at three throttle positions, the engine was matched with previously generated propeller performance data to determine which propellers would be best suited for the aircraft when maximum torque and minimum fuel consumption requirements are needed. Matching the appropriate

propeller to an RPA is an important design step that if completely incorrectly can cause substantial performance problems or increases in thrust specific fuel consumption. Taking the Brison engine data as an example, an engineer can locate peak power to match a propeller for best rate of climb. Additionally the performance data locates the lowest BSFC operating point which can be matched with the appropriate propeller to give best cruise endurance. If the RPA community does not have the engine performance data, they are forced to rely on the sparsely published data that already exists or their engineering estimations which may not scale appropriately to specific engines.

II. Theory and Previous Research

II.1   Internal Combustions Engines

The internal combustion (IC) engine has been around for over 100 years. The IC is currently the main power plant for a large variety of products that require the freedom of mobility that liquid fuel provides. The reason why the IC engine is used across such a wide variety of products has to do with the power density of liquid hydrocarbon fuels. Currently, liquid hydrocarbon fuels are the leading fuel source that is cost effective, easiest to distribute, and safe to use. Generally speaking, an IC engine uses a reciprocating piston that fits tightly inside a cylinder in which it oscillates. The piston is attached to a connecting rod which is mounted to a crankshaft that translates the reciprocating motion into angular rotation. The crankshaft is either then connected to a flywheel or it is connected to a power transmitting device depending on the engine's application.

The downward force on the piston is generated from the pressure caused by the combustion of a hydrocarbon based fuel with the appropriate amount of air inside the combustion chamber. The method of mixing the fuel with air, how the fuel mixture is ignited, and how the intake flow is controlled into the cylinder are the main factors that differentiate the types of IC engines.

II.2   Two-Stroke Spark Ignition Engines

The first engine type is the two-stroke engine, developed by Dugald Clerk in 1878 (6). The two-stroke engine is illustrated by Blair in Figure 3 (7) with the phases of filling and emptying of the cylinder illustrated in (a) through (d). In Figure 3 a, above the

piston, the trapped air and fuel charge is ignited by the spark plug which produces a rapid

rise in pressure and temperature. The increase of pressure drives the piston down (shown

in Figure 3b) and is considered the power stroke. As the piston moves down, it uncovers

the exhaust port, which allows the burnt gases to leave the cylinder and shortly thereafter,

the piston uncovers the inlet port, which lets a fuel and air mixture into the cylinder.

Figure 3c shows the process as the fresh charge pushes out the previous burnt gases. As

the cylinder begins to rise again, the intake port is closed and then the exhaust port is

closed. This short period of time can allow some of the fresh intake charge to exit the

exhaust port and this phenomenon is called short circuiting. Finally, Figure 3d shows the

exhaust port closing and this is called the trapping point as gases are no longer able to

leave the cylinder. From the trapping point, the piston begins compressing the intake

charge and becomes ready for the next spark. The entire process takes two strokes of the

piston (down and up) and consists of one whole revolution of the crankshaft. Since two-

stroke engines experience a power stroke twice as often as a four stroke, generally they

do not have intake valves or camshafts, and do not require a separate oiling system, their

power density is far higher than that of four stroke engines. Power density is defined in

Equation (1) as the engine rated power divided by the mass of the engine.

$$\rho_{Power} = \frac{P}{m_{engine}} \qquad\qquad (1)$$
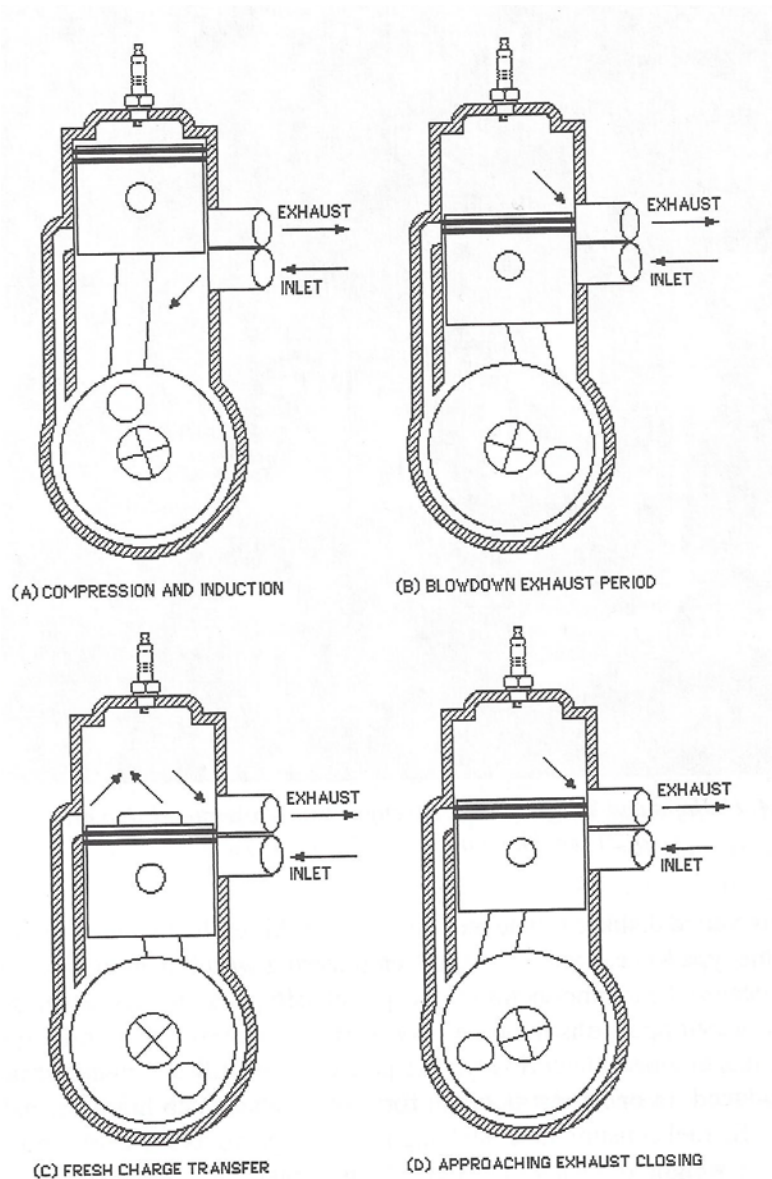
Figure 3: Various stages of operation for a two-stroke engine (From Blair 7)

In a two-stroke engine, the intake process differs from a four stroke engine due to the need to increase the intake charge pressure above the exhaust pressure in order to properly exchange the gases in the cylinder. This process is called scavenging and is one of the most important aspects affecting performance for a two-stroke engine. Figure 4 shows the three main types of contemporary scavenging configurations with the first

method being loop-scavenging. Loop scavenging uses multiple intake ports aimed away from the exhaust port that flow the intake charge across a flat piston and impinging on a wall opposite of the exhaust port. Figure 4b illustrates cross-scavenging and is the original / most popular method of scavenging for two-stroke engines. Cross-scavenging engines have an intake port on one side of the cylinder and the exhaust port located on the opposite side. The intake port or the cylinder top has a deflector which is used to deflect the intake charge in a manner that helps push out exhaust gases. The main difference between loop and cross scavenging is the location of the intake and exhaust ports on the same side for loop scavenging. The final type of scavenging is uniflow scavenging and is shown in Figure 4c. Uniflow scavenging brings fresh intake charge from the bottom of the cylinder and exhausts the burnt gases through the top of the cylinder (7).
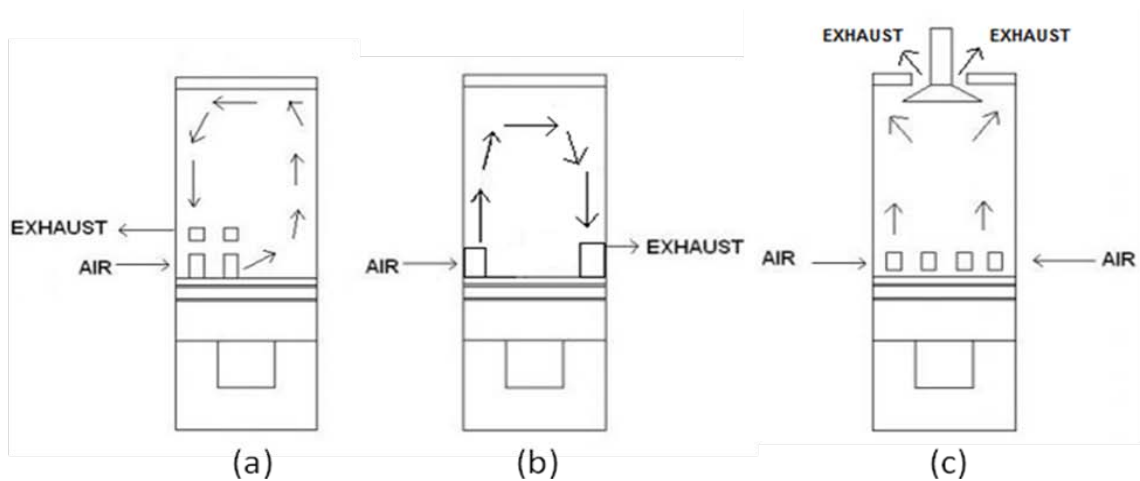
Figure 4: Common types of scavenging; (a) loop-scavenging, (b) cross-scavenging, (c) uniflow scavenging (Derived from Schmick 8)

The Brison 5.8 is a cross scavenging configuration and this is important to understand because according to Blair's modeling, cross scavenging engines do not

promote high scavenging efficiency under large throttle openings. Scavenging efficiency is defined as the mass of delivered air that has been trapped, m_{tas}, by comparison with the total mass of charge, m_{tr}, that is retained at exhaust closure. The unburned gases remaining in the cylinder from the previous cycle are m_{ar}.

$$m_{tr} = m_{tas} + m_{ex} + ma_r \qquad (2)$$

$$SE = m_{tas} / m_{tr.} \qquad (3)$$

The consequences of low scavenging efficiency at high throttle openings means the engine is not particularly fuel efficient since raw intake charge is escaping through the exhaust. Engines like the Brison have a lower power density than loop scavenging or the most efficient uniflow scavenging type engines.

The compression of the intake charge in a two-stroke engine can be accomplished using an external source (supercharger or turbocharger) or it can be accomplished via the crankcase. Crankcase pumping uses the piston and crankcase to compress the intake charge before it enters in the intake port. This type of pumping system is used in most small single cylinder two-stroke engines that are found in RC aircraft, chain saws, and string trimmers as examples. The major drawback of external pumps are their complication, purchase cost, and weight while the crankcase method of pumping normally utilizes the fuel as a lubrication source and therefore requires oil to be mixed into the fuel. Often external pumps have a typical sump oil system and do not require oil mixed into the fuel.

Two-stroke engines have the capability to be very light, have high power density, and be relatively inexpensive to manufacturer, but their primary tradeoffs are their

emissions and fuel consumption. The primary reason to use one in a small RPA is the engine's power density.

II.3   Four-Stroke Engines

Four stroke engines have four movements of the piston for each power stroke verses the two for a two stroke. A four stroke engine has an intake stroke, a compression stroke, expansion stroke which occurs after the spark, and an exhaust stroke. Therefore, there is one power stroke for every two revolutions of the crankshaft.   Separating the intake and exhaust into separate strokes prevents the four stroke engine from short circuiting and thus makes them potentially more fuel efficient and produce less harmful emissions.

Four stroke engines also have different hardware for intake valves. Instead of intake ports on a two stroke, four stroke engines generally have poppet valves that are actuated by a camshaft that runs at half the speed of the crankshaft. The additional valve train hardware, oiling system hardware, and camshaft make for a heavier engine when compared to two strokes. Therefore, a four stroke's power density is lower than a comparably powerful two stroke engine.

II.4   Compression Ignition Engines

Compression ignition engines were initially developed by Rudolph Diesel in 1897 (6) and are often referred to as diesel engines. The engine was developed to inject fuel directly into the cylinder instead of using the air intake tract. Instead of a mixture of fuel entering via the intake valve, diesel engines ingest air through the intake valve. The valve shuts and the piston begins its compression stroke. The diesel fuel is then injected

right before top dead center at peak cylinder pressures. Direct and indirect injection is used for diesels depending on their application.

Compression ignition engines do not utilize the spark plug to provide the ignition energy once the fuel is injected. Instead, the compression stroke compresses the air and fuel to a much higher pressure until the increased pressure causes a temperature rise greater than the ignition temperature of the fuel. Once this temperature is met, the fuel begins burning without the aid of a spark plug.

Compression ignition engines are generally more fuel efficient than their spark ignition counterparts. It is important to note that a compression ignition engine can be both two and four strokes, but modern day diesels are almost all four stroke engines. Compression ignition engines generally have a rather low power density because the engines are required to be much heavier due to the increased cylinder pressure. Additionally, the fuel injection systems are much higher pressure and require heavier fuel pump systems when compared to spark ignition engines.

II.5   Engine Parameters

In order to adequately compare one engine to another, several different parameters are used to identify differences. Before discussing performance parameters, standard geometric parameters need understanding. The most important geometry to understand include the cylinder, crankshaft, and piston geometry. Figure 5 describes each of these geometries and what they mean. The biggest references to understand are bottom dead center (BDC) and top dead center (TDC). BDC refers to the piston position at the bottom of the stroke while TDC refers to the piston position at the top of the stroke and

references to these positions are done based upon crankshaft position away from these two known positions. Often references to these positions are used for injection and ignition timing of the engine with respect to the angular position of the crankshaft at TDC or BDC. The crankshaft position is referred to as crank angle, θ, and the volume between the piston and the cylinder head at TDC is the clearance volume, V_c. Lastly, the total volume of the cylinder is called the displacement volume, V_d, and this is the volume swept by the piston from BDC to TDC.
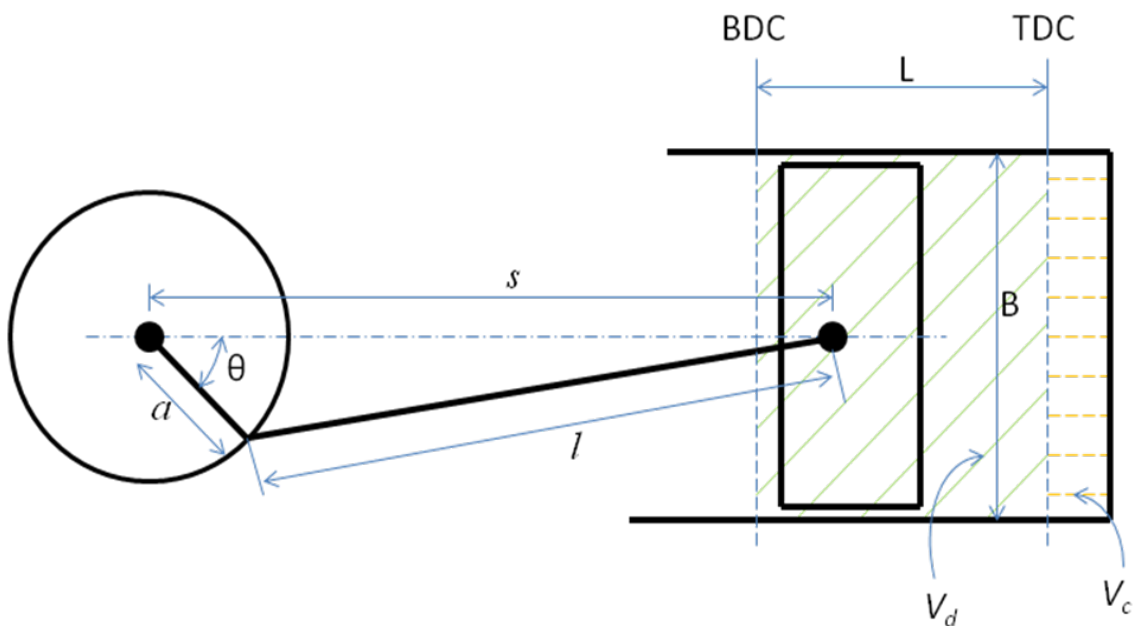
Figure 5: **Geometry of cylinder, piston, connecting rod, and crankshaft where B=bore, L=stroke, *l*=connecting rod length, *a*=crank radius, θ=crank angle (adapted from 5).**

The main reason this geometry is brought up is most engines are described by what type of ignition the engine is (compression or spark), how many strokes per power stroke (two or four stroke), engine displacement (all cylinder displacements added together), and power rating. Additionally, an engine's compression ratio relates the volume of the

combustion chamber at BDC to the volume of the chamber at TDC. Equation 4 shows

the geometric compression ratio relationship (7).

$$CR_g = \frac{V_d + V_c}{V_c}$$ (4)

Two stroke engines use a slightly different compression ratio analysis since

Equation 4 does not adequately describe the true volume of intake charge that the engine

really sees after short circuiting. For example, in Chapter III, the geometry of the Brison

will dictate a compression ratio of 19.4 (5). If the engine actually had this as a

compression ratio, auto ignition would be prominent and the engine would fail due to the

knock. Instead, the actual compression process occurs after the exhaust port is closed (L_{ts}

is the distance the piston moves from BDC to after the exhaust port is closed and V_{ts} is

the volume) and this is less than the geometric compression ratio used to describe four

stroke engines. This is an important distinction to make and when describing two-stroke

engines, trapped compression ratio is the value that should be compared to a four stroke.

Equation 6 gives the formulation for trapped compression ratio.

$$V_{ts} = \frac{\pi}{4} D^2 L_{ts}$$ (5)

$$CR_t = \frac{V_{ts} + V_c}{V_c}$$ (6)

Some of the most basic performance parameters for an engine are fuel

consumption, power, and torque. Power and torque are based upon the engine size and

type. A dynamometer is a contemporary way of measuring power via the dynamometer

holding the engine at a fixed speed measuring brake power, P_b. A load cell located at a

fixed distance on the dynamometer and is used to measure torque while a shaft encoder

on the dynamometer shaft is used to measure engine rotational speed. After power is

calculated by the dynamometer, fuel consumption can be calculated if the fuel flow rate,

$\dot{m}_f$, is known. Brake specific fuel consumption, BSFC, is the measure of fuel used per

power produced per unit time relates how well an engine can convert chemical energy

stored in the fuel to usable shaft work.

$$BSFC = \frac{\dot{m}_f}{P_b} \qquad (7)$$

Torque, T, is defined as a force, F, times a distance, b, given by Equation 8.

Torque is a measure of an engine's ability to do work while power, Equation 9, is the rate

at which an engine performs work. Power is calculated by taking the torque an engine

makes and multiplying it by the angular speed of the engine. The angular speed of the

engine is the rotational rate in revolutions per unit time, N, times the number of radians

per revolution, 2π.

$$T = F * b \qquad (8)$$

$$P_b = 2\pi * N * T \qquad (9)$$

Strictly comparing torque and power among engines is not an effective way of

describing how well an engine produces torque and power for its given displacement.

Figure 6 is a p-V diagram that shows the work produced on a piston in an ideal cycle.

The total work done on the piston would be the integral of the enclosed area on the p-V

diagram. This integral is often difficult to accomplish, so instead, the area of the shaded

rectangle is the BMEP and is calculated in Equation 10.
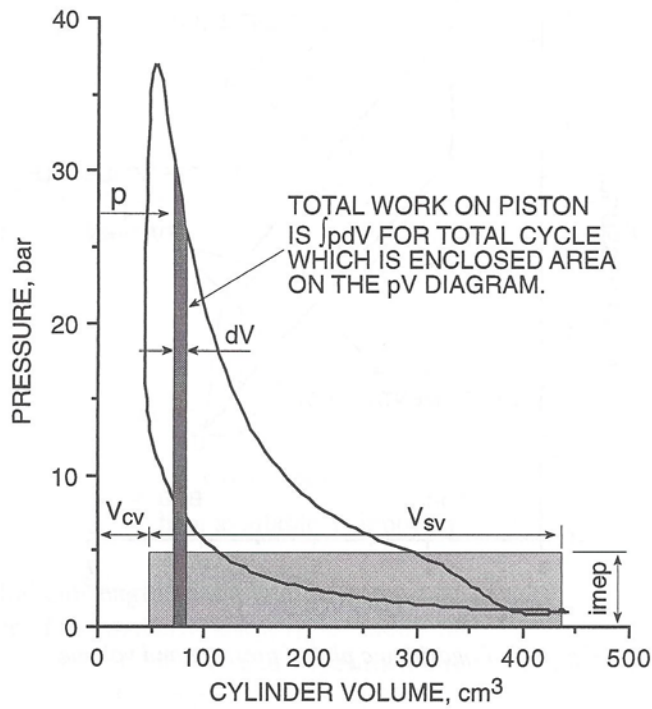
**Figure 6: BMEP equivalence shown in a P-V diagram of a power stroke
(Blair 7)**

BMEP is the effective yardstick for comparing engines, but it is important to note

that BMEP has nothing to do with the actual pressure the piston sees. Instead, BMEP

represents the constant pressure needed on the entire face of the piston all of the way

down the power stroke to generate the given brake power indicated on the dynamometer.

The term n_R is the number of crank revolutions per power stroke per cylinder and is equal

to two for a four stroke engine, and one for a two stroke engine.

$$\text{BMEP} = \frac{P_b * n_R}{V_d * N} = \frac{2\pi * T * n_R}{V_d}$$

(10)

Blair (7) completed a table of performance criteria derived from experimental

results for several classes of two stroke engines shown in Figure 7. Type A could be a

standard chainsaw engine or possibly a small UAS engine. Type B would be a small

motorcycle, while C a motocross bike, D an outboard motor or snowmobile engine. Likewise, type E could be an outboard boat engine, with F would be an electricity generator, and G/H could be truck engines. The main idea of this table is to introduce approximate ranges of BMEP for various size classes of two-stroke engines.

Engine Type	bmep, bar	Piston Speed, m/s	Bore/Stroke Ratio
Single-cylinder spark-ignition engines			
A untuned silenced exhaust	4.5 - 6.0	12 -- 14	1.0 - 1.3
b tuned silenced exhaust	8.0 - 9.0	12 -- 16	1.0 - 1.3
C tuned unsilenced exhaust	10.0 - 11.0	16 -- 22	1.0 - 1.2
Multi-cylinder spark-ignition engines			
D two-cylinder exhaust tuned	6.0 - 7.0	12 -- 14	1.0 - 1.2
E 3+cylinders exhaust tuned	7.0 - 9.0	12 -- 20	1.0 - 1.3
Compression-ignition engines			
F naturally aspirated engine	3.5 - 4.5	10 -- 13	0.85 - 1.0
G supercharged engine	6.5 - 10.5	10 -- 13	0.85 - 1.0
H turbocharged marine unit	8.0 - 14.0	10 -- 13	0.5 - 0.9

Figure 7: Some performance characteristics for different sized two-stroke engines (Taken from Blair 7)

II.6   Fuel Delivery

Modern day engines can use a myriad of fuel delivery systems depending on the price point for the engine, purpose of the engine, and emissions laws that govern the engine size class. The small RPA engines that power Group 1 and 2 aircraft tend to have fuel delivered via a small carburetor and often these are the same carburetors that are installed on small yard equipment. Larger RPA engines, like the Rotax 914, are sourced from the civilian aviation industry and some of these engines have already moved to fuel injection systems.

II.6.1 Carburetor Theory

The Brison 95cc engine is fed fuel through a carburetor. Carburetors work by using intake air that passes through a converging-diverging nozzle in the flowpath, often called a venturi. As the air passes through the venturi, the air accelerates which causes the pressure to drop. In the venturi, there is a fuel jet that is supplied with fuel at a higher than ambient pressure. The fuel is entrained into the airflow, breaks up into droplets, and starts to evaporate into the intake air stream. A butterfly valve, otherwise known as a throttle plate, is located downstream of the venturi and is used to regulate the amount of airflow into the engine. The term wide open throttle, WOT, or 100% throttle means that this valve is opened all of the way allowing maximum airflow through the engine. When the throttle plate is opened to less than 100%, increased vacuum is produced from the flow restriction and this is where vacuum is sourced for powering the Brison's diaphragm fuel pump. Additionally, when the throttle plate is closed, the fresh air flow is slowed down and less fuel is sucked into the intake stream. Figure 8 gives a pictorial example of how a basic carburetor works and is just an educational model as it does not represent any of the carburetors in this research.
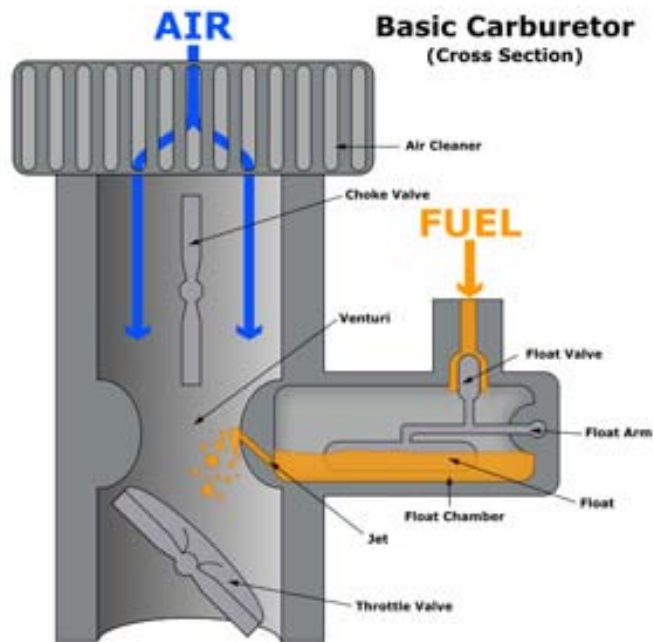
Figure 8: Basic representation of a simple carburetor (Supplied by 9)

The carburetor is not a one size fits all solution for any engine or operating

condition. The orifice or "jet" in Figure 8 is normally replaceable or adjustable in order

to meet certain air/fuel ratios and is often adjusted when the carburetor is used in vastly

different altitudes. Some carburetors employ transition jets that allow better fuel flow at

off design operating conditions, but even some of the most complex carburetors on the

market will often run different air/fuel ratios (AFR) at different engine speeds and

operating conditions. AFR is strictly the ratio of the mass of air in the cylinder after the

exhaust port closes over the mass of fuel in the cylinder. Inconsistent AFR is

unavoidable due to the tuning limitations of a carburetor (6). The inability to closely

regulate AFR across all engine loads causes varying power output, unreliable AFRs, and

increased fuel consumption. A poorly tuned carburetor can also negatively impact engine

performance. Modern day emissions regulations caused an evolution of the carburetor into the fuel injection systems of today.

II.6.2 Fuel Injection Theory

Electronic fuel injection made its way into the automotive industry in the late 1970s through the 1980s in order for manufacturers to meet strict emissions laws (6). The modern day electronic fuel injector is depicted in Figure 9. The main components are the housing, solenoid, and plunger. The injector works by normally being supplied 12VDC constantly while the engine computer switches ground "on" for the given pulse width of fuel that the engine computer commands. When the solenoid is energized by the switched ground, the pintle plunger moves up into the injector housing and opens the valve for fuel to mist out of the injector.
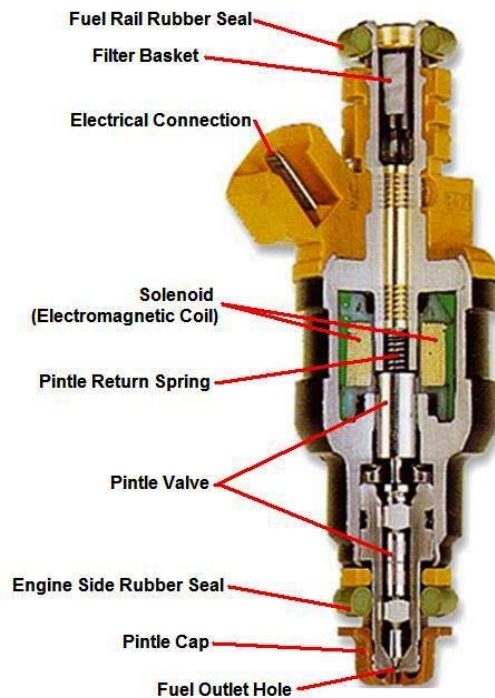
Figure 9: Typical fuel injector and its main components (Supplied by 10)

Electronic fuel injection is more than just a piece of hardware that replaces the carburetor, but instead it is a system that is integrated onto an engine made of many parts. A typical fuel injection system includes an electronic engine computer, the fuel injector, mounting hardware for the injector, pressurized fuel lines, mass air flow sensor or manifold pressure sensors, throttle position sensor, and sometimes an oxygen sensor (11).

There are three main types of fuel injection that can be used and all of them differ based upon where the fuel injector is located. Throttled body injection (TBI) is the most basic style of fuel injection and places a fuel injector aft of the throttle plate. Essentially this replaces the orifice of a carburetor with a fuel injector. TBI's largest advantages are its cost and ability to be easily retrofitted to a carbureted engine. One of the largest disadvantages is the fuel injected via a TBI can wet the walls of the intake tract and the wetted walls can act as a damper that slows reactions of the engine. This means that a sudden large throttle opening can cause the TBI system to over-fuel as ECU compensates for intake wetting by adding extra fuel. This means that the transitions of a TBI system can have slight erratic AFRs. Multiport fuel injection places an injector in the intake manifold just upstream of each intake valve and allows for more precise fuel metering to each cylinder. This system addresses the problem of fuel not equally distributing itself within the intake manifold of a TBI system. The most advanced style of fuel injection is direct fuel injection which uses a high pressure fuel injector placed directly in the cylinder head providing fuel directly into the cylinder (12). This type of fuel injection system does not require mixing of the fuel in the intake tract. Direct injection is known to ease engine starting since significantly less wall wetting occurs and better fuel

atomization is realized. Additionally, direct injection has distinct benefits combating pre-ignition and can allow for higher compression ratios yielding better BSFC.

Once the system is installed, there are two methods of determining the amount of fuel the injector needs to inject for a given AFR. The first method is the speed density method which uses a manifold pressure sensor and ambient air temperature sensor to determine the mass of air entering the cylinder using the ideal gas law and assuming the manifold pressure for in cylinder pressure (P_a) and ambient temperature (T_a) for air temperature in the cylinder.

$$m_a = \left(V_d * P_a\right) / \left(R_a * T_a\right) \tag{11}$$

Alternative method to the speed density method uses a mass air flow (MAF) sensor to determine air flow directly (6). The MAF is located upstream of the throttle plate and provides a voltage proportional to the flow rate. According to Heywood, there are five main advantages to measuring the air flow directly and these are: (1) automatic compensation for tolerances, combustion chamber deposit buildup; (2) dependence of volumetric efficiency on speed and exhaust backpressure is automatically accounted for; (3) less acceleration enrichment is required because the air-flow signal precedes the filling of the cylinders; (4) improved idling stability; (5) lack of sensitivity of the system if exhaust gas recirculation is used since only fresh air is measured. (6) Although there are advantages, the main disadvantage is mainly cost and complexity. If the intake system doesn't have adequate room to plumb in MAF, then the only choice a user has is the speed density system. In the case of a small UAS, the speed density system would most likely be used.

II.6.3 Previous Fuel Metering Research

Grasas-Alsina et al (13) completed research using a discontinuous fuel injection system on a 350 cc crank case compressed loop scavenged Montesa Crono motorcycle engine. The engine was hooked to an eddy current brake dynamometer and two different injection strategies were used to determine how they changed BMEP and BSFC.

The engine originally comes with a stock carburetor and the engine was characterized using this system. After completing the characterization, a low-pressure gasoline fuel injector was installed in the inlet duct between the carburetor and the engine. The engine was run at multiple throttle openings between 3,000 and 5,000 RPM and while varying injection timing. After this study, they installed injectors in the transfer tubes that supply the compressed intake charge to cylinder and the same test points were ran.

Several conclusions were discovered in Grasas-Alsina et al's research (13). The first conclusions for the inlet injection (TBI) were that injection timing did not affect engine performance. This is mainly due to the scavenging process mixing the air and fuel just like it does when fuel is supplied with the carburetor. The maximum power did not change, but the available power range was increased in the lower engine rpm band. Inlet fuel injection also realized a reduction of BSFC between 10% and 30% were realized at conditions less than peak power. Their largest conclusions were that TBI injection had little effect on engine performance if the air/fuel ratio is maintained. Unfortunately for a carburetor, maintaining AFR is difficult to nearly impossible, but if it were possible, the injection system would not necessarily increase performance.

Grasas-Alsina et al (13) felt the reason inlet injection did not decrease BSFC more was due to the poor trapping efficiency and short circuiting of their two-stroke engine. This is where the justification for transition tub injection came to play as the authors felt that with precise injection timing, a reduction of fuel consumption from injecting fuel after the exhaust port was closed could be realized. A fuel savings between 3% and 6% was observed and further reduction of fuel consumption might be possible with better atomization of fuel as the authors noted that the injection of liquid fuel into the combustion chamber might alter the combustion process in a negative manor.

The observations from Grasas-Alsina et al (13) provide good insight into what systems should be used on a small UAS. The transfer port fuel injection used in their testing is very similar to direct injection in today's automobile engines, but its added complications compared to its reduction of fuel consumption might not be a good enough trade off for low cost systems. The inlet injection system seemed to gain the most benefits with the least amount of modification.

II.7   Pressure Impact

Harari and Sher (14) studied the effect of atmospheric pressure on the performance of a two-stroke engine. Their study attempted to show the correlation between available torque of a two-stroke engine as altitude changes. Their study used a Sachs type SF2-350 Piston-port twin cylinder 700cc opposed-piston crankcase scavenged engine two-stroke engine. Engine power was measured by a Hofmann eddy-current dynamometer and ambient pressure of the intake was throttled to create a representative pressure drop that represents higher altitudes. A vacuum pump was used on the engine

exhaust side of pull a vacuum that represents altitude as well. Data was collected

between 6,000-7,000 RPM and a pressure range of 44-100kPa with the highest altitude

tested of 7 km. Their results show that maximum engine power has an approximate linear

dependence upon ambient pressure. Their results show that available torque decreases as

inlet pressure decreases as inlet pressure decreases, but the published data did not give

predicted trend data.

Shin, Chang, and Koo (15) established a computer code that predicts power and

torque of Harari and Sher's (14) test engine over a range of engine speeds and altitudes.

The code simulated sea level, 3 km, and 5 km to predict brake mean effective pressure,

engine brake horsepower, and BSFC. Figure 10 and Figure 11 show their prediction of

BMEP and BSFC for changing altitudes.   The main conclusion that can be derived from

this data is a linear dependence of BMEP on ambient pressure while BSFC increases with

a non-linear dependence on altitude.
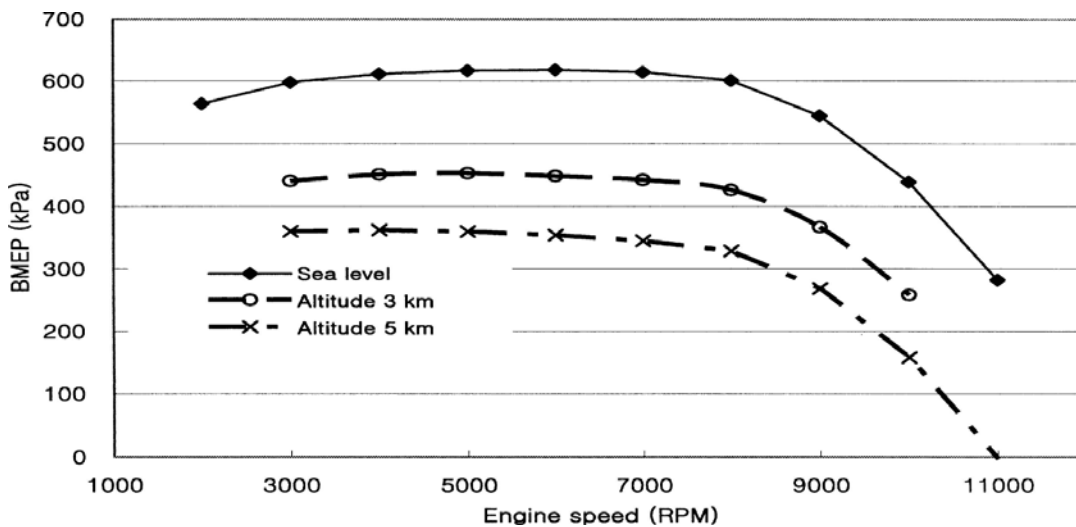
Figure 10: Computer model of pressure effects on BMEP (15)
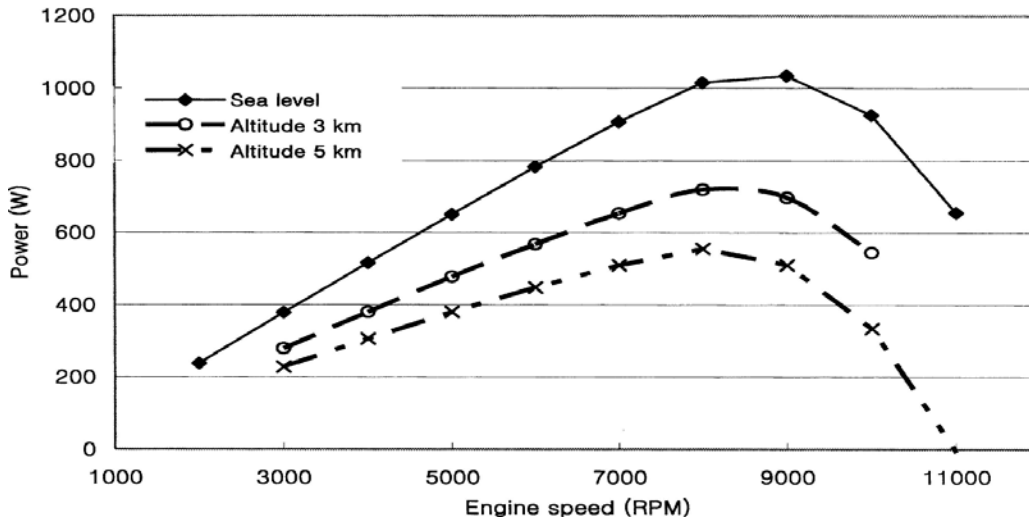
Figure 11: Computer model of pressure effects on output power (15)

Taylor (16) provides a more concise approximation for predicting power of a myriad of engines. Taylor shows predicted brake mean effective pressures of liquid cooled aircraft engines, four stroke diesel engines, two-stroke engines, and multi-cylinder engines. Figure 12 is shows the effects of air density on BMEP for various types of engines.
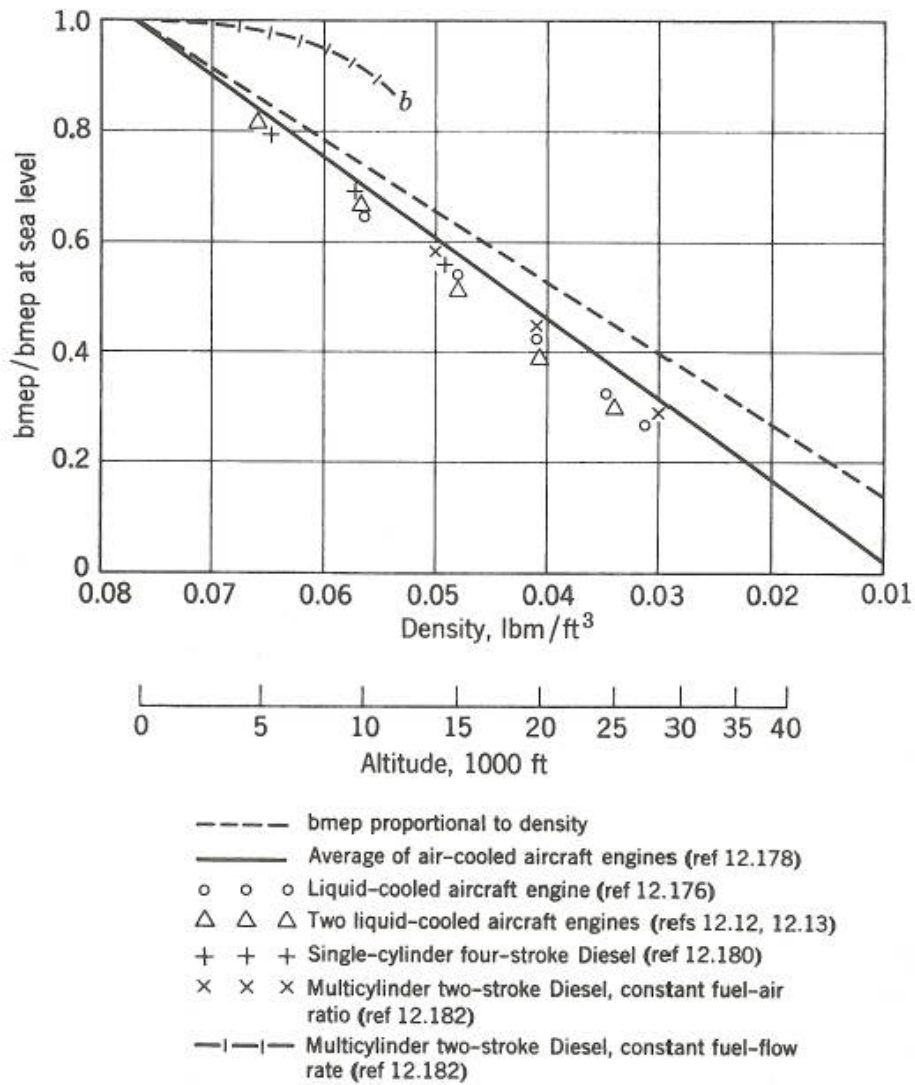
Figure 12: Taylor's experimental data for BMEP change due to altitude (16)

A quick look at the figure shows that at 5,000 feet MSL, the predicted BMEP is

83 percent of the maximum BMEP at sea level. 10,000 feet MSL provides 73% of

available BMEP and these data points will provide useful to compare test data against

since all of Taylor's data is derived from actual test data and not theoretical equations.

Additionally, the data is presented in a non-dimensionalized for that allows any engine's

peak BMEP to be put into the figure and a prediction of BEMP at altitude can be quickly approximated (6).

II.8 Temperature Impact

Watanabe and Kuroda (17) studied the effect of inlet air temperature on the power output on a crankcase compression two-stroke engine. The author's effort focused on determining a correlation of the power output of the engine as a function of the absolute inlet temperature in a range of 4.5 °C to 40 °C. The test engine was a 60 cm^3 Schnuerle scavenging type engine ran over a speed range of 1,000 RPM to 4,000 RPM. Six electric heaters with a total capacity of 900 W were used to heat the inlet air allowing a maximum carburetor inlet air temperature of 50 °C. Air flow rate was measured upstream of a surge tank with a round nozzle. The surge tank was 690 times the size of the engine volume and had a gummy diaphragm attached to reduce pressure and flow pulsations to allow for more accurate air flow measurements. Engine power was measured using a 2 hp electric dynamometer and was corrected back to standard conditions using Equation 12.

$$(N_b)_S = \frac{p_S}{p} N_b \tag{12}$$

where N_b is break power, p is the atmospheric pressure, and the subscript s denotes reference conditions. The authors derived a relationship between the power output and the scavenging pressure to show that as the inlet temperature increases the power will decrease due to a decrease in scavenging pressure with increasing ambient temperature. This result also compares well with compressor theory where an increase inlet temperature for a fixed inlet temperature will result in lower pressure ratios. Figure 13

backs up the author's claim that as inlet temperature increases, the pumping efficiency of the crankcase compression system decreases supplying less inlet pressure to the cylinder during the scavenging process.
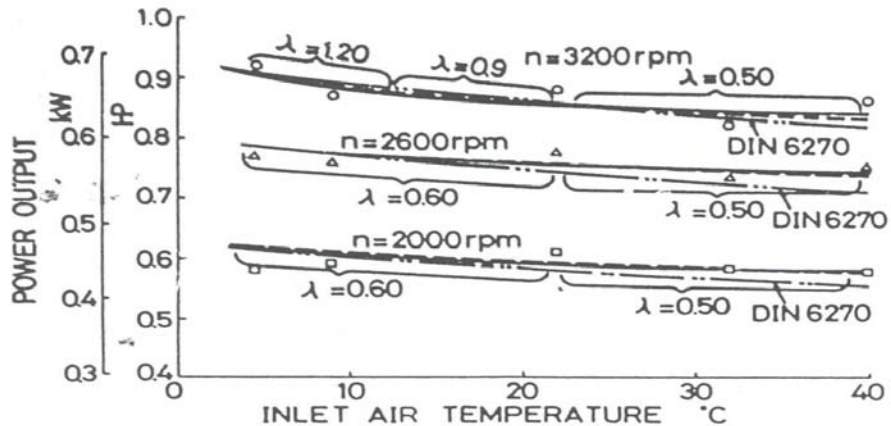
Figure 13: Inlet air temperature's effects on output power of a two-stroke engine (17)

II.9   Combustion Background

The main purpose of this section is to briefly outline the combustion process in an IC engine as well as provide some insight to the relationships used to describe fuel mixtures. Equation 13 outlines the global chemical equation for combustion of an organic fuel with air as the oxidizer. It is important to understand that Equation (13) is in general form and that there are many intermediate reactions occur along the way and often the end result creates hundreds of different products than the academic ones in this equation (18).

$$C_mH_nO_pN_qS_r + X\left(R(O_2)+S(N_2)+T(CO_2)+h(H_2O)\right) \rightleftharpoons$$
$$P_1(CO_2)+P_2(N_2)+P_3(O_2)+P_4(H_2O)+P_5(CO) \qquad (13)$$
$$+P_6(C_xH_y)+P_7(NO_2)+P_8(NO)+P_9(SO_2)$$
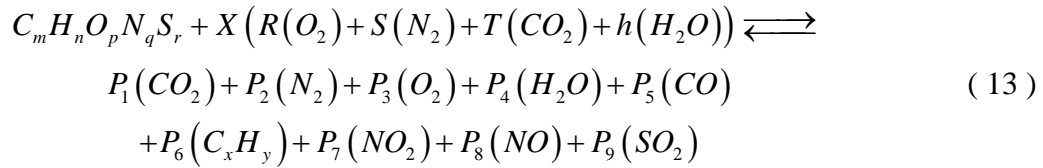
Air / fuel ratio is one of many ways to describe the combustion characteristics and

it can be arranged in different manners depending on the industry doing the research.

Fields of combustion often refer to the mixture of air and fuel as the equivalence ratio.

The equivalence ratio, ϕ, is commonly used to indicate quantitatively if a fuel-oxidizer

mixture is rich, lean or stoichiometirc. Common IC engines run a stoichiometric AFR of

14.7 with values less than 14.7 being rich and greater being lean. To convert AFR to

equivalence ratio, Equation 14 shows how to do this. Values of ϕ greater than unity

indicate fuel rich and less than unity fuel lean. Lambda is another means of determining

mixture characteristics and is shown in Equation 15. Lambda is often used by oxygen

sensor manufactures and these sensors are normally referred to as lambda meters. For

lambda, values less than unity are fuel rich and greater than unity is fuel lean. The

current research will be sticking with AFR as the primary indication of mixture, but it is

important to understand that the same indicators are represented in these other ways (18).

$$\phi = \frac{F/A}{(F/A)_{St}} \qquad (14)$$

$$\lambda = \frac{A/F}{(A/F)_{St}}$$
<div align="right">(15)</div>

II.10 Impact of Air-to-Fuel Ratio and Previous AFR Research on Two-Stroke Engines

Air / fuel ratio is one of the most important engine parameter to monitor if peak power, low BSFC, engine temperatures, and emissions concerns are of high interest to the user. Unfortunately, a stoichiometric AFR of 14.7, for gasoline engines, does not provide the optimal ratio for all of the previous engine characteristics. Therefore, tradeoffs are required on some of the performance parameters in order to meet the needs of more important characteristics that are determined by either the user or in some cases external factors.

AFR studies are completed for all types of engines, but detailed research on these small low budget COTS two-stroke engines is sparse. Blair (7) introduces research of three different size classes of two-stroke engines. When tuning an engine, there are two misfire limits that are quickly established based upon listening to the engine. Blair suggests the rich misfire limit for a two stroke starts at anything lower than 9 while the lean misfire limit is around 19. These are suggested boundaries that when applied to a small Homelite® 42cc two-stroke manifested themselves at 11.5 for the rich limit and 16 for the lean limit.

Additionally, the AFR of the engine impacts the amount of power the engine produces, the amount of fuel it burns, and the hydrocarbon (HC) emissions of the engine. Blair outlines work completed on modeling the chainsaw engine, but has actual test data on a Queen's University of Belfast (QUB) custom designed research engine. The engine

<div align="center">49</div>

is a 400 cross scavenged crankcase compressed engine that was designed for research

purposes.   Figure 14 displays performance curves for BSFC and BMEP for 100 percent

throttle and 3,000 RPM. The individual values of BSFC and BMEP are good for

comparison, but the real value of this figure shows where peak BMEP was observed as

well as lowest BSFC. In the test engine's case, peak BMEP is at around 12.2 AFR while

lowest BFSC is 15.1 (7). The figure clearly shows that an engine cannot have both

maximum BMEP and lowest BSFC with a single AFR. Additionally, AFR plays a huge

roll in HC emissions, but is outside the scope of this research. Therefore, engine

manufacturers are forced to compromise and design to the mission of the engine.
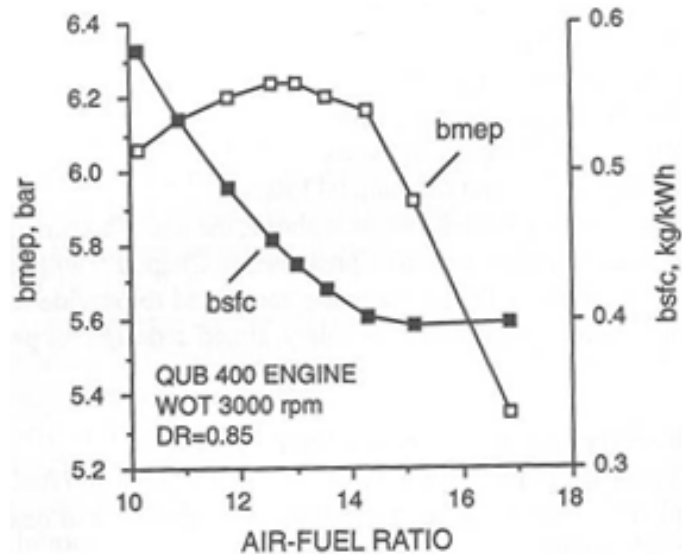
Figure 14: Locating optimal BSFC and BMEP based on AFR (7)

III. Test Setup and Apparatus

The primary objectives of this research are to characterize the Brison 5.8 with the carburetor, change the fuel metering system to fuel injection, and analyze the engine with the fuel injection system in order to improve the reliability of the engine. In order to do any of these tasks, several research tools were built. The first tasks to complete involved receiving the test facility from Schmick and determining the causes of several shortcomings. Once all of the test facility's shortcomings were addressed, the carbureted Brison was tested. After determining the stock engine performance metrics, a fuel injection system was selected and installed onto the Brison. Finally, performance metrics were tested on in the altitude chamber using the fuel injection system.

III.1 Existing Test Facility

The test facility utilized in this investigation was developed by Schmick (5). The primary goal of the research was to determine how a small IC engine performance varies as a function of temperature and pressure. The original test facility was designed to recreate altitude conditions of roughly 15,000 feet MSL in order to test the performance changes of the engine. Prior to the test stand's development, no test facility existed that can test both pressure and temperature affects on a small scale two-stroke RPA engine. The current reseach goals for this test facility were to complete the build up of the facility in order to characterize the power, torque, and BSFC of the engine at altitudes between sea level and 15,000 feet. After characterizing the engine, the next goal was to convert the carburetor on the engine to a fuel injection system in order to chase an increase of

reliability. After conversion, the engine would be characterized again to check for performance improvements.

This facility was received configured to test a Brison 5.8 in^3 single cylinder two-stroke spark ignition crankcase scavenged engine. This engine from the factory utilized a Walbro SDC-80 pump style carburetor with high and low speed needle valves.

Table **1** gives the engine parameters.

Table 1: Brison engine measurements (19)

Property	Value	Property	Value	Property	Value
Displacement*	5.7 in^3	Connecting Rod Length+	2.8 in	Intake Port Open/Close Angle	59.7° B/ATDC
Swept Volume Displacement+	5.89 in^3	Type	2-stroke, crankcase scavenged	Exhaust Port Open/Close Angle	81.3° B/ATDC
Bore+	2.165 in	Geometric Compression Ratio++	19.4:1	Crank Radius+	0.8 in
Stroke++	1.6 in	Intake Port Area+	0.31 in^2 / port	Exhaust Port Area+	0.626 cm^2
Intake Port Arrangement	2 ports 180° offset				

*Manufacturer advertised value   +Measured Value   ++Calculated Value

Table 2 shows the test stand capabilities established to investigate the change of performance with altitude of the Brison engine. The test stand was desiged to be capable of emulating flight conditions from takeoff conditions up to 15,000 feet MSL. The pressure was controlled with a Vorteck 5-V k-trim automotive supercharger and a series of control valves that were used to restrict the flow rate of the chamber's cooling air. Throttling of the cooling air creates the atmospheric pressure inside the chamber. The supercharger serves as a compressor and was driven by a 20 hp Emerson Motor

Corporation electric motor model AF18. The speed of the motor was controlled through

a Delta VFD-F variable frequency drive.

Table 2: Basic Test Stand Facts as Designed

Test Engine	Brison 5.8 95cc 2-Stroke
Altitude Chamber Pressure Range	Ambient Pressure to 8.2 psig
Altitude Chamber Temperature Range	Ambient to 13°F
Dynomometer	Magtrol 2WB65 eddy current (Up to 10HP)
Fuel Tested	Avgas 100 Octane Low Lead mixed 100:1 with Amsoil Synthetic 2 Stroke Oil
Fuel Flow Meter	Max Machinery 213 rotary piston with model 294 transmmitter (0.00089 cc/pulse)

Figure 15 is a flow diagram of the major components of the test facility as

received from Schmick (5). The fuel system is shown in yellow, the engine inlet path in

blue, the engine cooling path in green, the coolant system in red. Also shown in Figure

15 is the compressor and oiling system, the dynamometer and water coolant system, and

the engine controls. The fuel supply system consisted of a fuel flow meter, a fuel filter, a

fuel tank, and a set of valves. The fuel valves directed and isolated fuel in the system.

Fuel flow rate was measured by a Max Machinery model 213 rotary piston flow meter

with a model 294 transmitter. Additionally, Figure 16 is an actual photo of the test

facility identifying key components of the test stand. The picture gives a better idea of

what the components look like when they are referred in later sections. Further details of

the facility and capabilities as supplied are outlined in Schmick et. al (19). Detailed

procedures for operating the test facility are located in Chapter III, Section 3.
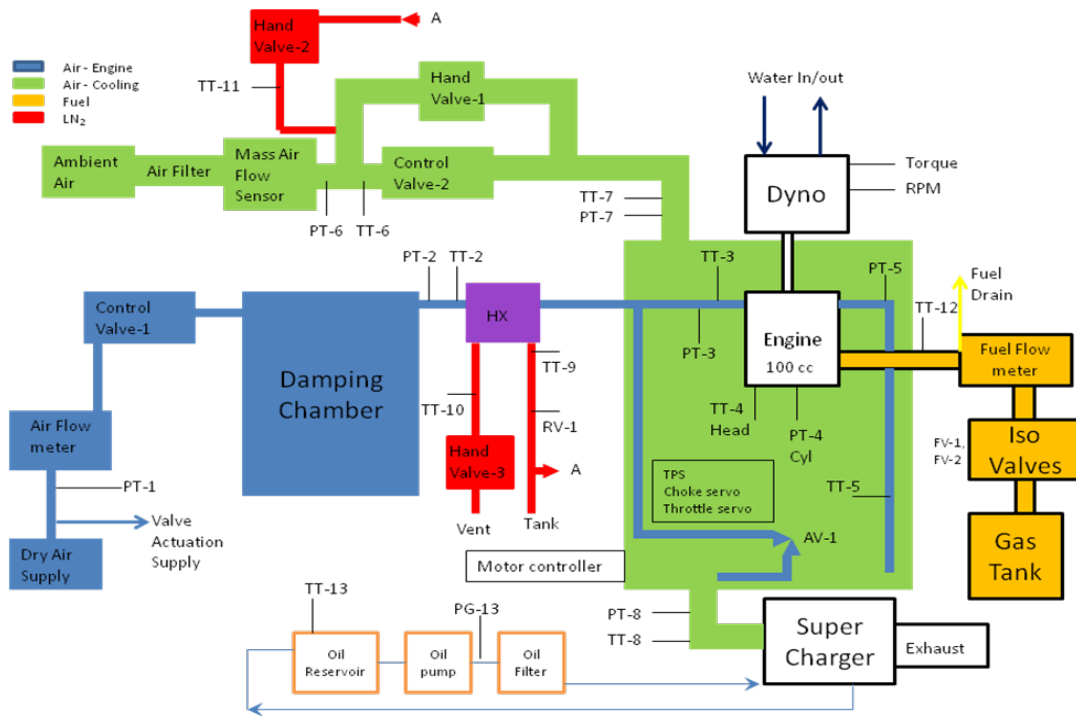
Figure 15: Test facility configuration as received (5)
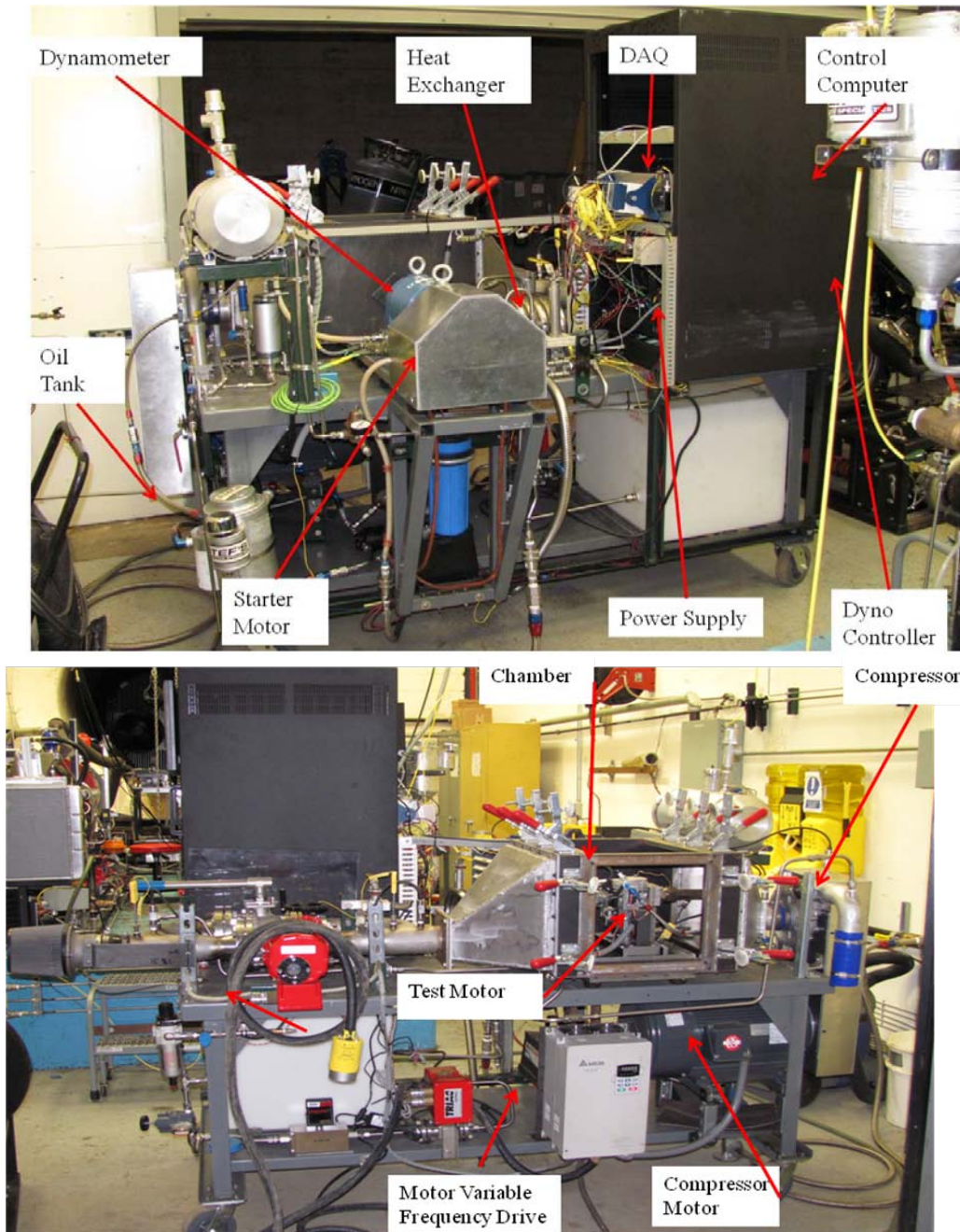
Figure 16: Test facility with key components identified (19)

III.2   Initial Test Facility Upgrades

The test facility as received was complete, but required several modifications before the current research could take place. The following is a list of deficiencies that were either identified by Schmick in his Future Work (5) section of this thesis or

discovered upon initial operation of the facility. This list served a set of initial facility objectives that needed to be overcome to bring the facility to the level needed to begin accomplishing the research objectives.

1. The altitude chamber fell short of the 15,000 foot MSL altitude pressure goal. The ability of the facility to recreate temperatures at altitudes worked as designed, but 10.1 psia was as low as the facility could go and this represents roughly 10,000 feet MSL. Additionally, the VFD would experience over-current faults that were not understood.

2. Previous test experience showed that the original inlet manifold design proved to be inadequate for the engine to properly start. Pressure drops in the inlet were notionally 2 psi and the engine was never reliably run with the inlet.

3. The compressor lubrication system reached peak oil temperatures (>200°F) too quickly and an oil cooling system was recommended.

4. BMEP, torque, and HP values for the test data of the engine proved to be uncharacteristically low based upon the expectations of the Brison 5.8. Further investigation was needed to address why the performance characteristics were so low.

5. Data provided for the different throttle positions proved to be difficult to actually replicate. Throttle positions from the installed throttle position sensor (TPS) proved to be inaccurate and wildly varying up to 800% in error due to vibration.

6. After receiving the test stand, the engine would not start after adjusting the carburetor to factory specifications. Further investigation was needed to determine the cause.

7. The engine starter on the test facility would sometimes become jammed with the gear on the output shaft of the dynamometer. The jamming could cause the starter and dynamometer to become locked up and wouldn't allow the engine to spin. This failure needed repair before further operation.

8. Schmick wrote in detail that a better process for engine output shaft alignment with the dynamometer input shaft might be required.

III.2.1 Fixing Altitude Chamber Pressure Leaks (Facility Objective 1)

While most of the key components already existed for the test facility, the research could not begin until the key issues / deficiencies were addressed. The first task to tackle was the reason why the altitude chamber did not achieve the 15,000 foot MSL design pressure of 8.2 psia. The first problem found was the shaft seal that seals the area around the output shaft of the engine and the altitude chamber box was damaged in the build process of the test facility. The engine was allowed to move while the starter was engaged and the seal was permanently damaged. Additionally, the Plexiglas window sealing gaskets were made of a material that was too brittle for constant installation and removal of the windows. The material was cracked in several places and each of these cracks along with the failed shaft seal caused the altitude chamber to leak. Lastly, small pressure leaks were found at the entrance and exits of the cooling air for the altitude chamber. These leaks were the main reason why the altitude chamber failed to meet its 15,000 foot MSL pressure altitude design goal.

In order to fix these issues, a new shaft seal was ordered from American High Performance Seal and installed in the wall of the altitude chamber. Additionally, rubber

sealing material from McMaster Carr (part number 8722K622) was ordered to make new window gaskets for both the top and side of the altitude chamber. The new rubber gasket material was chosen because it is much more flexible than the previous graphite based material, less brittle than the previous material, and able to withstand temperatures up to 400°F. The material came in 24" by 24" sheets and the gasket was cut out of these sheets of rubber. Photos of both the old brittle graphite material and the new rubber material are shown in Figure 17.
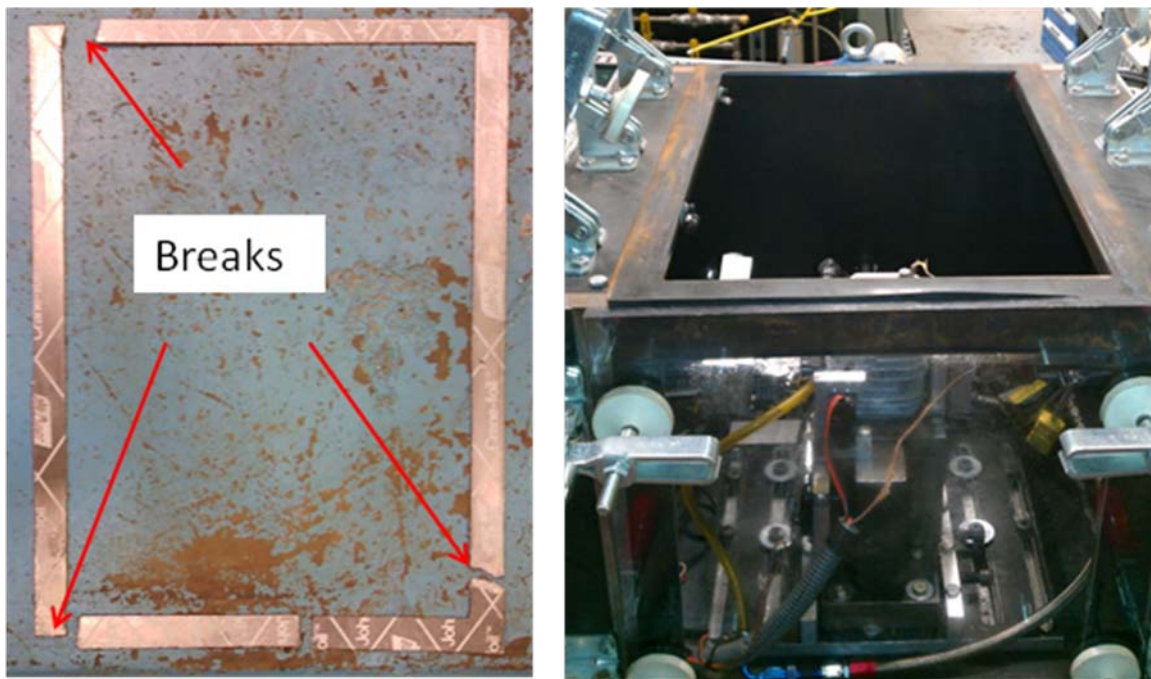
Figure 17: Left photo shows the old graphite based gaskets and its failure points. The right photo shows the new rubber gasket material

The leaks along the entrance and exit of the chamber were more difficult to solve. These leaks formed around the corners of the chamber where the aluminum diffuser meets the steel body of the chamber. The main cause of these leaks is speculated to be from warping of the aluminum diffuser during welding. In order to fix the leaks, Pro-Seal 34 from Pro-Seal Products was ordered from McMaster Carr due to its flexibility

after curing, temperature withstanding capability, and its resistance to degrading from oil based products. Pro-Seal was applied using a caulking gun around both the entrance and exist surfaces. After completing all three of the chamber sealing upgrades, the chamber was tested to determine its ability to generate simultaneous pressure and temperature conditions. Hand Valve 1 was fully closed at the start of each test, compressor oil pump turned on, and the compressor was started. The compressor speed was increased until the compressor output pressure reached 16 psia. Once that pressure is reached at the output side of the compressor, it was found that the variable frequency drive (VFD) would go into an over-current condition and shut down.

The shut-down occurrence was occurring way before the goal of 15,000 feet pressure altitude or maximum RPM of the electric motor. It was found that when the output pressure of the compressor reached levels above 16 pisa, the compressor would cause an over-current error in the VFD and the VFD would shut down the electric motor. A way around the failure was found by increasing compressor speed until reaching 16 psia of output pressure. After reaching 16pisa, Hand Valve 1 was closed and compressor speed was increased again until 16pisa of output pressure was reached.   In order to meet the 10,000 foot and 15,000 foot goals of the test facility, gradually closing Control Valve 2 while monitoring the compressor operating map is necessary so the user can watch for compressor stall. Once the low corrected mass flow stall limit is reached, the compressor speed can then begin to be increased once more. Following this process is how the pressure limits of the altitude chamber were determined. As well, this procedure is important in general for taking the altitude chamber to pressures below 13psia. Current overload of the VFD was also observed when trying to take the altitude chamber back to

sea level static (SLS) conditions as the output side of the compressor would increase past 16 psia and the VFD would go into overload. It is important to note that whenever SLS conditions are discussed in this research, Dayton, Ohio at 750 feet MSL is the actual reference condition. The overload conditions can be mitigated by reducing the compressor speed to 50% and then opening Control Valve 2. Once open, the speed of the compressor can be reduced and Hand Valve 1 can be opened fully without risk of current overload and the final data can be collected to present the overall pressure envelope the test facility can create for the engine.

III.2.2 Getting the Engine to Start (Facility Objectives 2, 4, & 6)

The next upgrade of the test facility included working on why the engine was so difficult to start. The original setup was nearly impossible to start and this was initially attributed to both the carburetor being set incorrectly and the initial inlet design. The initial inlet design to the carburetor included 1/2" stainless steel tubing with both pressure and temperature transducers installed. As Schmick (5) identified in his thesis, this inlet design caused peak pressure to oscillate rapidly when starting the engine and this can be seen in Figure 18. The oscillations were on the order of 3 psia and it was speculated that these oscillations were why the engine failed to start.
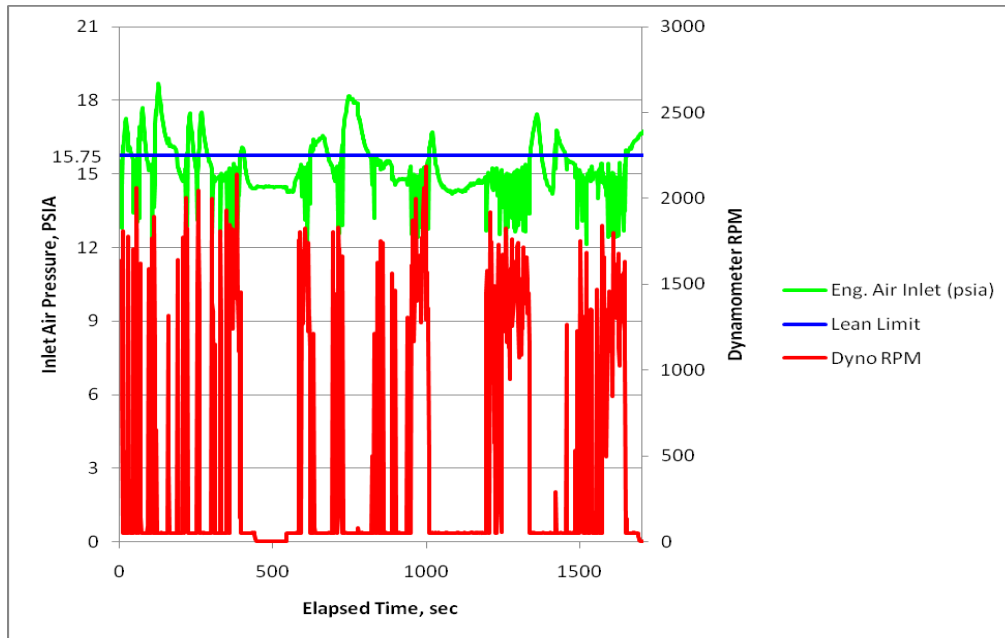
Figure 18: Inlet pressure and engine speed versus time for 16 February 2011 testing (5)

To troubleshoot the starting issues, the inlet tubing was removed from the carburetor. Troubleshooting the engine separately from the inlet monitoring equipment was necessary for two reasons. The first was to be able to isolate the cause of the starting problems and the second was to initially baseline the engine without any inlet modifications. This baseline was important in order to fully understand if the test equipment installed on the inlet were negatively affecting performance.

After removing the inlet tubing from the carburetor, it was determined that the choke servos were operating backwards from the indicated operating procedures. When the engine was choked in the LabVIEW VI, the servos were commanding a non-choke condition and the reverse was true for the un-choked condition. This was determined to be the cause of the unstable engine operation and the LabVIEW VI was changed to indicate the proper choke conditions. Additionally, since the choke was backwards, it

61

was assumed that the high and low speed carburetor adjustment needs were out of adjustment. Therefore, the needles were set to the factory specifications of 5/8ths of a turn for the low speed needle and 3/4 of a turn for the high speed needle. It is important to note for Walbro carburetors, these adjustments are done from the screw being bottomed out in the carburetor and adjusted out. The combination of the choke being set backwards and the carburetor being out of adjustment were suspected to be the primary causes of why the engine underperformed in previous research by Schmick.

Once the carburetor was adjusted, attention was put onto the inlet design. The inlet air for the carburetor is sourced from shop air and is cooled independently of the chamber air via a heat exchanger. This setup is required because LN_2 is used as the primary cooling medium for the chamber and the concentrations of oxygen and nitrogen in the air of the chamber is no longer representative of what the engine would see at altitude. Unfortunately, the current inlet design utilizes 1/2 inch stainless tube which caused 3 psia drops in pressure at the face of the carburetor. Figure 19 shows the original inlet configuration. Calculations showed that the intake line was creating an inlet Mach number between 0.4-0.5. This high Mach number coupled with the flow oscillations caused by the piston stroke resulted in un-starts of the engine. These lines and fittings caused a restriction in air flow which caused the intake pressure to drop 2-3 psi during engine startup. An attempt was made to increase the intake line pressure up to 16 psia prior to starting the engine. This pressure increase allowed the engine to start but it was not enough to keep the engine running or test the full range of engine performance.
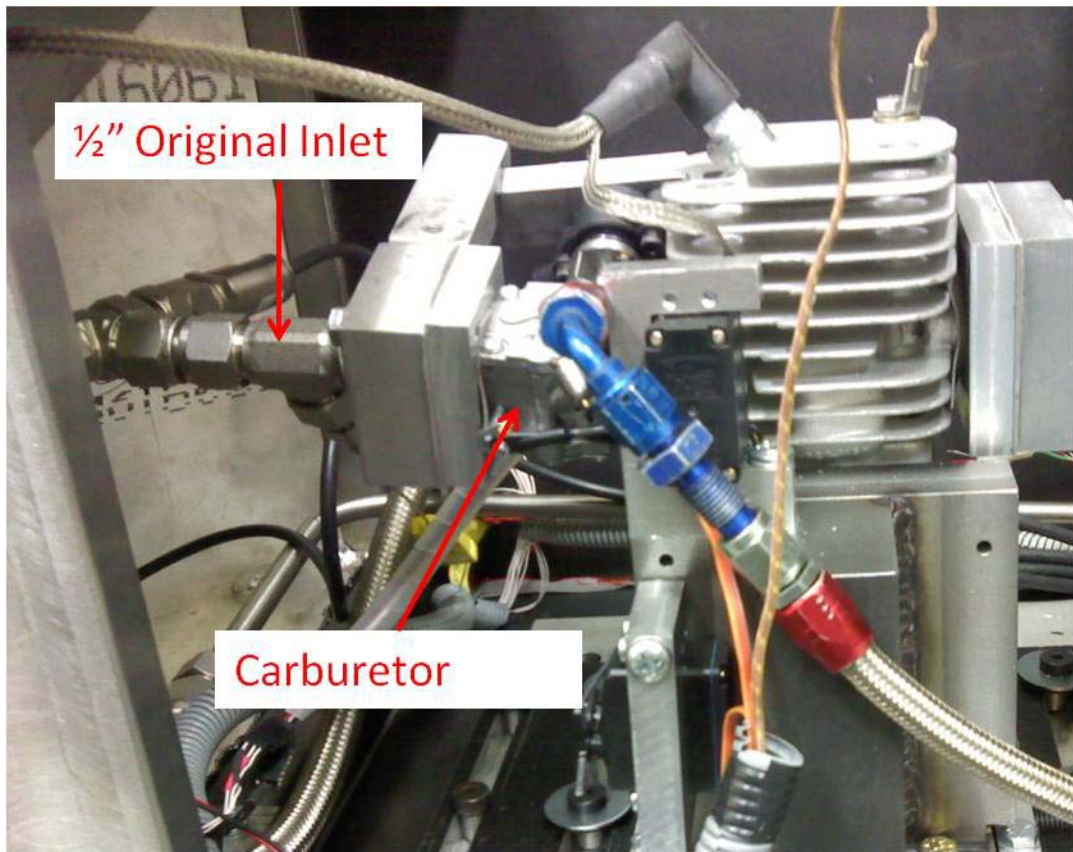
Figure 19: Original inlet configuration causing the pressure drops at the carburetor

To alleviate the problem, reducing the inlet Mach Number to less than 0.1 was desired in order to avoid compressibility effects. The new design incorporated a 3 inch steel pipe cut to 5 inches in length with stainless steel caps welded on the ends. The modified intake line added 33.5 in^3 in volume directly upstream of the engine intake. This additional volume kept the intake line pressure from dropping dramatically (<0.1psi with additional volume) and allowed the engine to operate over the range of inlet pressure and temperature conditions as required. This increase in intake volume is much larger than needed to maintain a Mach Number less than 0.1 and Figure 20 shows the new design. The additional volume of the intake allows for easier engine inlet valve operation

as the extra volume provides a buffer of air while the inlet valve is manipulated when transitioning engine rpm test points.

Figure 20: New 3 inch stainless pipe used as an intake manifold

Although additional volume was needed in front of the intake manifold, the supplied damping chamber was not close enough to the face of the carburetor to supply that increase in volume. When testing with the new manifold, the damping chamber actually caused significant problems for controlling the inlet pressure. As the pressure increased in the intake system, the chamber would expand and cause the system to react slowly to changes of the control valve. This posed a major problem because the engine was very sensitive to intake pressure and quick adjustments to the pressure were required. The damping chamber actually slowed these adjustments down and made running the engine impossible. The solution to this problem was to remove the damping chamber from the system. The intent of the chamber was to dampen air oscillations from negatively affecting the air mass flow meter upstream of the chamber. Further investigation showed that since the control valve was after the mass flow meter and the

mass flow meter is supplied via 70psi shop air, the mass air flow meter actually saw

choked flow conditions. Since the flow is chocked, the pressure oscillations from the

engine would never get far enough upstream to disturb the mass flow meter's readings.

The new manifold design was successful at reducing the inlet Mach Number, but

initial test data, discussed in Chapter IV, showed that the inlet manifold had several

negative impacts on the engine. These impacts included:

1. Engine performance suffered by as much as 12% when compared to data without

   the inlet. Adding extra air flow or reducing air flow did not increase performance.

2. Managing the air flow into the engine while managing throttle position and engine

   speed proved to be very difficult. In order to run the engine with the manifold,

   the inlet pressure had to be between 13.8 and 14.3 psia. Maintaining this pressure

   consistently during start-up or while transitioning between RPM set points was

   nearly impossible. Transitioning the engine between RPMs means adjusting the

   engine RPM by increments of 20 RPM on the dynamometer and gradually

   opening the inlet air control valve until the engine ran smooth again (no more

   missing or coughing of the engine). Often the engine would stall during this

   process and this meant starting over again at 3,000 RPM.

3. Even when the engine was running in steady state with the inlet attached, trying to

   transition the altitude chamber to a lower ambient pressure while the engine ran

   proved impossible. As soon as the chamber pressure dropped below 14pisa, the

   engine would immediately cease operation. It was found that the carburetor is not

   air tight and had leaks were causing intake air to leak out of the carburetor.

   Additionally, the carburetor and its diaphragm fuel pump require the ambient

pressure around the carburetor to be roughly the same value as what the inlet face

is seeing. The inability to run the engine with the difference of pressure made it

impossible to collect altitude data information.

4. The numerous attempts to run the engine with the inlet caused a carburetor to fail

due to over pressurization of the intake during the starting process. This cased

some of the rubber seals to fail and ultimately required a carburetor replacement.

After replacing the carburetor, the inlet manifold was scraped.

III.2.3 Installing an Oil Cooler (Facility Objective 3)

The next modification to the test facility involved installing an oil cooler to the

compressor lubricating oil system. The current setup allowed the compressor oil increase

in temperature to over 200°F within 15 minutes of compressor use and the issue would

only get worse as the temperature increased in the test cell. Therefore, an oil cooler was

sourced from Derale. (P/N 14-401051). The oil cooler was installed and the cooler

placement on the stand is shown in Figure 21. The new oil cooler allows continual

operation of the test facility in any ambient temperature while keeping oil temperatures

below 120°F.

Figure 21: New oil cooler installed to reduce compressor oil temperature

III.2.4 Addressing Starter Gear Jamming

After addressing the oil cooler, the last problem to tackle was the starter which
would not disengage from the gear mounted on the dynamometer output shaft. Figure 22
shows the state of the starter and the gear as the facility was received.
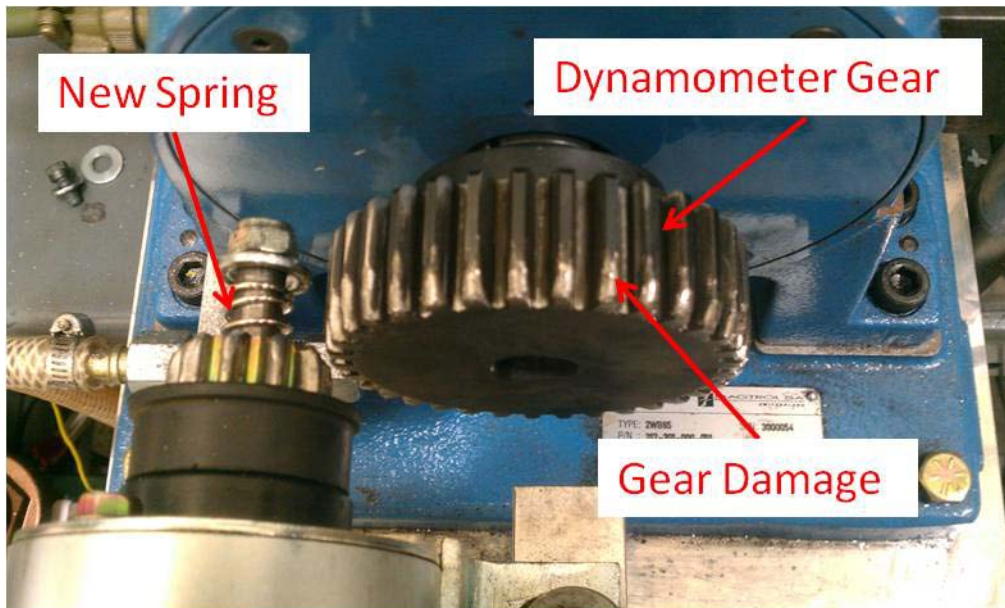
Figure 22: Starter spring replacement and dynamometer gear damage

A spring on the starter shaft that pulls the starter gear away from the dynamometer gear. This spring as supplied by the starter manufacturer was weak and deformed. Replacing the spring with a thicker and stronger spring restored starter function. Additionally, the gear on the dynamometer had burrs on the teeth due to repeated starter operation with the weak spring. The burrs were filed down and smoothed out. After all of the functional modifications were made to the test facility, the next step was to begin collecting baseline performance specifications for the Brison 5.8.

III.3 Carburetor Testing

The first round of tests involved running the engine with the supplied Walbro SDC-80 pump style carburetor as a baseline in order to have the ability to compare modifications made to the engine. For these baseline tests, the inlet line was removed and no LN_2 was flowed through the system. Standard operating procedures for the carbureted test facility are included in Appendix A: Carbureted Operating Procedures.

Before getting started, a safety check of the test stand is necessary as well as gathering the correct personal protection equipment. Safety glasses and hearing protection are required. Additionally, no loose fitting clothing items are allowed and a long sleeve shirt is required. If running LN_2, the oxygen sensor needs to be turned on and warn at all times to test for affixation and the proper safety gear for the LN_2 is required (gloves, safety shield, apron).

After getting all of the correct safety gear, the first thing required was to shake the engine to check if any of the bolts were loose that hold the engine to the test facility or that hold the head onto the engine block. Both sets of bolts were known to come loose and their failure can cause a catastrophic failure of the test facility and their locations are found in Figure 23. The head bolts are larger than the block bolts and usually just tightening them with an Allen wrench was adequate. The block bolts are long with few threads that lock into the block. These bolts actually loosed during testing or in one case broke off inside the block which occurred in the final days of testing. Broken bolts required replacement of the engine. If all of these bolts break off, nothing will be holding the engine to the test stand and if this happens, severe damage to the test facility will occur. Checking couplers, bolts, screws, and wiring for any loose connections caused by engine vibration was the next step in while checking out the test stand. Test stand vibration is an issue with this test facility and careful inspections for looseness was constantly needed.
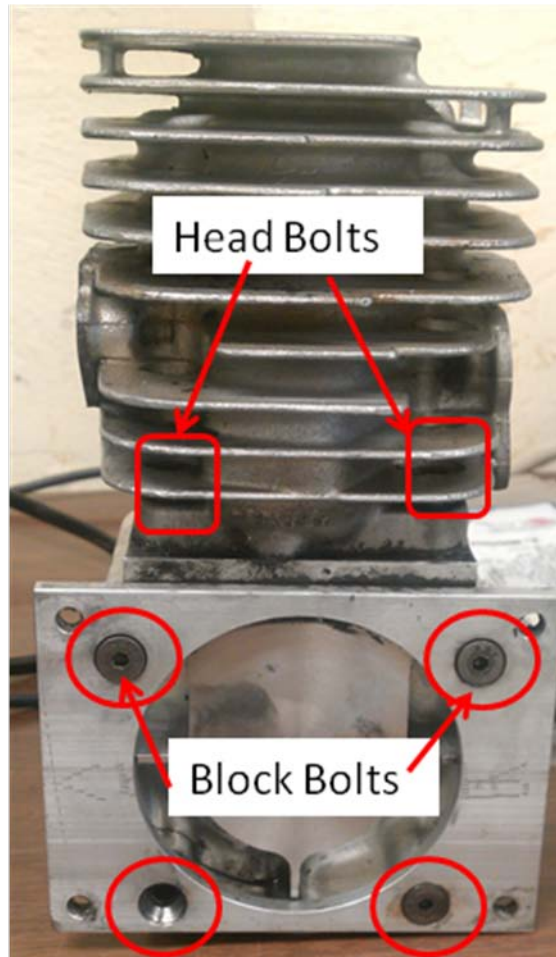
Figure 23: Broken block bolts and loosening head bolts are both areas that require daily checks to prevent damage

After inspecting the test stand, the 120VAC power was plugged in, the 480VAC power for the supercharger plugged in, 100 psi shop air plugged in, cooling water for the dynamometer plugged into water supply, and the exhaust hose plugged into the stand and routed to safe ventilation. The reason all of these connections were required daily was because the test facility is a mobile test facility. The stand is built on four caster wheels which allow the facility to be moved around the test location. The test location for the duration of this thesis is in Building 71A 5 Stand which is controlled by the Air Force Research Lab Propulsion Directorate.

After all supply lines were routed, the test cell exhaust fans were turned on as well as the 12VDC and 24VDC power on the main test cell control panel. While at the control panel, the 'Reset' button was switched to power the control panel power relay and then active the "Main Water Supply Valve" in order to activate dynamometer cooling water flow. After turning the water on, the exhaust fans were switched on, test cell door was closed so others cannot access the cell during testing, and the roll up door was cracked to allow fresh air into the test cell.

Once in the test cell, the 480VAC circuit breaker was flipped on, the dynamometer cooling water valve on the stand was opened, the shop air valve on the stand was opened, the manual fuel control valve was opened, and power on the computer was enabled. Once the computer was powered on, LabVIEW was opened and all of the sensors were verified to see if they were working properly. Working properly included checking the thermocouples to see that they all matched the ambient temperature of the test cell, pressure transducers to check if they were reading 14.3 psia, dynamometer output to make sure it was reading 0 RPM and torque. If any of these values were incorrect, either the sensor failed or the calibration settings in LabVIEW needed correcting. This was done by going to the top of the LabVIEW VI and selecting the calibration tab where all of the sensor calibrations are located for adjustment. Figure 24 shows the Altitude Chamber LabVIEW VI in its final configuration.
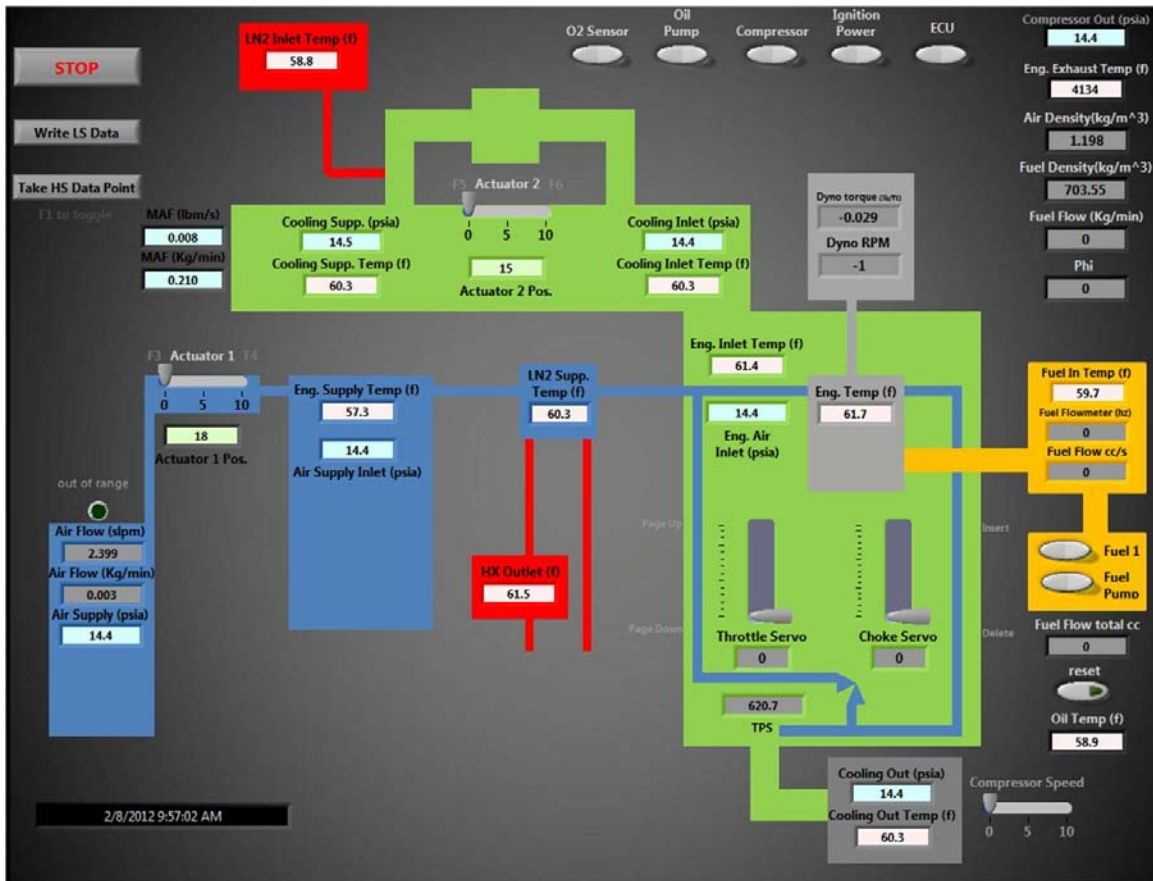
Figure 24: LabVIEW VI for the Altitude Chamber

Once ready to test, the oil pump was turned on so it could pressurize the

lubricating oil to 35 psig. Once at pressure, FV-1 was opened and the supercharger was

turned on. It is important to remember that the supercharger cannot be operated at speeds

greater than 50% at SLS conditions without reducing cooling air flow as stated in the

previous section. After the supercharger was running, the altitude in the chamber was set

to the required test point by closing Hand Valve 1 and gradually closing Control Valve 1.

All of the valve numbers are shown in Figure 15

The Magtrol Dynamometer controller was turned on via the black power switch,

dynamometer brake enabled, and set to the starting RPM of about 2,400 RPM. Less than

2,400 RPM is too slow for starting and faster than 3,000 RPM is just a little fast to start

the engine and increases risk of backfire. The engine RPM was set by pressing the "Set Point Max Speed" button, turning the "increase/decrease" wheel until the RPM was reached, the "shift" button pressed, and then the "max speed" button is pressed to lock in the RPM. If the RPM is not locked in, small vibrations or a bump of the adjustment knob can change the dynamometer operating condition and cause a faulty data point. Additionally, the RPM can be changed by the tens, hundreds, or thousands place by using the "up/down" buttons to move the cursor (20).

The PID settings for the dynamometer are very important for stable engine operation. The engine is not governed in any way and therefore if the dynamometer was not set up properly, the engine can over speed and cause damage to the dynamometer and the couplers. The limiting factor of the system was the couplers as they are speed limited to 7,500 RPM. In practice, 7,500 RPM is all that will be used. The first setting to ensure was correct is the Proportional Gain (P). The proportional gain was set to 20% and this was completed by pressing the "P" button, turning the dial until the correct value was reached, and then pressing "shift" to save the value. The next setting to change was the Integral gain; which was set to 20%. The final setting was the Derivative gain and that was set to 1%. The three settings were set where they are because they were the most effective combination of settings found at keeping engine RPM steady while holding to an RPM as close to the set RPM as possible. Steady operation of the engine was possible with higher P, I, or D settings, but generally too much brake pressure was applied at those higher settings which cause the engine to run much slower (200 RPM or more) than the set RPM.

The PID settings are incorrect if engine variations or surging become too great. Engine operation should be smooth sounding to the observer with visible engine RPM variations to be within 60 RPM of the set RPM. To fix the surging, the Derivative gain should be increased, but increasing the derivative gain caused the dynamometer to undershoot engine RPM. Additionally, the PID settings did not need changed for the duration of testing and if engine surging was observed, generally there is another cause outside of the dynamometer PID settings. Undershooting just means the engine will run under what the set RPM indicates and therefore test points can be 200 or more RPM lower than intended (20).

After the dynamometer was set, the next step was to turn on the ignition, and fully choke the engine. A throttle of about 25% is all that was required. The engine will not start in the full choke position. Instead, the engine will pop as the engine as it tries to fire. Once the pop happens, the choke needed to be opened back up and the starter engaged again. Often, the choke and un-choke process takes a few tries before the engine will start. It is also important to understand not to run the starter for more than a second or two when the choke is closed. Running the starter too long caused the engine to flood. If the engine was suspected to be flooded, removal the spark plug was required to dry it off with shop air before trying to start the engine again.

Once the engine was started, the test points were ran. Normally, 500 RPM increments were fine and test points taken for roughly 10 seconds per point. The reason 10 seconds was used is because the LabVIEW VI writes data at 33 Hz. This meant that a data point was recorded 33 times per second and therefore, 10 seconds of data was needed in order to get a true average of the performance data. Instantaneous data is not

presented in Chapter IV because the instantaneous torque can wildly vary depending on the crankshaft position in reference to the combustion event. Therefore, 10 seconds allows for many combustion events to occur in order to get a good average reading of the 330 data points recorded. Additional time can be added, but when running test conditions between 3,000 and 7,500 RPM, engine head temperature became a concern and increasing the amount of time spent at each test point rans the risk of overheating the engine before completing the test points (>400°F). Overall testing per test condition took over 10 minutes and testing much longer than that at full throttle can cause the engine to overheat. Therefore the engine was reduced to 2,500 RPM to cool off between test conditions or the engine was shut down while leaving the compressor running to assist cooling the engine. Shutting the compressor down with a hot engine can actually allow the engine to get hotter while it sits. The overheating condition was not an engine limitation, but instead a facility limitation that does not direct enough airflow around the engine. There are three primary reasons why the engine was returned to 2,500 RPM after running a given test condition. These are:

1. Take data at 2,500 RPM to test if the engine output changed during the test. This was a repeatability test to ensure nothing changed while running the test condition.

2. Continuously running the test stand at high RPMs can cause the engine to overheat. Allowing the engine to rest at a lower RPM gives the engine an opportunity to cool. Additionally, there are no baffles inside the test chamber that would direct all of the air around the cooling fins of the engine. The RC

community often uses baffles to direct air from the prop around the engine to maintain adequate cooling.

3. Returning to 2,500 RPM allows all of the rotating machinery to gradually slow down at a controlled rate before turning off the engine. As well, slowing an engine to idle is common practice to reduce the risk of backfiring. Backfiring can cause damage to an engine.

Once testing is complete, the previous operating steps were completed in reverse order to shut the test facility down.

Initial attempts to collect the baseline data for the carburetor led to some significant problems with the test facility. The largest problem manifested itself in the elastomer spiders used in the Lovejoy GS28/38 couplers used to couple the engine to the driveshaft that goes to the dynamometer. Initial failures of the spiders are displayed in Figure 25. The failures of the spiders would occur sometimes after 20 minutes of testing or sometimes within a few minutes of testing depending on RPM. Several spiders were replaced in an effort to understand why these failures were occurring.
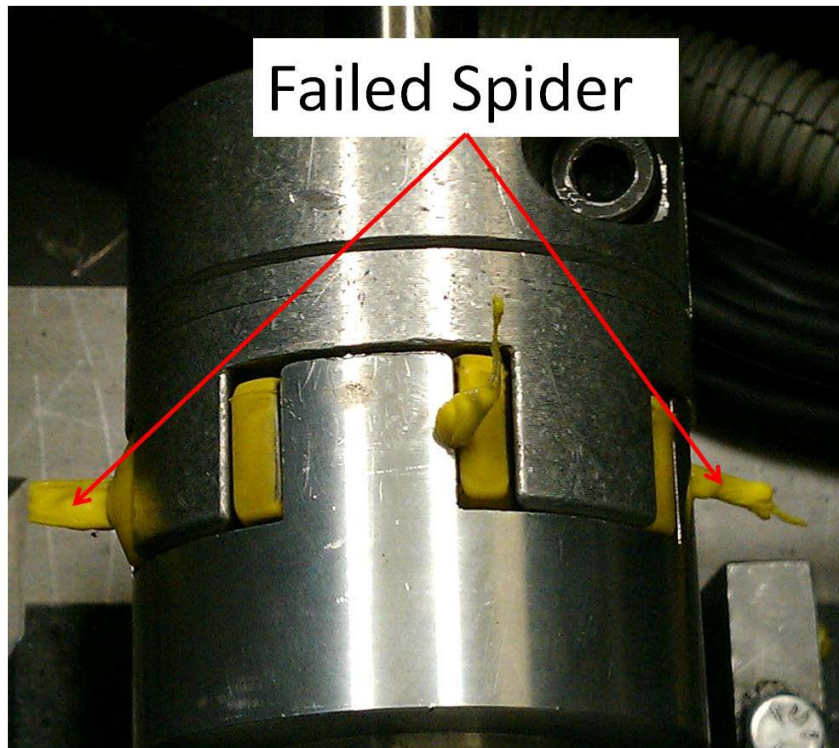
Figure 25: Failed Lovejoy spider

A call to Lovejoy, the manufacturer of the spider and coupler, gave insight into the potential cause of the problem. Hysteresis inside the elastomer spider was causing the material to heat up in the center of the coupler faster than the spider was able to transfer the heat out into surrounding aluminum of the coupler. Another suggested cause of the heating included vibration due to the instantaneous torque from the engine. Additionally misalignment was considered as a cause of the melting spiders, but LoveJoy's engineers insisted that misalignment causes these elastomers to degrade into small balls of the spider material that ejects the spider. Additionally, the nature of how the spider material would wick out of the center of the open sections of the coupler was more indicative to vibration hysteresis than misalignment. A new harder was sourced from LoveJoy as the yellow spider (92 Shore A GS) is a much softer general use spider

and the performance specifications are located in Table 3. The red spider is more suited for high load industrial applications and it was ordered for the facility.

Table 3: Lovejoy spider choices and their performance characteristics (21)

Spider Type	Color	Material	Temperature Range		Sizes Available	Typical Applications
			Normal	Maximum		
80 Shore A GS	Blue	Urethane	-50° to 176° F	-80° to 248° F	14-24	Electric measuring systems
92 Shore A GS	Yellow	Urethane	-40° to 194° F	-50° to 248° F	14-55	Electric measuring systems and control systems
95/98 Shore A GS	Red	Urethane	-30° to 194° F	-40° to 248° F	14-55	Positioning drives, main spindle drives, high load applications
64 Shore D GS	Green	Urethane	-20° to 230° F	-30° to 248° F	14-55	High load applications torsionally stiff spider material

The next item addressed was the shaft that connects the engine to the dynamometer. Initial inspections showed that the shaft had a keyway cut along the entire length of the shaft. Although the keyway was cut, the only places were keys filled the void of the shaft were at the ends of the shaft where the couplers were located. The rest of the keyway was open and this was suspected to cause an out of balance situation. In an effort to correct this situation, a new solid shaft was ordered and 1 inch in length keyways were machined into the ends.

Although a new spider material was ordered and shaft replaced, attention was given to the alignment of the engine with respect to the dynamometer. Laser alignment hardware and the expertise to use the hardware were supplied by Mr. Dave Peabody of the AFRL Compressor Research Facility in AFRL/RZTE. He manufactured the mounting fixture for the laser in order to check the alignment against the coupler's tolerances for alignment. A laser was mounted to the dynamometer input shaft and a receiver was mounted to the engine crankshaft. The coupler tolerances were entered into the computer and both the dynamometer and the engine crankshaft were rotated

independently to check axial, radial, and angular misalignment. The tolerances for the

LoveJoy GS28/38 Curved Jaw couplers are located in

Table **4**. The alignment checkout of the engine with the dynamometer proved that the

facility's hardware was in fact aligned within the specifications allowed by LoveJoy.

Table 4: Lovejoy Curved Jaw coupler alignment specifications (21)

Size	Spider Shore	Axial Misalignment (in)	Radial Misalignment (in)	Angular Misalignment (degrees)
28	92	+0.059 / -0.027	0.006	1,0
	98		0.04	0,9
	64		0.003	0,8
38	92	+0.070 / -0.027	0.007	1
	98		0.005	0,9
	64		0.003	0,8

Since trapped heat was a suspected cause of the yellow spiders to melt, cooling air

was introduced to the coupler on the outside of the altitude chamber. The choice to only

include it on the outside of the chamber and not on the inside was mainly due to fact that

the outside spider was the only one to fail prior to the addition of the red spiders. Once

the red spider was installed on the outside coupler the engine was ran to check for spider

failure. This time, the inside yellow spider failed and therefore warranted a replacement

with a similar red spider. Additionally, since the outside spider always failed before the

inside spider, it was assumed that the air around the outside couple was stagnated and it

made sense to add cooling air. The cooling air was supplied via shop air that was already

available on the test facility. Some ¼ inch tube was bent in place and a manual valve was

installed to control the cooling air. Figure 26 displays the cooling air fixture.
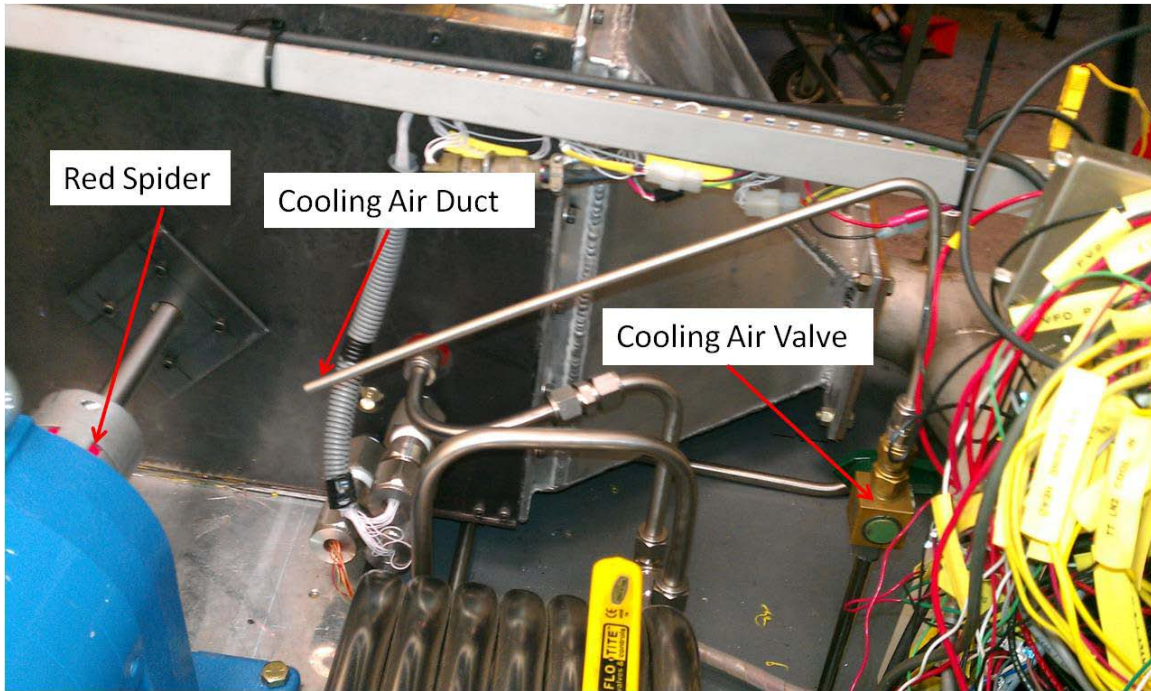
Figure 26: Exterior coupler cooling duct installed

After installing cooling air, the engine was run and preliminary data was collected to check out all of the measurement devices and to exercise all of the subsystems. Initial stand checkouts showed the fuel flow meter was indicating about half of the fuel expected to operate the engine. BSFC was just too good and when data is too good, it's an indicator that something is wrong and the values should be scientifically questioned. Initial BSFC calculations from the carburetor were around 0.4 lb/(hp-hr) and values this low are indicative of modern day direct injected gasoline engines. Further investigation of the fuel metering system found that the flow meter and the LabVIEW VI were never calibrated together. Therefore, a separate test to verify fuel flow was needed. To accomplish this, the fuel hose was removed from the carburetor and placed into a graduated cylinder. The fuel control valve was actuated along with a stop watch for 10 seconds in order to verify both the fuel flow rate and the total fuel flowed indicators in

LabVIEW. Since the fuel flow is primary gravity feed with the assistance of the

carburetor's fuel pump, the fuel flowed at a constant rate throughout the testing. Figure

27 shows the graduated cylinder setup. As anticipated, fuel flow rates were half of what

was actually flowing through the system and a change in how LabVIEW was counting

the pulses from the flow meter was needed to solve the problem.

**Figure 27: Fuel line and graduated cylinder used for fuel flow meter
calibration**

Another phenomenon when running the initial tests manifested itself in initial

plots of the data. Data showed unexplained dips in power and the dips were actually

being caused by a small screen filter inside of the carburetor. The screen was removed

and metal shavings were found to be plugging the screen. The sources of the shavings

are unknown, but they are most likely from initial manufacture of the fuel system of the

facility. After cleaning the carburetor, the next step was to tune the carburetor.

Provided engine documentation (22) yielded approximate ranges for the high and

low speed needle. The low speed needle was specified to be positioned between 5/8 to

7/8 out and this needle controls idle and low speed fuel delivery. The high speed needle was specified to be positioned at 1 turn out and this needle supplied additional fuel for high speed operation. Both of these adjustments start with the needles screwed all of the way into the carburetor and then turned out the specified turns.

These adjustments provide a rough engine tune. Further adjustment was needed based on operating conditions and this was done purely based upon listening to the engine. This manual tuning of the engine was initially accomplished without an oxygen sensor. The engine was run at idle until it was warmed up to operating temperature. The low speed needle was adjusted out until the engine began to miss based upon too much fuel. The needle was then adjusted back in until the missing stops. Then, to tune the high end, the engine was run at wide open throttle, 8,000 rpm, and the same procedure was completed. With both needles set, the engine was traversed through its rpm operating range to check for stumbles or missing. If missing occurred, small adjustments to the low speed needle were completed. If engine surging was experienced, this meant the engine was hitting its surge limit and this means the mixture is too lean. Surging is experienced when trying to increase engine RPM via the dynamometer controller and is observed when the engine quickly rams up in RPM and then shuts down.

Carburetor adjustments were required daily to ensure optimal operation of the engine due to many factors. Engine vibration, changes in ambient pressure, and changes in temperature were some of the factors that influenced carburetor needle settings. Therefore, daily checks on how the engine runs are needed before taking any data. As a warm up procedure, the engine was run across its full RPM range to ensure there was no missing, backfiring, or surging occurring.

Additionally, the Brison 5.8 creates significant vibration as it approaches RPM operations greater than 5,000 RPM. Due diligence is needed when running the stand to ensure bolts that loosen due to vibration are tightened during the testing process. Special attention is needed to ensure the head bolts are tight on the engine head. These bolts have a tendency to loosen over time even with liberal Loctite application. Additionally, all mounting hardware for the carburetor needs to be checked, exhaust hardware, and engine attachment hardware on a daily basis. Failure to check these things can cause parts to fall off of the facility or for the engine to come apart while testing.

Vibration while troubleshooting the engine caused several components to fail. The first components were the existing throttle position sensor (TPS) and its mounting hardware. Bolts continuously sheared off due to vibration and vibration from the engine caused the TPS to oscillate rapidly giving inconclusive throttle position information (800% error). To remove risk of the mounting hardware coming off and being sucked into the supercharger, the TPS and its mounting hardware were removed for carburetor testing. A new TPS measuring system was used for the later installed fuel injection system.

Another problem experienced involved the plastic throttle body spacer supplied with the engine. The plastic spacer was used to mount the carburetor to the engine intake port. Unfortunately, the part is made of plastic with brass inserts for the carburetor attachment bolts to mount. Failure occurred around the brass inserts as they separated from the plastic and caused the spacer to fracture in half while testing. A new aluminum spacer was machined with the help of Ben Naguy. Ben assisted with the precise machining required to create the vacuum port and path on the engine side of the spacer.

Both the broken spacer and the new spacer are shown in Figure 28. The aluminum spacer added the appropriate amount of strength needed to withstand the vibration and if this problem is seen in the field by the operators, a possible solution to future failures.

Figure 28: Top left is original spacer, top right is new aluminum spacer, and bottom is broken spacer

The first set of tests involved tuning the carburetor at sea level static (SLS) conditions and running the engine up to 10,000 feet MSL of pressure. This simulated a realistic operational situation where the RPA was tuned at a low elevation location and taken to a high elevation without the user changing the carburetor. No temperature effects were investigated in this data and therefore the engine was operating at near ambient temperatures for all tests and the inlet design was not used. The second set of test involved leaning the mixture for each operating condition other than ambient

pressures. This strategy is called optimized tuning. For every 5,000 feet tested both the low and high speed needles were adjusted in (leaned) by $1/8^{th}$ of a turn. The engine is then run to verify smooth operation at the optimized altitude. All test points are at wide open throttle. The needle configuration is shown in Figure 29. This simulates a user knowing the conditions the RPA is flying in and adjusting for those conditions.

Figure 29: Walbro SDC 80 with low(L) and high (H) speed needles identified. Left side faces the engine and right side faces the inlet manifold

Testing was also attempted with the inlet attached to the carburetor, but running the engine while metering the amount of air entering the carburetor proved to be an extremely difficult task to manage. In order to start the engine, the inlet had to pressurize to roughly 18 psia. Once pressurized, the starter can be quickly engaged to see if the engine will fire. After several tries, the engine would fire and run sporadically until more air flow was introduced. Actuator 1 was then increased until the engine began to run smoothly at 3,000 RPM. Once the engine is running smoothly, the engine RPM could be increased by 20 RPM and then the air adjusted to smooth the engine back out. As the RPM is increased, the engine will begin to miss and this is the sign that more air is needed. The process of gradually increasing RPM with air volume can be repeated until the next test point is reached to take data. Some test data was taken using intake inlet, but

unfortunately, testing with the inlet caused several problems that could not be easily solved. The first problem involved leaks in the carburetor. The Walbro SDC-80 carburetor has many holes, ambient pressure ports, and fittings that were never meant to hold pressure. This was observed when trying to reduce pressure inside of the altitude chamber while the inlet remained at SLS conditions. As soon as a pressure differential of 1 psia was reached, the engine shut down. Repeated attempts to troubleshoot this phenomenon caused a failure of the internal rubber diaphragm for the fuel pump in the carburetor. Further testing with the inlet was canceled and all carburetor data was completed with the inlet removed. The initial inlet test data as well as all of the carburetor testing is introduced in Chapter IV.

III.4 Fuel Injection Testing

Running the tests with the carburetor highlighted some significant operating difficulties and performance disadvantages that should be addressed. After running these tests the carburetor system was torn down and removed. The supplied fuel system was converted to a port fuel injection system to attempt to better control the fuel flow ratio over the full operating range. A fuel injector is an electromechanical solenoid actuator that meters fuel into the engine via the amount of time it is open and the fuel pressure supplied to the injector (6). Replacing the carburetor with an injector warranted adding a low pressure fuel pump to the fuel system as the current carburetor also acted as the fuel pump. In addition to a fuel pump and fuel injector, an engine control module needed developing in order to properly control the amount of fuel the injector introduces to the engine. The control module regulated the amount of time the injector was open, the

injector pulse width, and the period between injections. The SAE Surface Vehicle Recommended Practice, J1832, (23) identifies the necessary functional parameters of a fuel injection system as well as the ways to design for system reliability and proper engine performance.

A commercial-off-the-shelf throttle body fuel injection (TBI) kit from Ecotrons (24) was integrated onto the engine. The fuel injection kit included a 10.58 lb/hr fuel injector, generic fuel pump, engine computer, Pro-Cal tuning software (25), intake air temperature sensor, manifold pressure sensor, engine temperature sensor, and 28mm throttle body housing with throttle position sensor attached. The main rational for choosing the Ecotrons system was the kits extra low maximum flow rate fuel injector. Some of the smallest automotive fuel injectors flow a maximum of 14 lb/hr and these flow rates were too high for the class of small engines like the Brison. Figure 30 is supplied from Ecotrons and gives an overview of what is included in the kit. Some of the pieces were used as supplied, others were modified, and some pieces were replaced with different equipment more suitable for the test facility. None of the supplied fuel lines were used and the supplied ignition module was not used either. The reason for this is the Brison already comes with a capacitive discharge ignition box and changing both the ignition source and the fuel source would make determining the causes of changes in performance more difficult to quantify.

**Figure 30: Ecotrons sourced fuel injection system as received from the company
(Supplied by 24)**

Additionally, a Bosch LSU4.9 oxygen sensor with the CJ-125 driver chip was

installed in order to visually see the AFR as tuning changes are made (26). The LSU 4.9

(shown in Figure 31) is a wide band lambda (λ) sensor. Equation 15 defines lambda as

the actual air-to-fuel ratio divided by the stoichiometric air-to-fuel ratio.

Figure 31: Bosch LSU 4.9 oxygen sensor

The LSU 4.9 has the capability to measure lambda down to 0.65 and up to infinity (26). Additionally, this O_2 sensor has an integrated heater installed that is capable of reaching sensor operating temperatures (700°C) within 30 seconds of initial power on. The sensor is made for use in gasoline, diesel, and E85. The use of AVGAS will degrade the O_2 sensor over time due to the leaded fuel, so a careful eye is needed to watch for sensor failure over time. Signs of included flashing error codes on the sensor diagnostic software and slow reaction when exposed to clean air. The sensor instructions state that the sensor should be installed as close to the exhaust port as possible. Installation too close to the exit of the exhaust pipe to ambient air can cause inaccurate readings from the sensor because of mixing with non-exhaust gases. Figure 32 displays the installation of the sensor in the supplied M18 bung.
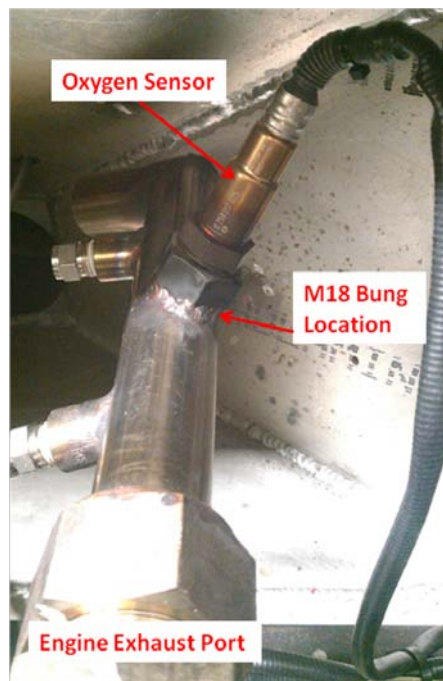
Figure 32: Exhaust Bung and Oxygen Sensor Location

Setting up the Oxygen sensor involved using a separate program that was supplied with the ECU. The O_2 sensor has several calibrations than can be changed via the supplied the software. The supplied display currently is set up to output AFR, but it can be set to display lambda if that value is desired. The software is not necessary for proper operation of the O_2 sensor, but it is required to make changes. All of the changes are outlined in the "Accurate Lambda Meter" instruction manual.

Furthermore, the engine computer had the ability to tune the engine with the wideband Bosch oxygen sensor and this allowed the engine to tune itself for pressure changes due to altitude. Since this was a generic kit, a new throttle body spacer and gaskets were machined to fit the engine and throttle body. New servo control linkages were designed to move the throttle plate. The new attaching hardware is displayed in Figure 33.
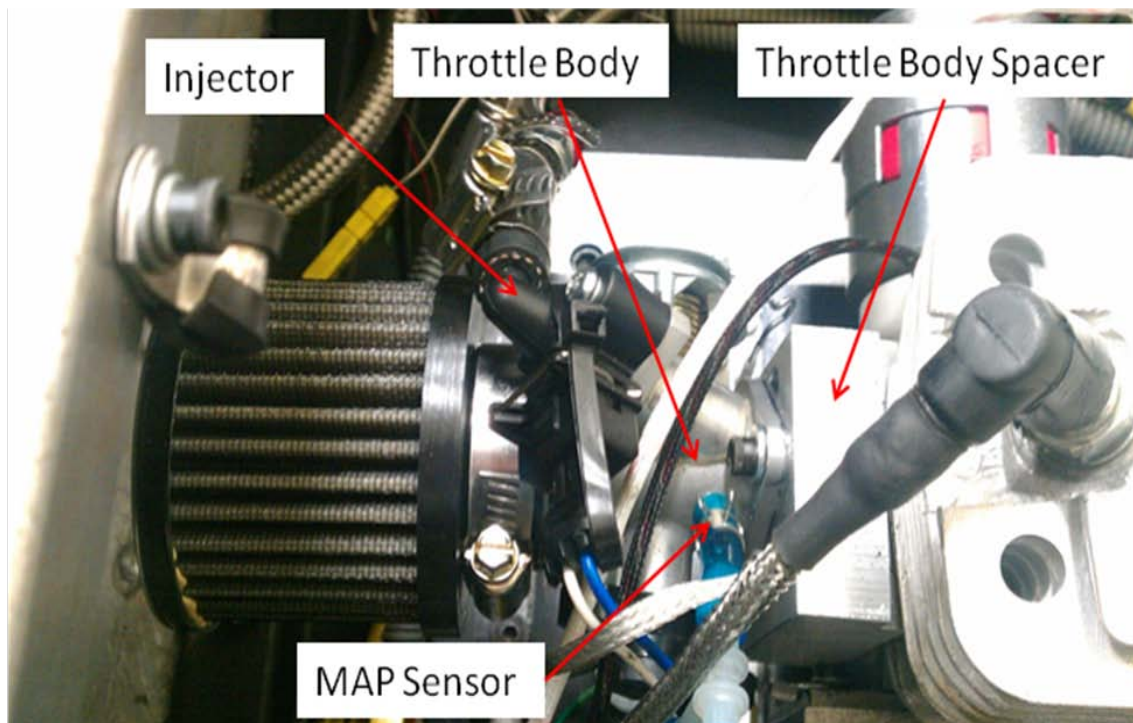
Figure 33: Fuel injection system installed with new throttle body, spacer, injector, sensors, and air filter

The supplied ECU wiring harness is intended for use in converting carbureted motorcycles to fuel injection. In order to install the system on the test facility, several modifications to the harness were required. The first modification was to remove all of the electrical tape covering the wires of the harness and cut the harness in half since the ECU would not be installed inside the altitude chamber. The main reason this decision was made was to avoid complication and delay time of installation because of the power requirements of the ECU, size of existing pass though wiring, and the need to constantly monitor ECU information via the test facility's computer. In order to avoid full disassembly of the altitude chamber in order to install more wire pass through connectors, the existing two Conax Technologies 12 wire pass through were utilized to pass the sensor signals and power through the altitude chamber. To free up enough pass through

wires from the carburetor configuration of the test stand, the choke wires, exhaust

pressure sensor wiring, and old throttle position wiring were removed. All of these

systems would no longer be needed with fuel injection and therefore their removal does

not reduce the capabilities of the test stand. Their removal will however require re-

wiring for carburetor installation if needed. In their place, the wideband oxygen sensor,

supplied throttle position sensor, manifold pressure sensor, intake air temperature sensor,

injector voltage and ground, and engine temperature sensor wiring were installed. The

wire diagrams for the pass through connectors and the associated plugs are included in

Appendix B and Appendix C.

The next modification to the supplied wiring harness was the fuel pump wiring.

The fuel pump was originally configured to be powered through the ECU harness via the

pre-wired relay. Instead, the fuel pump was wired separately from the ECU harness in

order to be able to isolate any fuel supply problems when changing parameters on the

ECU. Initial testing of the fuel system showed that the fuel pump was activated for 3

seconds when the ECU power switch (key on) was switch on and then turned off. The

ECU would then command the pump to run full time once the engine was started. This

strategy works fine for motorcycle use, but can be difficult to deal with when

troubleshooting the system. The choice to wire the fuel pump to a separate power supply

and switch was in anticipation of any future problems. The fuel pump wires on the ECU

wire harness are capped and can be used later if deemed necessary.

The last modification to the harness involved powering the components. The

ECU power is supplied via the starter battery on the test stand and the fuel pump is

powered by an external 12VDC power supply. None of the fuel injection or oxygen

sensor systems could be wired into the stand's existing 12VDC power supply as they only can supply 2.5A. This is the reason why there is a separate DC converter for the fuel pump (3 amp draw) and the ECU and oxygen sensor are powered via the battery. The oxygen sensor's power draw is normally 700mA, but the sensor has an internal heater that is used to heat the sensor to an operating temperature of 700°C. When the heater is running, the sensor draws 2A requiring it to be wired directed to the battery. After the power supply modifications were made, the ECU serial cable was installed and plugged into the computer.

After running all of the wire, supplied sensors, and fuel system, the engine's Hall Effect sensor was integrated into the supplied engine computer. Since little documentation comes with the Brison engine, little was known about the Hall-Effect sensor on the crankshaft except that 5VDC was supplied to the sensor. Originally, the sensor signal wire was cut, spliced for a spark signal, tested, and spliced to supply spark signal to the ECU. Figure 34 identifies the Hall-Effect sensor on the Brison 5.8.

Figure 34: Brison Hall-Effect sensor

Hall-Effect sensors are configured a few different ways. The sensor on the Brison watches for a single magnetic tooth that triggers the spark pulse. The trigger tooth is located at 28 degrees before top dead center on the crankshaft. Other sensors have multiple teeth with one tooth that identifies top dead center. When testing with oscilloscope, the signal wire on the Brison produces 4VDC power all of the time until the trigger tooth passes sensor. When the tooth passes, the signal drops to 0VDC. The Ecotrons engine computer required at least 2VDC pulses from the sensor and this signal was acceptable. The spark signal wire from the Hall-Effect sensor was hooked to the ECU and the wiring was finished.

Numerous attempts were made to try and start the engine with no success. The fuel injector was pulled to check for fuel when cranking the engine over. No fuel was pulsing from the injector, so the fuel system was checked for fuel pressure. The fuel system was operating properly at 40 psia, so attention was put on the fuel injector. The fuel injector wires were scoped. The fuel injector is supplied 12VDC power all of the time the ECU is powered. When the ECU wants to fire the injector, the ECU switches the ground wire on the injector. Switching of the ground wire is how the ECU controls the pulse width of the injector. Scoping the injector ground wire showed that the fuel injector was receiving the correct pulse width from the engine computer and therefore the fuel system was verified to be working properly.

After establishing the fuel system was operating properly, attention had to be put back on the ignition system since the engine would not fire. Originally, spark signal was being checked by scoping the spark signal wire from the Hall-Effect sensor without being connected to the ECU spark pickup wire. As soon as the Hall-Effect signal wire was

hooked to both the ignition box and ECU, the signal would attenuate from 4VDC pulses

to 400mV pulses. The ECU requires at least 2 VDC pulses in order to establish engine

RPM. The signal was therefore boosted in order to supply the ECU with 4V pulses and

the boosted signal came from the pull-up resistors inside the capacitive discharge ignition

(CDI) box that comes with the Brison. The signal wire was traced through the ignition

box and the signal wire was soldered in after the sensor signal was boosted. After this

fix, the spark signal wire provided a signal as shown in Figure 35.
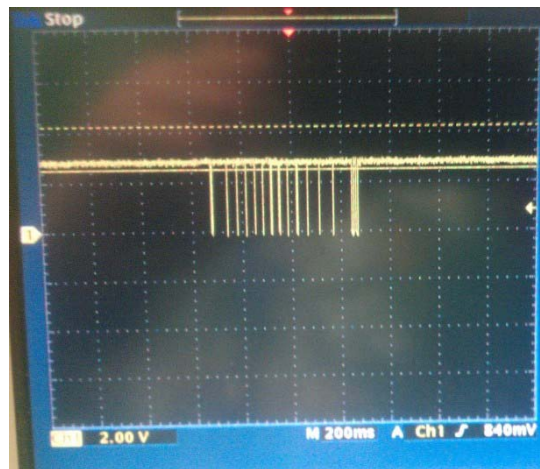
**Figure 35: Ignition signal from Hall-Effect sensor showing 4VDC drops when the
magnet passes the sensor**

Understanding the key fundamentals of how an engine operates becomes

important when troublshooting why an engine is not operating as intended. In all

combustion cases, a fuel, an oxidizer, and a heat scource are needed at the right time in

order to create combusion. When troubleshooting an engine, each of these sources needs

to be investated independently in order to better understand what is not operating

properly. In the previous case, had the spark plug been removed and checked for spark

intially, a significant amount of time would have been saved in the troubleshooting

process since the reason for lack of combusion was the spark signal attenuation.

Once the entire system was wired into the test facility, the ECU's calibrations were adjusted to match the engine. The first calibration required programming the ECU so it knows what to expect for the spark signal. The ECU is programmed via the Pro-Cal software suite installed on the test stand computer. Hundreds of parameters are available for user programming, but two parameters needed changing to get started. The parameters are located by opening Pro-Cal and clicking on "add advanced calibrations". The first calibration, "VAL_CKP_Pulse_Polarity," tells the ECU if it will see voltages spikes when the trigger passes on the Hall-Effect sensor or if the signal drops. In the Brison's case, the signal drops from 4VDC to 0VDC and therefore a value of 1 is required for entry. . In order to make any of these changes to the ECU, the changes must be made in Pro-Cal, saved to the computer, and then burned to the ECU. There is a "Burn to ECU" button that must be pressed while the ECU is powered in order to program the ECU with the new calibrations. This is true for any calibration that is changed in Pro-Cal. Failure to burn to the ECU will result in the ECU not utilizing the changes (25).

The next calibration required tells the ECU how many teeth are on the Hall Effect sensor. In the Brison's case, only one tooth exists at 28 degrees before top dead center (BTDC) and therefore a value of 1 is placed in the calibration "Val_nTeethTot."

The final ignition system calibration tells the engine computer how many of the teeth on the crankshaft are magnetic signal teeth. In the Brison's case, the single tooth is also magnetic and therefore a value of 1 is placed in the "Val_nTeethMiss" calibration. After completing the ignition system calibrations, no changes were needed since initial setup.

The next system to calibrate is the air and fuel system. The ECU was supplied with generic fuel tables. The ECU programming used for the Brison is a throttle position based load mapping system since the engine is a two-stroke. A four stroke would use a volumetric efficiency versus RPM fuel mapping table. The ECU had a 12 RPM interval by 16 throttle position table with load values indicated for each operating location. The user has to tune the engine for each throttle position verses rpm location by inputting the correct load value in the cell. Load by definition is the actual air mass charged into the cylinder divided by the ideal air mass that can be filled into the cylinder or it can be the brake mean effective pressure over the maximum brake mean effective pressure (25). In order to accomplish the tuning, the engine was started and the first operating point of throttle at 100% was dialed into the engine. The dynamometer controller was set to 2500 RPM (the first point in the load table) and the oxygen sensor signal was observed for the AFR. If the AFR was less than 13, the engine was shut down and a lower load value was placed into the corresponding cell. The new table was "burned to the ECU" and the point was run again until the correct AFR is reached. The decision to go with an AFR of 13 is discussed in the results section of this research.

The previous steps of tuning the ECU are considered open loop control. Open loop control utilizes the manifold pressure sensor, throttle position sensor, and intake air temperature sensors to determine which operating point on the tuned table to reference for the load value. No feedback from an oxygen sensor is used. All of the calibration settings needed to run the open loop configuration are shown in Figure 36.

CV_SSFLAM

CV_SSFLAM

Name	Value	Unit	Description
CV_SSFLAM	1.0000		"code variant, sensor signal POT "
CV_SSWO2	1.0000		"code variant, non-linear close-loop adaptations "
VAL_CDI_pulse_width	500.0000	us	"CDI trigger pulse width "
VAL_CKP_Pulse_Polarity	1.0000		"= 1 voltage high, =0; voltage low"
VAL_CylNum	1.0000	-	"Number of cylinders"
VAL_NidlDsr	1500.0000	RPM	"desired idle speed, LLD"
VAL_Nmax	8000.0000	Rpm	" max engine speed allowed "
VAL_nTeethMiss	1.0000		"number of missing tooth on the tooth-wheel, usually 1 or 2;"
VAL_nTeethTot	1.0000		"Total number of teeth on the tooth-wheel, including the missing tooth"
VAL_Qstat	79.9966	g/min	"Injector static flow rate, in g/min"

Figure 36: Advanced calibration menu set up for open loop configuration
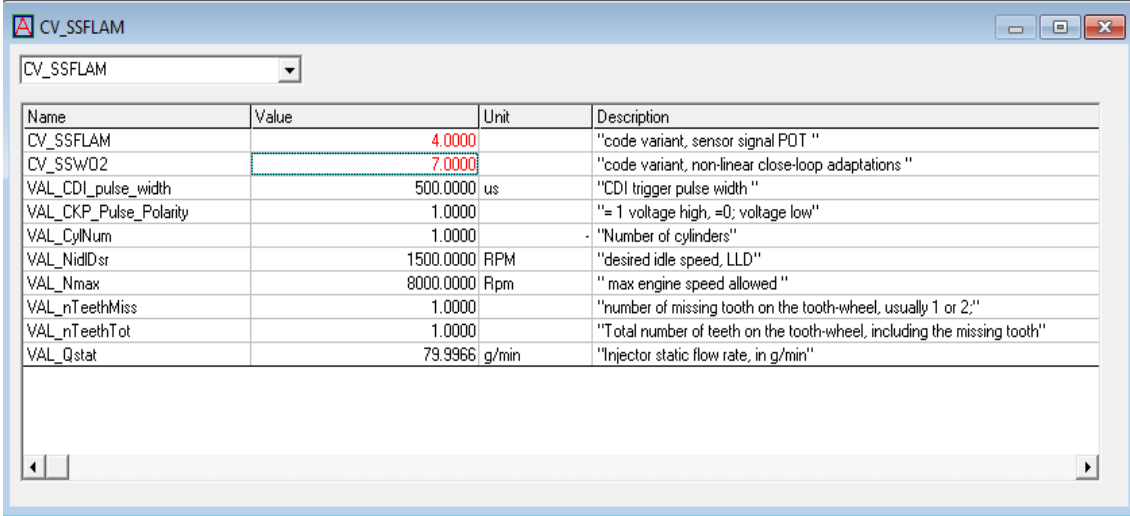
Once all 192 operating conditions of the table were tuned, the ECU can be put into the closed loop control which used readings from the manifold air pressure sensor to test for changes in pressure and the O_2 sensor to provide feedback to ECU regarding the air-to-fuel ratio. The final load values for all throttle positions and RPM settings are displayed in Table 5. The red values are the load values, x axis displays RPM intervals, and the y values represent throttle position intervals.

Table 5: Final TPS vs. RPM load values

	Y/X	2500	3000	3500	4000	4500	5000	5500	6000	6500	7000	7500	8000
	0	0	0	0	0	0	0	0	0	0	0	0	0
	3.9139	28.3125	28.3125	24.6797	22.6172	22.6172	20.8594	20.1797	18.4453	16.9688	16.6172	16.2422	15.8672
	6.5262	32.2969	32.2969	30.2813	26.1094	26.1094	25.5469	24.0469	22.6875	20.2969	20.2969	20.2969	19.2891
Y: Tps;	9.1324	40.8047	40.8047	34.9922	32.6016	32.6016	28.5469	28.9688	26.8594	25.3594	24.75	24.75	23.7422
[%]	13.0478	46.2422	42	42.4688	38.9297	38.9297	34.2891	32.625	19.9922	25.0078	25.0078	26.8594	26.1797
"throttle	16.9632	54.4688	42	42	44.3203	40.0078	34.9922	25.0078	19.9922	25.0078	25.0078	25.0078	25.0078
position	20.8786	45	42	42	42	40.9922	34.9922	25.0078	15	15	25.0078	25.0078	25.0078
with	24.7925	62.7422	42	42	40.9922	40.9922	34.9922	19.9922	15	15	19.9922	25.0078	30
respect	32.6172	64.4063	55.0078	49.9922	49.9922	49.9922	40.0078	43.0078	34.9922	34.0078	42	34.9922	34.9922
to lower	39.1449	64.9922	58.0078	52.9922	52.0078	49.9922	45	46.0078	55.0078	48	48	34.9922	34.9922
mechanic	45.6711	64.9922	64.9922	67.9922	60	55.0078	45	49.9922	49.9922	49.9922	40.0078	31.9922	34.9922
al stop"	52.1927	64.9922	70.0078	70.0078	67.9922	55.0078	48	52.0078	52.0078	52.0078	40.0078	34.9922	37.9922
	58.7158	64.9922	70.0078	70.0078	70.0078	64.9922	64.9922	64.9922	64.9922	64.9922	64.9922	60	60
	65.242	64.9922	75	75	78	85.0078	94.9922	79.9922	79.9922	79.9922	79.9922	70.0078	70.0078
	78.2898	64.9922	75	75	78	85.0078	90	90	90	90	85.0078	75	75
	99.9939	64.9922	75	75	78	85.0078	90	90	90	90	85.9922	75	75

X: N; [Rpm]   "Engine speed in Rpm"

Closed loop is enabled via two calibrations in the advanced calibrations menu. "CV_SSFLAM" is set from 1.0 to 4.0 and "CV_SSWO2" is set from 1.0 to 7.0. In practice, the tuning process would be accomplished by an experienced engineer prior to providing the aircraft to the end user who would not need to make any further adjustments in the field and the system could be operated without an oxygen sensor and in an open loop ECU configuration.

After the engine was running stably, the closed loop mode was enabled to allow the ECU to self-learn from the analogue output of the oxygen sensor. The ECU will adjust injector pulse width based upon how rich or lean the O_2 sensor was reading. The closed loop control was also known as fuzzy logic in other engine computers. All of the calibrations used to operate in closed loop operation are shown Figure 37.

Figure 37: Advanced calibration menu set up for closed loop configuration

With a properly tuned ECU, the fuel injection system was ready for the fuel injection test matrix.   Installation of the fuel injection system required significant modification to the test facility and its standard operating procedures. Operation has a

similar flow as with the carburetor, but there are some simplifications. Appendix D

includes the detailed operating procedures for the test facility with fuel injection. A

general flow of how to operate the stand starts with a detailed inspection of the engine

and all of its attached hardware. Once again, this step cannot be neglected as vibration is

still an issue for the test facility. After the inspection, the first step is to connect the

exhaust hose, dynamometer cooling water, shop air supply, 115VAC, and 480VAC. The

next step is to power on the lab computer, open the manual fuel isolation valve, and open

the cooling water supply valve.

The next step is to open FV-1 and power on the fuel pump via the 12VDC power

supply located next to the starter battery. The fuel pump is connected to be separately

powered via the power supply instead of being powered through the ECU as originally

configured from Ecotrons. It is important to open FV-1 (Figure 38) before turning on the

fuel pump as the pump uses the fuel to cool the motor and if run dry too long, the pump

can overheat and fail. Once fuel is flowing, the Magtrol Dynamometer controller can be

turned on via the black power switch, dynamometer brake enabled, and set to the starting

RPM of about 2,400 RPM. Less than 2,400 RPM is too slow for starting and faster than

3,000 RPM is just a little fast to start the engine. The RPM is set by pressing the "Set

Point Max Speed" button, turning the "increase/decrease" wheel until the RPM is

reached, press the "shift" button, and then the "max speed" button to lock in the RPM. If

the RPM is not locked in, small vibrations or a bump of the adjustment knob can change

the dynamometer operating condition and cause a faulty data point. Additionally, the

RPM can be changed by the tens, hundreds, or thousands place by using the "up/down"

buttons to move the cursor (20).

As before, the PID settings for the dynamometer did not change for fuel injection operation. The proportional gain was set to 20%, the integral gain to 20%, and the derivative to 1%. If engine variations became too great, the derivative was increased, but increasing the derivative gain caused the dynamometer to undershoot engine RPM. Undershooting just means the engine will run under what the set RPM indicates and therefore test points can be 200 or more RPM lower than intended. Settings are changed via the same manor explained in the carburetor section

After setting the dynamometer, the ignition was turned on, oxygen sensor turned on, supercharger powered on, ECU powered on, throttle set closed (0%), and the oil pump for the supercharger turned on. Once the oil pump reached above 35 psig, the supercharger RPM was increased from 0. If the test point included SLS conditions, the supercharger was set to a level of less than 50% on the LabVIEW VI or to an output pressure less than 16 pisa in order to prevent over current errors in the VFD. If the test point was at a lower pressure, the same steps as in the carburetor section were needed to lower the pressure of the altitude chamber. The last step before starting the engine was to open the coupler cooling air valve greater than 50% to cool the coupler. Attention was paid to the coupler while running the stand to monitor its conditions while running.

After turning on the cooling air the engine was started with a flick of the starter switch. Once the engine is running, the ECU will take the engine through a warm up cycle that is a gradual ramp down in fuel until the engine is running at 158°F. Once that temperature was reached, the engine will be running off of the program fuel maps and attention can be made to the AFR readings of the O_2 sensor. From here, the throttle can be advanced to the position necessary or the dynamometer RPM settings can be adjusted.

There are a couple of notes when running the facility. It is important to understand that running the engine at speeds greater than 6,000 RPM too long can cause engine temperatures to peak above 400°F and an effort should be made to keep temperature below that threshold. Test points always begin at 170°F and no lower in order to avoid testing while the ECU is adding extra fuel to the mixture. Beginning each test point at 170°F allows for a standardized process of collecting data that is the same across all tests as engine performance could change based upon engine temperature.

As well, the engine creates a lot of test stand vibration at speeds above 5,000 RPM, so watching for loose items becomes an important consideration while taking data. The vibration is a function of the engine having no flywheel to dampen the power stroke of the Brison and the engine being rigidly mounted to the test facility. The use of capacitive discharge ignition removed the need to use a magneto and flywheel on the engine, thus saving valuable weight on an aircraft. The drawback of removing the magneto flywheel is there is not a means to dampen the vibration from the engine. Often RC enthusiasts mount these engines on flexible engine mounts that allow the engine to move instead of transferring the motion to the aircraft frame. These mounts could not be used in testing because of the need to keep the engine ridged to maintain alignment of the couplers.

Once the test point is reached, data can be recorded via the LabVIEW VI. Typical test points were taken for roughly 10 seconds and the next test point is established since data acquisition is at 33Hz. For the same reasons as discussed in Section 3 of this chapter discussing the carburetor testing, the data was averaged over the 10 second test point and this is what is plotted in Chapter IV. Additionally, Pro-Cal has

the ability to monitor all of the fuel injection engine sensors, ECU parameters, and injector parameters. To take data with Pro-Cal, open the software on the computer, press the connect button so the software will connect via the serial connection, click on view, view list, and then click the green arrow which commands the software to view the variables in the list. Here, any of the variables the ECU uses to run can be watched. Some of the important ones to watch are the spark signal and the injector pulse width. Much more can be examined using this software as well as a built in oscilloscope to view the signals if troubleshooting is needed. Further investigation is left to the user to try via the Ecotrons' instruction and tuning manuals (25). Once the testing is completed, the previous steps should be done in opposite order.

Additionally, a new test facility diagram is included in Figure 38. This diagram shows the final configuration of the test stand after the necessary improvements were made to make the test stand functional as well as the addition of fuel injection of the fuel injection system.
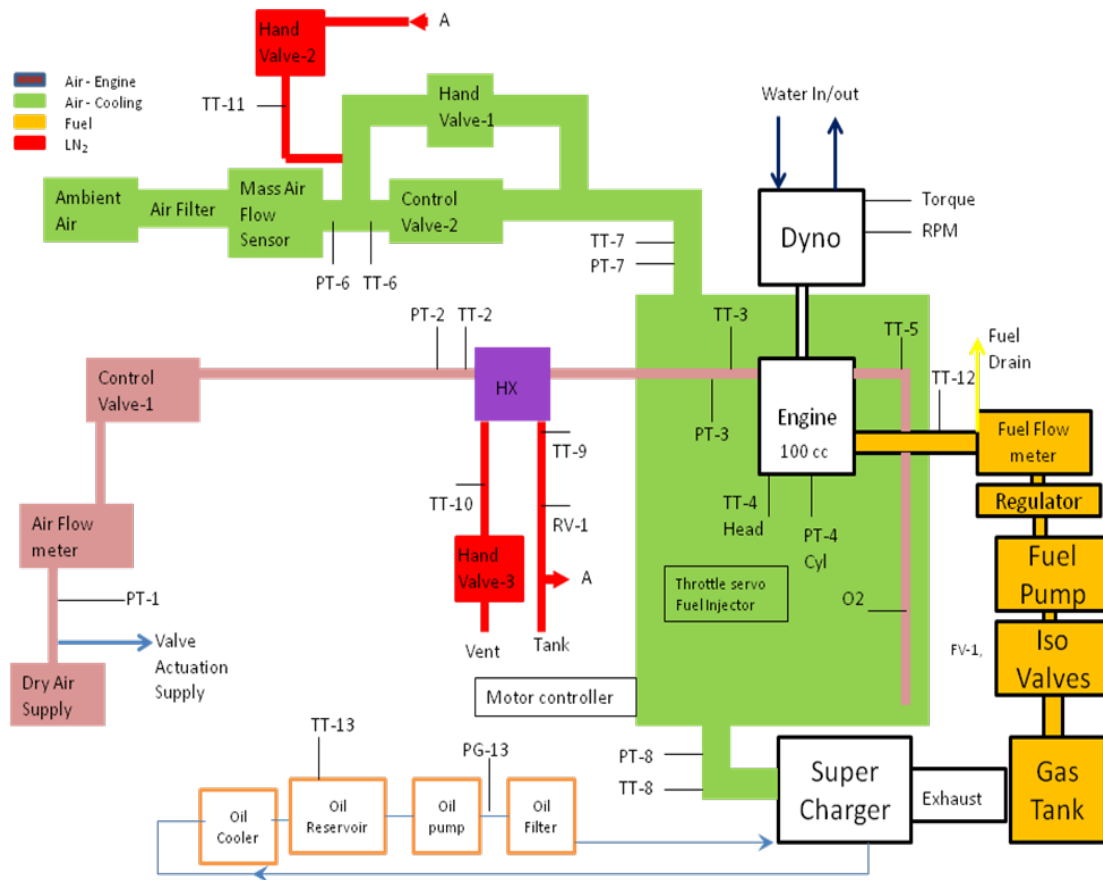
Figure 38: Final configuration of the test facility

The last study completed on the test facility before collecting data was an uncertainty analysis on power, BSFC, and BMEP. The same test condition used for the repeatability analysis was used for the uncertainty analysis and the test data as well as the component measurement uncertainties are shown in Table 6. The uncertainty analysis used was developed by Kline and McClintock and is shown in Equation 16 and the final uncertainty results are sown in

Table **7**. The uncertainty analysis gives insight to the variations seen in the test data presented in Chapter IV. Variations in HP, BSFC, and BMEP seen on the graphs that are

greater than these uncertainty values can be considered actual performance variations and not changes due to manifestation of error (27).

$$u_R = \left[\left(\frac{x_1}{R} \frac{\partial R}{\partial x_1} u_1 \right)^2 + \left(\frac{x_2}{R} \frac{\partial R}{\partial x_2} u_2 \right)^2 + \cdots + \left(\frac{x_n}{R} \frac{\partial R}{\partial x_n} u_n \right)^2 \right]^{1/2}$$

(16)

Table 6: Uncertainty Analysis Test Points and Component Values

Measurement Device	Uncertainty	Measured Value	Units
Torque (Dynamometer)	0.7% of reading	4.099921632	lb-Ft
Engine Speed	0.01% of reading	4037.727867	RPM
Fuel Flow Meter	0.2% of reading	0.664345351	cc/sec
Pressure	+/-0.5% of span	14.05785009	psi
Temperature	0.75% of full scale	55.20884972	°F

Table 7: Final Uncertainties

Uncertainties			% Uncertainty
Power	0.022066	HP	0.70%
BSFC	0.00878	lb/(hp-hr)	0.73%
BMEP	0.373	psi	0.70%
Temperature	3.9 to 17.1 deg F		9.06%
Pressure	0.15	psi	1.07%

IV.   Results

The original test facility supplied by Schmick (5) was not ready to take data as supplied. Section III.2 of this research was primarily focused on fixing the issues found with the facility in order to begin taking data on the test facility. After these issues were addressed, work on achieving the established goals of this research could commence.

The primary goals of this research are:

1. Upgrade the test facility so it is capable of taking reliable test data

2. Run the Brison 5.8 as it comes from the manufacturer to create baseline performance maps for the engine at SLS, 5,000 feet, 10,000, and 15,000 feet.

3. Convert the Brison 5.8 to fuel injection and test the engine at SLS, 5,000, 10,000, and 15,000 feet to see if performance gains were met

4. Map the final engine at 100%, 75%, and 50% throttle settings in order to size an appropriate propeller for the Brison 5.8.

IV.1 Results of the Modifications Completed to the Initial Test Facility

An initial set of experiments were performed to determine the limits of the facility to provide specific environmental conditions. The first test was run using only the compressor and control valves to vary the chamber pressure. Testing resulted in a minimum pressure of 8.21 psia or about 15,260 ft altitude. The fixes to the chamber validated the chamber pressure design and when combined with previous results indicates that testing of engines is possible with the current design up to 15,000 ft simulated altitude conditions. Additionally, temperature testing of the facility was needed to verify its new capability. This study established that the system could achieve temperatures

down to 13.0 °F while maintaining chamber pressures around 8.5 psia. The temperature

was maintained by injection LN_2 into the cooling air inlet stream while the compressor

was maintaining the chamber pressure at 8.5 psia. Figure 39 shows the limits of the

system as determined by the capability tests. The upper limits of pressure and

temperature are currently set by ambient conditions within the test lab which were

recorded at 65.0 °F and 14.8 psia.
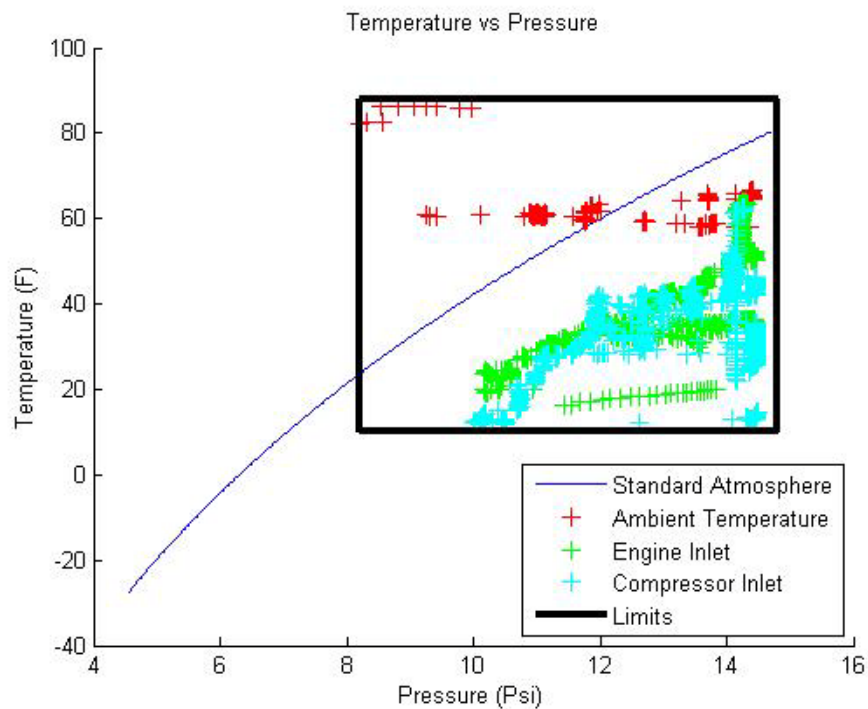
Figure 39: Chamber temperature versus chamber pressure for system limits testing

The intent of the first engine test was to run at sea level standard day conditions to

provide a baseline of performance against which the altitude data could be compared.

The major focus was to investigate the effect of a combined pressure and temperature

condition on engine performance. Although temperature conditions are an important

research objective, the new intake line was disconnected for these tests as it was

unknown if or how the intake system might adversely affect engine performance. Since there isn't any published data for this engine, it was important to have a true baseline of engine performance before any modifications were attached to the intake for altitude testing.

IV.2 Carburetor Results

As discussed earlier, first attempts to start the engine lead to numerous adjustments to the test facility. After the adjustments were made, initial test runs were completed at 100% throttle from 3,000 to 7,500 RPM. Figure 40 shows the results of the first runs of the engine at sea level static conditions. This graph shows the performance losses between ideal carburetor tuning and a fuel rich scenario. The fuel rich scenario just meant adjusting the high and low speed needles out an additional $1/8^{th}$ of a turn. The graph shows that the lower half of the RPM band (under 5,000 RPM) had a much lower (10%) power output in the rich AFR. The AFR is unknown at this point, but the misfiring of the engine was apparent.

The point of this testing was to understand how small changes in the carburetor tuning needles off of their ideal setting ($1/8^{th}$ in this case) can make large impacts in engine performance. The problem here lies in the ability of the user of the RPA in the field to adjust the carburetor to be at its idea settings. The ideal carburetor settings found in this research required the use of the dynamometer and fuel flow meter. The user in the field does not have these feedback mechanisms to determine the optimal tuning settings. The settings change based on ambient temperature, pressure, and manufacturing tolerances so specifying specific needle orientations is not possible either. Instead, the

user is more likely to not adjust the carburetor correctly and therefore will not see optimal

performance of the engine during flight. If the adjustments are made to be too rich, the

poor tuning will only compound on itself as the aircraft reaches higher altitudes where a

leaner mixture is necessary.
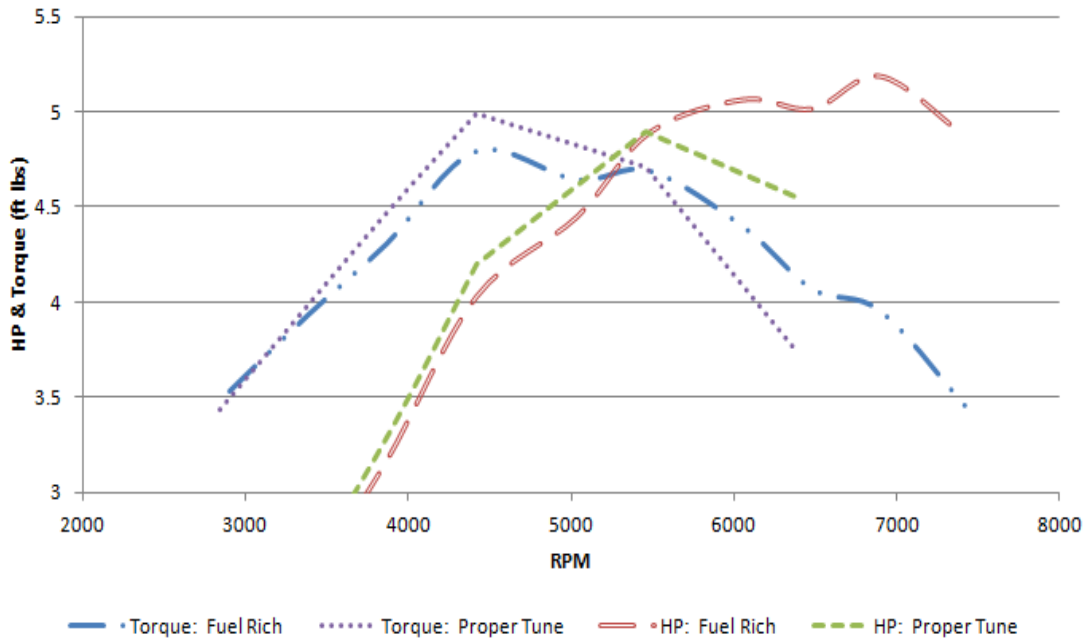
Figure 40: Results of studying the performance changes due to carburetor maladjustment

The problem with this data was that the rich tune actually produces more power at

the high RPM end of the test runs. This is inconsistent with the expected results.

Additionally, the test points were collected at 500 RPM increments, but the lines do not

show smooth transitions between test points. This lead to questioning the data produced

because the performance curves should be smooth in order to have predictable engine

performance. Sharp changes in engine performance indicates either a fuel, air, or ignition

problem in the system. Further investigation showed a significant amount of metal

shavings and debris caught inside of the carburetor. Several screens were full of metal

and it is anticipated that the partial clogging of the carburetor might have caused the unexpected performance characteristics of the engine. Additionally, the fact that the engine produced more power under what was expected to be rich AFR means the initial carburetor settings were still not ideal (lean in this case) and more tuning was needed.

Initial practices of finding the proper tune based upon engine sound was actually incorrect, an additional factor was introduced to tune the engine. After tuning the engine based upon sound, data was taken at SLS between 3,000 and 7,500 RPM and BSFC was calculated. If large spikes were observed or if a large increase of BSFC was measured, additional carburetor adjustments were required. The point of this test was to create smooth BSFC curves.

After cleaning the carburetor and working to properly tune the carburetor, additional test data shows more anomalies. The first sets of criteria in analyzing the test data is to look for any trends that are not expected or their standard of deviation was too high. Figure 41 shows the incorrect BSFC versus engine RPM for these tests. To the untrained eye, these results look great with the lowest BSFC being around 0.45 lb/(hp-hr). Unfortunately, when something is "too good to be true" it often is. Two-stroke engines are characteristically higher in BSFC than four stroke engines, but this graph alludes to the Brison being just as fuel efficient as some modern day fuel injected engines. The combination of these facts led to investigation of the fuel metering system on the test facility. As described in Chapter 3, the fuel metering was discovered to be incorrect and once corrected, the data looked more realistic to comparable engine test data.
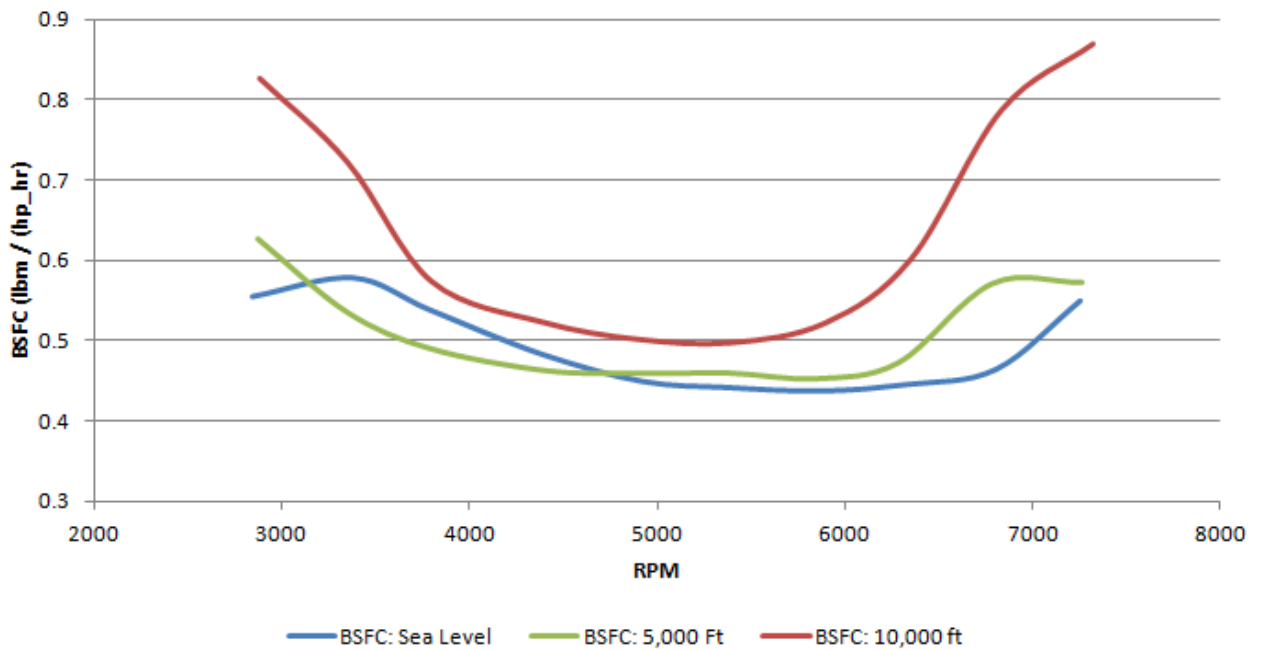
Figure 41: Initial BSFC

As discussed in Chapter 3, some limited test data was run with the inlet manifold intact. Running with the manifold provided to be very difficult as discussed and eventually the manifold was discarded because of the performance impacts, extreme difficulty of taking data, destroying the rubber fuel pump diaphragm in the carburetor, and finally the carburetor's inability to operate with an inlet pressure different from ambient pressure. The data is displayed in Figure 42 and it is easy to see the manifold was adversely impacting engine performance. From this point on, metering the intake air was scrapped until a new manifold design can be made that does not affect the engine performance.
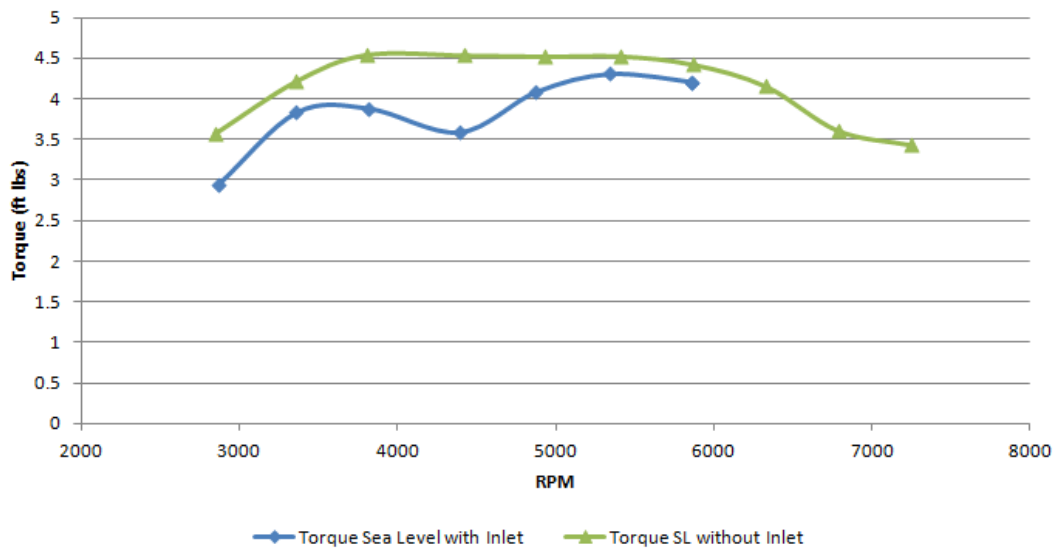
Figure 42: Torque values with the inlet manifold was attached to the carburetor

The final data collected belongs in two groups. The first set of data collected involves HP, BMEP, and BSFC versus rpm for three different altitudes. Table 8 shows the test matrix for these tests and does not include 15,000 feet as a test point. The reason why 15,000 feet is not tested for the duration of this research is previous testing above showed that the engine will not run on a SLS carburetor tune at 15,000 feet. Data showed that running at 10,000 feet was difficult and when the altitude chamber was brought to 15,000 foot pressure conditions, the engine would die during the transition to the altitude. Lastly, the carburetor data represents the baseline data for the engine as it comes from the manufacturer. As discussed in Chapter III, each test point of the test matrix had roughly 10 seconds of data recorded in a steady state configuration. The data was averaged and the standard deviation for each test point was calculated in order to calculate the coefficient of variation used later in this chapter. With the help of Matt Rippl, a Matlab code was established that inputs each of the data files from LabVIEW

and completes the averaging and standard deviation calculations. The code is listed in
Appendix E.

Table 8: Brison carburetor test matrix

| **SLS carburetor tune at local conditions (14.3pisa)** |
| Local: 100% throttle 3,000-7,500 rpm, 14.3psia |
| 5K AGL: 100% throttle 3,000-7,500 rpm, 12.2 psia |
| 10kAGL: 100% throttle, 3000-7,000 rpm, 10.1 psia |
| **Engine tuned optimized for each altitude (~1/8th turn)** |
| Local: 100% throttle 3,000-7,500 rpm, 14.3 psia |
| 5K AGL: 100% throttle 3,000-7,500 rpm, 12.2 psia |
| 10kAGL: 100% throttle, 3000-7,000 rpm, 10.1 psia |

Figure 43shows the horsepower versus speed curves for the carbureted test matrix
using an optimized tuning strategy. The carburetor in these conditions was tuned for
each operating altitude. Essentially, the carburetor was tuned for each 5,000 foot increase
in altitude. The adjustment was a 1/8th of a turn in for both the low speed and high speed
needles. It is important to note that for these cases, the engine was leaned for the
operational altitude; therefore, it would not run at the ground altitude. An operator
cannot lean the engine for a known high altitude condition and expect the engine to
perform at SLS. The engine will not operate at SLS when the carburetor is preemptively
leaned to compensate for altitude. When attempts were made to run the engine in this
lean condition, the engine surged violently and was unable to sustain operation. To
simulate the operational altitude in the rig the altitude chamber was brought to the test
altitude and then the engine was started. This strategy represented an RPA operator
tuning the engine in the field as takeoff altitude increases from the home station tune. It
is important to note that if the RPA was going to be used 5,000 feet or more above the

takeoff altitude that the carburetor cannot be tuned for those operating altitudes as the

surging from a lean condition will not allow for adequate takeoff performance.
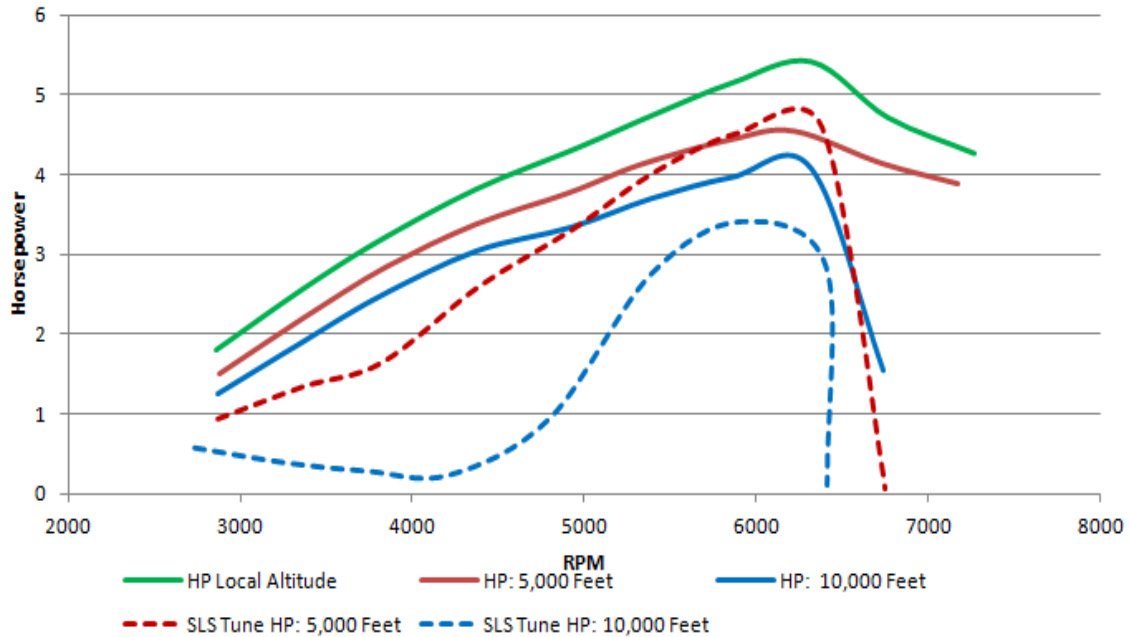
Figure 43: Power curves for SLS tuned and optimally tuned carburetor

Figure 44shows engine performance with a standard sea level static (SLS)

carburetor tune and the optimized tune. This stock SLS tuning strategy represents the

engine manufacturer or RPA user tuning the engine at the home base and then taking the

aircraft to a different altitude in the field for use. In many cases, the RPA manufacturers

do not allow adjustment to the carburetors after manufacturer testing and this tuning

strategy would represent engine performance in that situation. The strategy also

represents the effects of altitude if the RPA is actually flown from close to sea level to

10,000 feet without the ability to adjust fuel metering in flight. Lastly, if the RPA user

has little experience with the platform and lacks the understanding needed to tune the

engine at all, this is the kind of performance one could expect if the user makes no

changes to the carburetor. It is important to note that the 10,000 foot altitude run shows a range of 3,000-4,500 rpm where the engine was effectively struggling to run. At the 4,000 RPM point comparing 10,000 feet operating altitudes there is a 91% reduction in available engine power if the carburetor is left at the SLS tune condition. This means, if the user attempts to perform a takeoff maneuver while the engine was operating in this extreme rich condition, one could expect almost certain aircraft power plant failure.

Figure 44 represents the brake specific fuel consumption versus engine RPM for all three operating altitudes. Figure 44 also represents the optimized carburetor tune. The figure shows that roughly 6,200 RPM is the most efficient operating point for the engine and this RPM should be used to find an appropriate propeller size and shape that generates power at this RPM.   However, there is an increase in BSFC when using the stock SLS tune at high altitudes and this is apparent in Figure 44 Having an optimal tune for all altitudes actually causes the BSFC's to stay consistent among all flying altitudes.
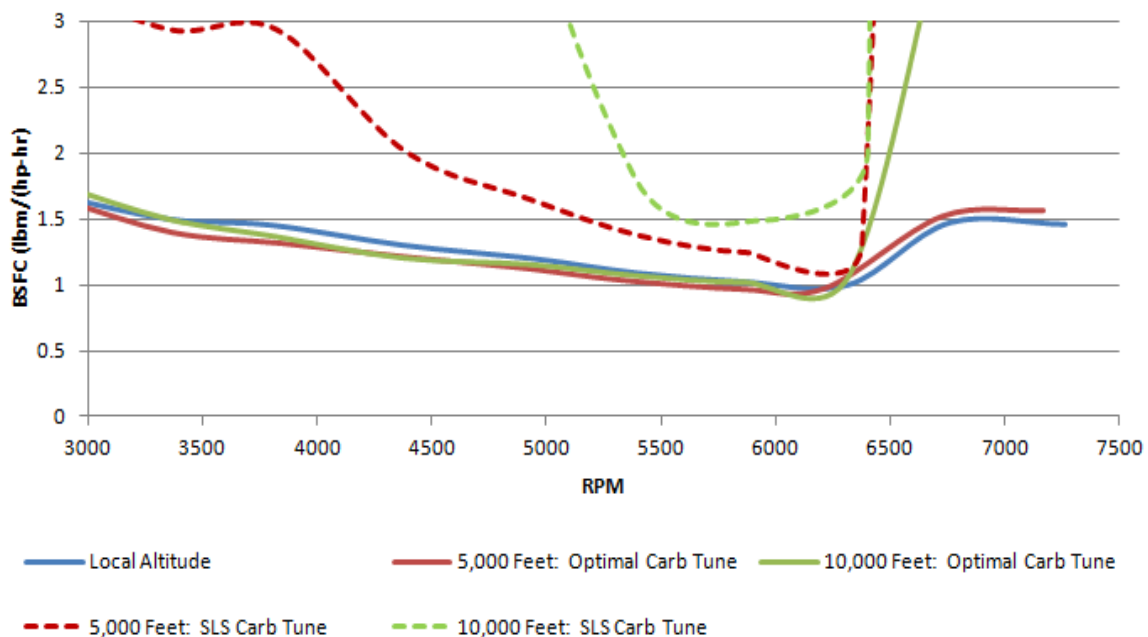
Figure 44: BSFC Optimized Tuning with Carburetor and SLS tuning

BMEP is the work per cycle divided by the cylinder volume displaced per cycle. (6). BMEP allows engineers to compare engine designs with other well established engines of different sizes. Taylor (16) gives several relationships of how BMEP changes with respect to pressure and temperature and this was shown in Figure 12. Taylor's experimental data shows that for small engines, BMEP decreases to 72% of SLS BEMP at 10,000 feet altitude and 82% at 5,000 feet altitude and this published data trends very close to what was observed for the Brison. When the air-to-fuel ratio was held closer to constant (solid lines) the reduction of BMEP with altitude was proportional to the change of pressure. When the fuel was allowed to flow at a constant flow rate regardless of altitude, BMEP is reduced and erratic. The last thing to understand based on all of the carburetor figures is the condition shown as the optimized tuning of the carburetor is unrealistic performance data for the end user. This tuning strategy took weeks to accomplish and requires the test facility to accomplish. The tunes optimized for altitude will not run at SLS conditions. The reason that the optimized tune is not a realistic comparison model is not due to the user's lack of knowledge, but instead a lack of appropriate feedback equipment to determine the optimal tune. As said before, BSFC data along with sound were used to tune this engine. In order to create BSFC data, a dynamometer and a fuel flow meter are required pieces of hardware that the user does not have. Therefore expecting engine performance to look like the optimal tuned data is unrealistic. The stock SLS tuning conditions that are displayed as the dashed lines are more realistic to what a user would experience.
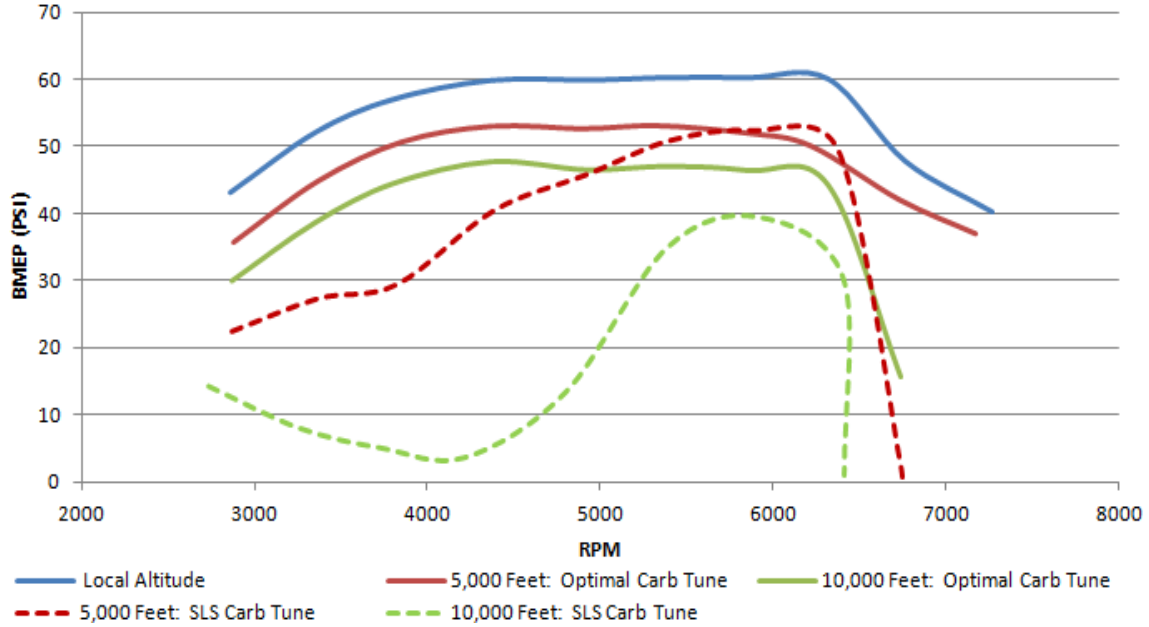
Figure 45: BMEP with optimized and SLS carburetor tuning

The last metric to look at for the carbureted data is the coefficient of variation for the BMEP. The coefficient of variation (COV) gives insight into the repeatability of each combustion event. The higher the COV percentage, the less repeatable the combustion event and the source of the lack of repeatability in these tests is most likely the engine misfiring due to the engine reaching the rich misfire limits (AFR>9). Figure 46 shows the COV data for the SLS tune since the SLS tune is what is most likely going to be seen in the field. The red and green lines show large variations in engine performance and allude to the lack of combustion repeatability for the 5,000 and 10,000 foot flight conditions. The lack of repeatability for the combustion events is one of the primary motivators for installing fuel injection on the Brison 5.8.
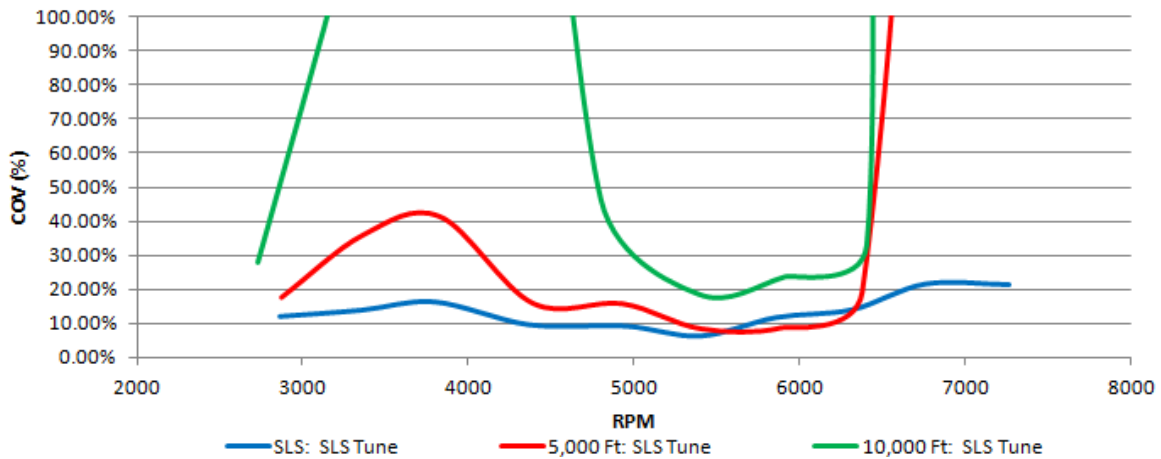
Figure 46: SLS Tuned COV of BMEP for the carburetor

IV.3 Throttle Body Injection Results

The next set of data collected involves the installed throttle body fuel injection system. The tests were run in the same manner as the carbureted runs except there was no need to tune the engine for each operating condition. Table 9 includes the test points for the fuel injected engine and this table also does not include 15,000 foot flight conditions. The reason for this was the carburetor did not run at 15,000 feet and therefore the decision was made to forgo testing at 15,000 feet since there was not any data to compare to. That that being said, there is no reason why the TBI system could not run at 15,000 feet since it automatically corrects for changes in ambient pressure. Lastly, all of these tests were all performed at ambient temperatures in open loop configuration.

Table 9: Throttle Body Injected Test Matrix

SLS: 100% throttle 3,000-7,500 rpm, 14.3psia
SLS: 75% throttle 3,000-7,500 rpm, 14.3psia
SLS: 50% throttle 3,000-7,500 rpm, 14.3psia
5K AGL: 100% throttle 3,000-7,500 rpm, 12.2 psia
5K AGL: 75% throttle 3,000-7,500 rpm, 12.2 psia
5K AGL: 50% throttle 3,000-7,500 rpm, 12.2 psia
10kAGL: 100% throttle, 3000-7,000 rpm, 10.1 psia
10kAGL: 75% throttle, 3000-7,000 rpm, 10.1 psia
10kAGL: 50% throttle, 3000-7,000 rpm, 10.1 psia

The ECU has an altitude correction factor it used for reducing injector pulse width as the manifold pressure sensor indicated an overall decrease in intake pressure. Closed loop control would also use the feedback from the oxygen sensor to determine if the mixture was too rich or too lean. Initial testing found that using closed loop for an aircraft that is going to dynamically change altitudes at magnitudes of thousands of feet within minutes is not the best strategy. When taking data at altitude, the closed loop would end up leaning the fuel table to accommodate a stoichiometric ratio while operating, but as soon as the engine was brought back down to SLS conditions, the new table developed at altitude would have adjustments that caused the fuel mixture to be too lean. Operationally, a fuel table too lean will cause engine damage, lack of power, and decreased reliability upon landing and this would be the opposite effect this research is trying to achieve. Therefore, once the fuel table was tuned, the open loop configuration was enabled and the oxygen sensor was only used as a reference to observe the AFR while taking data.

The dashed lines in Figure 12 indicate horsepower for the carburetor in the SLS tuned condition. The solid dotted lines indicate the new horsepower data for the TBI

system. Readily apparent from this data was that the fuel injection system was able to

match the performance achieved from the optimally tuned carburetor data in Figure 47.

Matching this performance proved to be extremely difficult. Tuning the fuel mapping for

the fuel injection system requires many iterations of running the engine at specific

throttle settings and engine speeds while watching the oxygen sensor and is the most

labor intensive aspect of converting the Brison to fuel injection. If the O_2 sensor reads

low, then the load value in the fuel mapping tables needed to be lowered and the opposite

was true if the oxygen sensor read lean. This took much manual iteration for each of the

192 operating conditions in order to get the engine to settle on a specific AFR.

Matching optimal carburetor performance really means the TBI system is able to recover

the 91% power loss at 10,000 ft without any user adjustment. This indicates that optimum

performance could be achieved without the need to retune the engine over the entire

flight envelope. In fact the user can be removed from this process completely. This

highlights that carburetor training for the end user can also be eliminated. The data

highlights that the aircraft can have more repeatable and reliable performance

characteristics all while reducing the responsibility of the user.
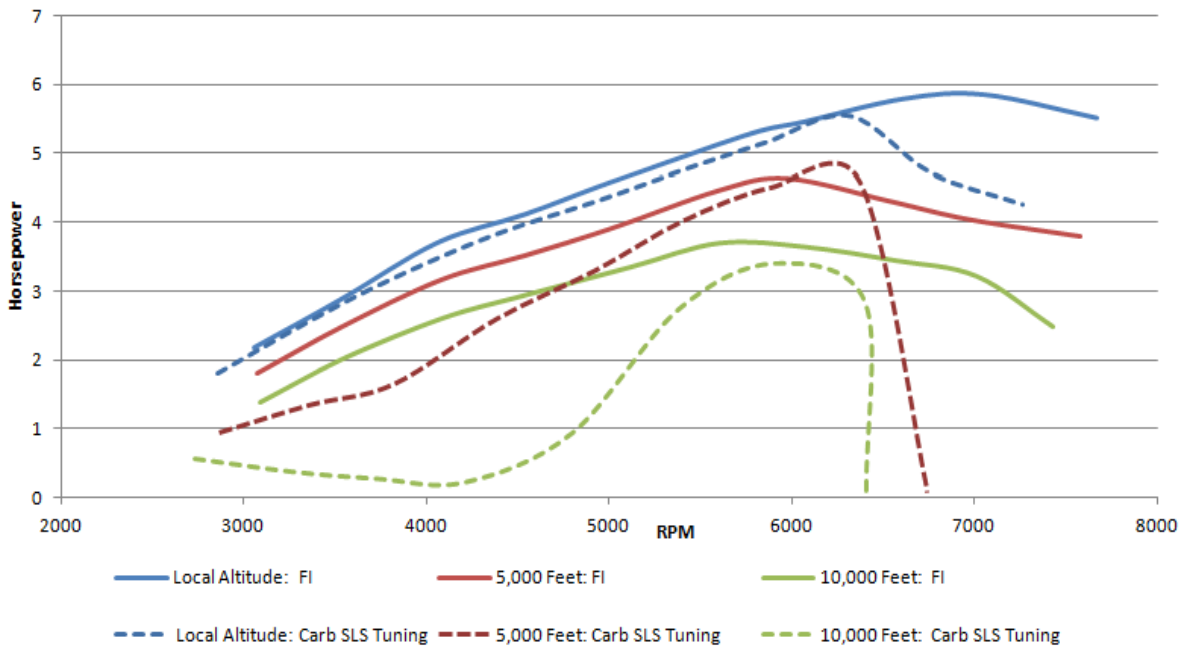
Figure 47: HP Curves at altitudes comparing TBI vs. Carburetor

Figure 48 provides a representation of the brake specific fuel consumption of the engine for both the carburetor and the TBI system. Figure 48 clearly shows that the TBI system was able to match the carburetor's lowest BSFC, but the ability to tune for the air-to-fuel ratio for lower fuel consumption in the outside extremes of the graph allows for decreased BSFC. Two-stroke engines suffer from a condition called short circuiting as discussed in Chapter II. Short circuiting is the condition where some fresh air mixture was wasted through the exhaust port. This occurs because in a two-stroke engine, the intake and exhaust ports are open at the same time. Blair shows several figures where BSFC was at its highest in the low rpm region and quickly ramps down due to its minimum at peak powers. This phenomenon was likely due to short circuiting, but can also be sourced from the carburetor's inability to closely measure fuel flow rates in all conditions, and fixed exhaust port tuning. TBI was unable to fix short circuiting, but the

ability to lean the mixture at low RPM operations where cylinder head temperatures are less of an issue allowed for lower BSFC. Both the low and high RPM extremes show a reduction in BSFC of greater than 100% when looking at the 10,000 foot altitude condition. Reducing BSFC allows for longer flight times on the same charge of fuel and increasing flight times by as little as 20% is a substantial increase in mission capability. In many cases when looking at Figure 48, flight endurance at RPMs other than 6,000 RPM could be more than doubled since BSFC is less than half of what was observed with the carburetor.
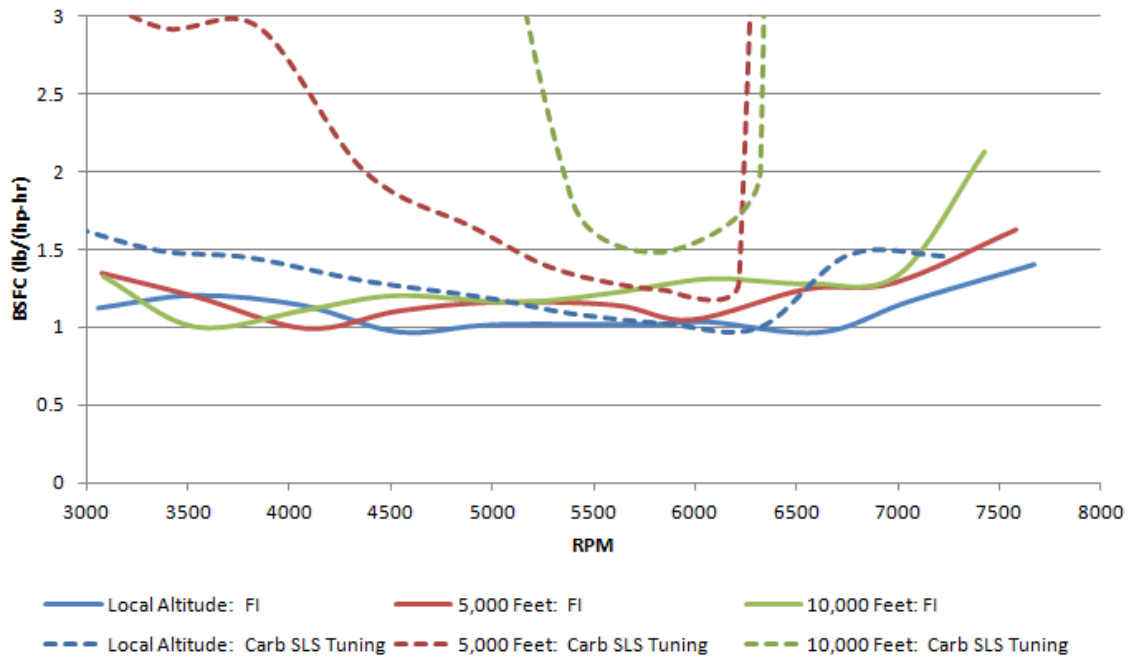
Figure 48: BSFC curves at altitudes comparing TBI vs. carburetor

Additionally, Figure 48 shows a more consistent BSFC performance with TBI than with the carburetor. The flat BSFC performance across 3,500-6,500 RPM was due to the ability to tune the engine at each operating condition versus only having a high and low speed needle to tune on the carburetor. Air-to-fuel ratios were tuned to approximately 13.1 as a compromise between tuning for peak power and tuning for best

BSFC. If peak power was desired, an AFR of 12.5 should be used while low BSFC is reached by tuning for an AFR of 15.5. Tuning to AFR readings of greater than 14.5 caused rapid heating of the cylinder head and managing head temperatures to less than 350°F became difficult. The choice to compromise between peak power and low BSFC while maintaining a manageable engine temperature lead to choosing an AFR of 13.

Figure 49 displays the BMEP of all three altitudes and both fueling strategies. The main objective of this figure was to show that the fuel injection was able to match the optimized tuned carburetor case while also extending engine performance slightly past what the carburetor was able to handle at high rpm conditions. It was important to understand that several weeks of dynamometer testing was accomplished to get the carburetor tuned properly for each test altitude. The user of the aircraft will never have the time or the dynamometer resources necessary to tune the carburetor to match these conditions. A more realistic expectation will be the Fixed SLS Tune setting shown in the dashed lines. Comparing this case to the TBI curves reveals a significant improvement in performance. Achieving this condition does necessitate a tuning process for the engine. However, this can be accomplished prior to the aircraft reaching the field. No further adjustments or time will be needed by the end user once the aircraft is on station.
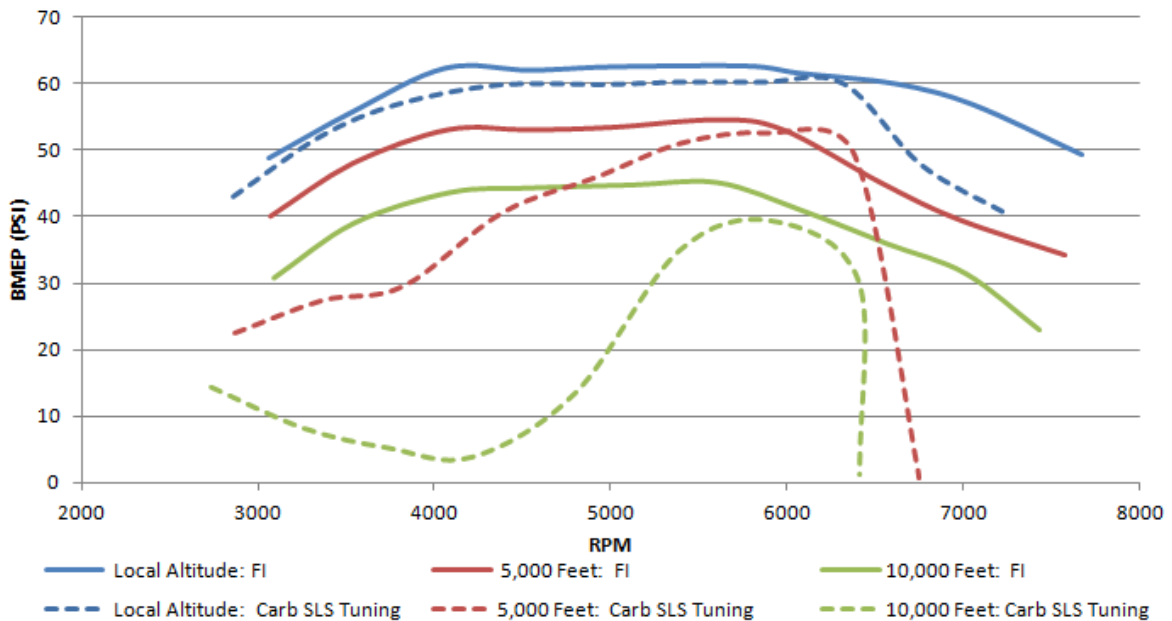
Figure 49: BMEP curves at altitudes comparing TBI vs. carburetor

A common complaint regarding carbureted engines is cold starting. With the carburetor, starting the engine when it was cold often took several attempts while constantly adjusting both the choke and throttle to get the engine to fire. Failure to start with the carburetor is a significant problem that can be frustrating to the operator since flooding often requires spark plug removal. Sometimes, these RPAs only have one opportunity to start due to mission requirements. If the engine fails to start due to flooding, the RPA is deemed a failure. The TBI system eliminates startup concerns. The system is calibrated to automatically enrich the fuel mixture when the engine is cold and reliable starting on the first try is consistent with the TBI setup.   Now, the operator can start the engine at any operating altitude with no concern for the fueling system.

IV.4 Performance Investigation of the Brison 5.8

To complete the understanding of the Brison 5.8, several investigations were accomplished. These studies were obviously specific to the Brison, but the same studies

are used across major IC engine laboratories to qualify engine performance. Additionally, this process gives a potential roadmap for the Air Force to use in obtaining performance metrics on Group 1 and 2 RPA engines that allow for proper propeller selection.

1. Repeatability of the combustion event by analyzing coefficient of variation (COV) for BMEP.

2. What AFR does the engine produce lowest BSFC and highest BMEP.

3. Partial throttle performance of the engine as well as a sensitivity analysis to determine how changes in throttle affect engine performance.

4. Match available COTS propeller performance data with Brison 5.8 for best cruise fuel consumption and rate of climb (ROC)

IV.4.1 Repeatability Investigation using BMEP COV

After determining that the TBI system was working properly and that it does increase the operating envelope of the engine, some repeatability analysis was completed comparing the coefficient of variation for BMEP of the carbureted engine versus the fuel injected engine. COV of BMEP is used because it indicates how repeatable each power stroke is compared to the average power created. If large variations are found, that means that the combustion event is not consistent while a low COV implies that each combustion event is similar to the last. Figure 50 shows the TBI system averages much lower COVs when comparing high altitude flight conditions. The dashed curves represent the fuel injected data while all solid lines reference a SLS tuned carburetor. For conditions at 5,000 feet, 100% throttle, the average COV is 35% less for the TBI system

than for the carbureted system. Another interesting piece of information is the overall

increase in COV after 6,000 RPM. This proves that loop scavenged engines, like the

Brison 5.8, have poor scavenging efficiency at high RPM as the engine is not

experiencing repeatable combustion events like it was at 5,000 RPM. The COV shows

that the combustion event is less repeatable implying that the engine might be misfiring

more often at these speeds. If emissions data were taken at these RPMs, higher exhaust

emissions would be expected in this region.
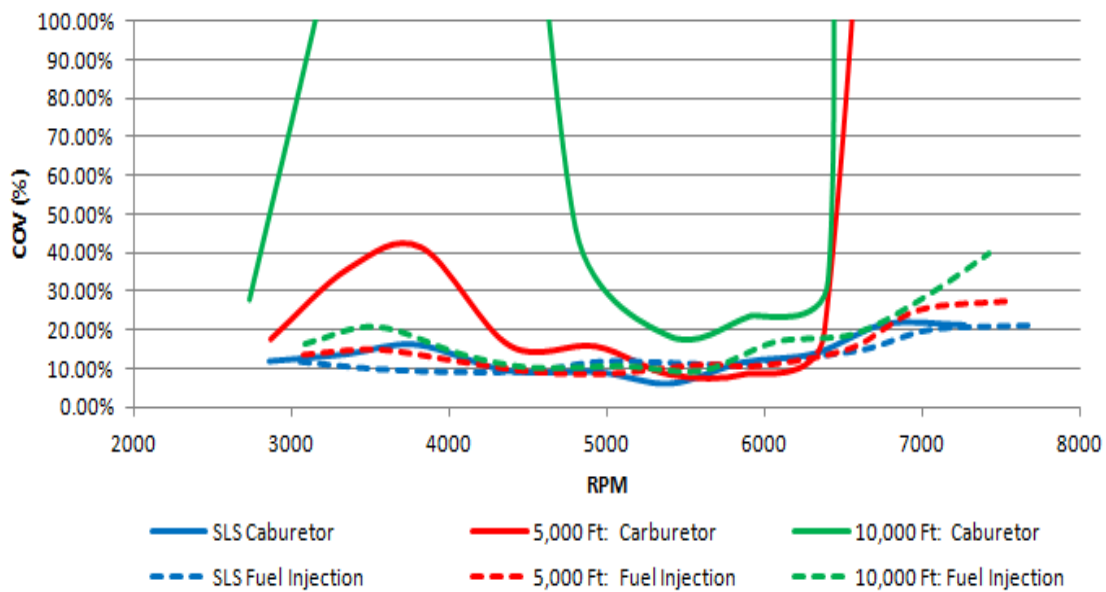
Figure 50: COV comparison showing TBI provides consistently lower COV across all engine operating conditions

IV.4.2 Throttle Sensitivity Study

The next study was performed using the TBI equipped Brison. The engine was

set to a constant 4,000 RPM, SLS conditions, and the throttle was varied from 100% to

5% in 5% intervals using the throttle position sensor output in ProCal. The data shown in

Figure 51 shows that peak BMEP drops after 90% throttle, but power output after that

drop stays fairly constant until about 30%. After 30%, power drops off rapidly. COV

was calculated (Figure 52) at these operating points as well and shows that at 4,000 RPM,

COV is around 14% until the throttle is less than 30%.
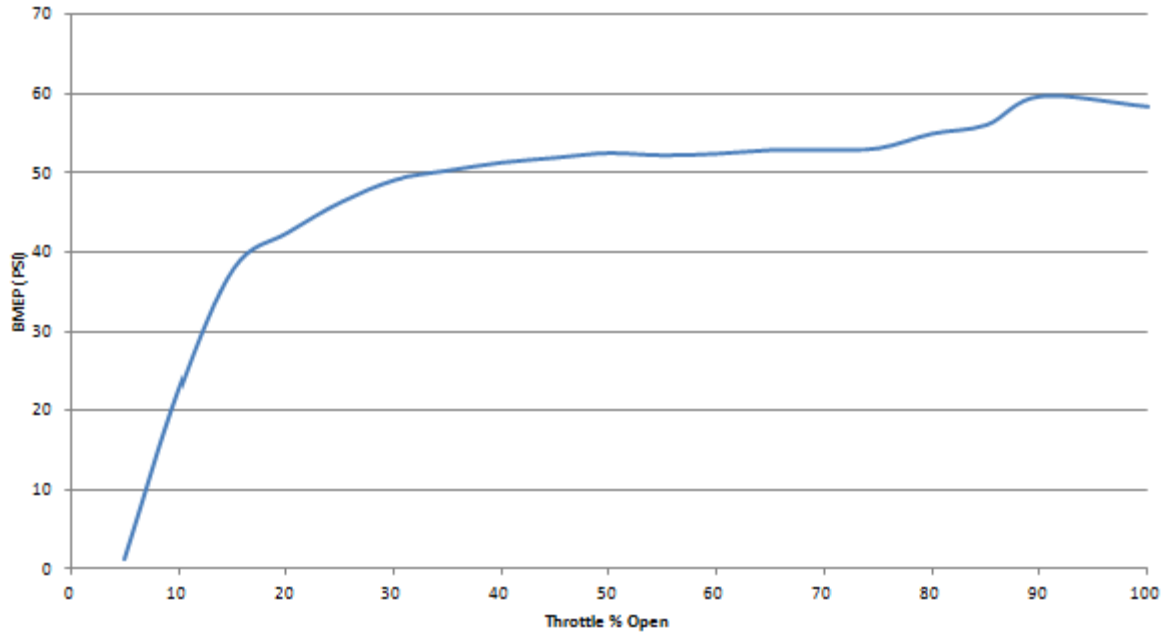
Figure 51: BMEP for different throttle positions at 4,000 RPM SLS (left)
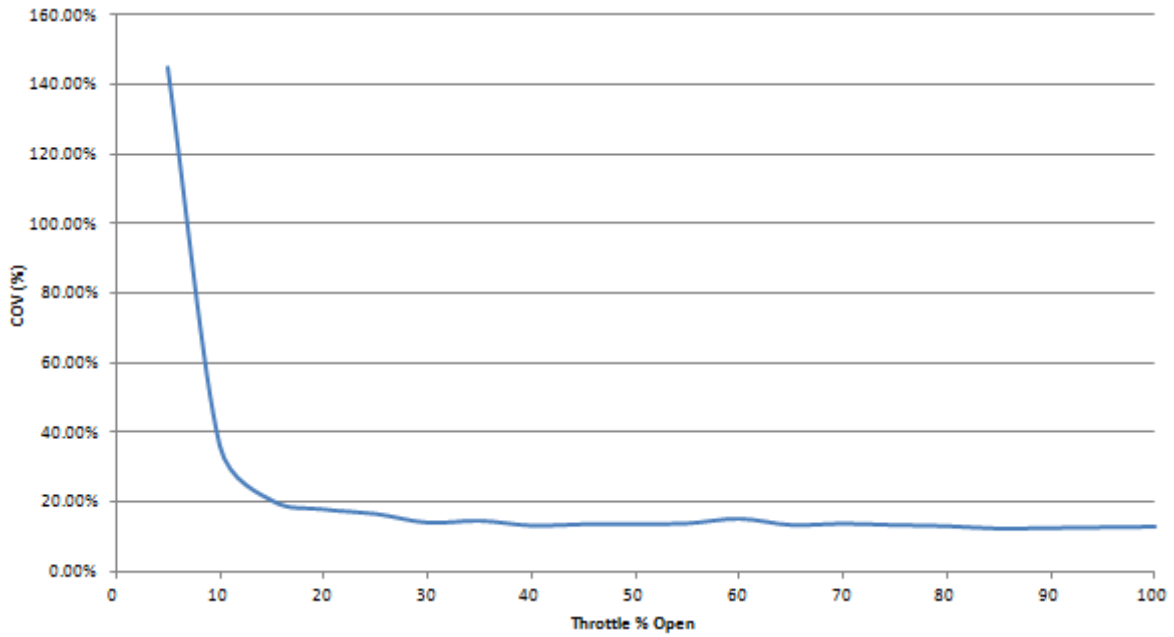
Figure 52: COV BMEP for the same throttle position test (right)

IV.4.3 *Test Stand Repeatability Over Time*

The next study took the same 4,000 RPM test condition and ran the engine for 5 minutes. Data was recorded for 10 seconds at a time every 30 seconds. This study was completed to investigate the repeatability of engine performance over time. Figure 53 shows that BMEP stays at around 53 psi for the duration of the test. This data gives insight towards the repeatability of testing completed with the test facility.
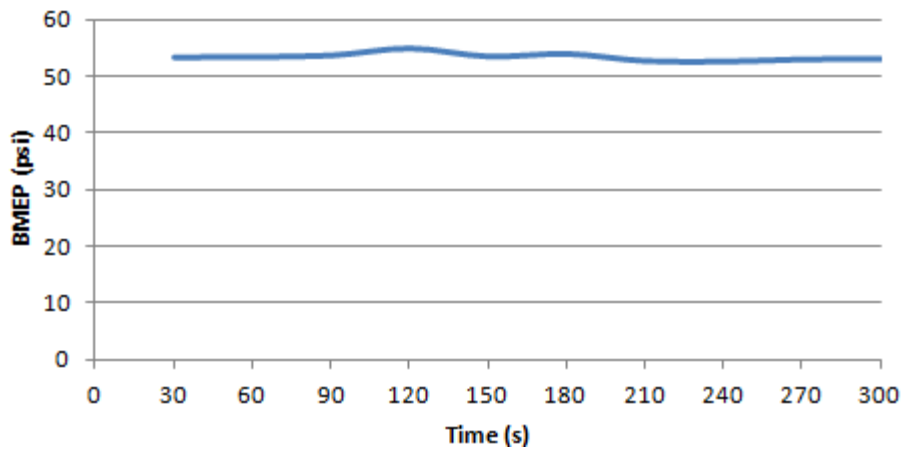
Figure 53: BMEP variation for 4,000 RPM over 5 minutes

IV.4.4 Partial Throttle Performance Testing

Now that repeatability for engine performance is established, a partial throttle test was completed for throttle settings of 75%, 50%, and 25% at SLS conditions. This test is unlike the sensitivity study as this test maps the entire engine operating range at the partial throttle settings. The test was completed in the same manner as the 100% throttle tests except the throttle position was reduced to a set position and left there for the duration of the test. Figure 54 represents the available engine power and Figure 55 shows the BSFC for these operating conditions. The figures show that the available power difference between 100% throttle and 75% throttle is negligible and there is good reason for this. When selecting the fuel injection system, a 28mm diameter throttle body was selected as it was the closest size available that compared to the 21mm diameter carburetor. Since the throttle body was oversized, engine performance difference between 100% and 75% throttle was not expected. However, 50% and 25% throttle show appreciable performance difference and these throttle settings represent what an operator

129

would use for a best cruise scenario when the aircraft is trying to maximize flight endurance.
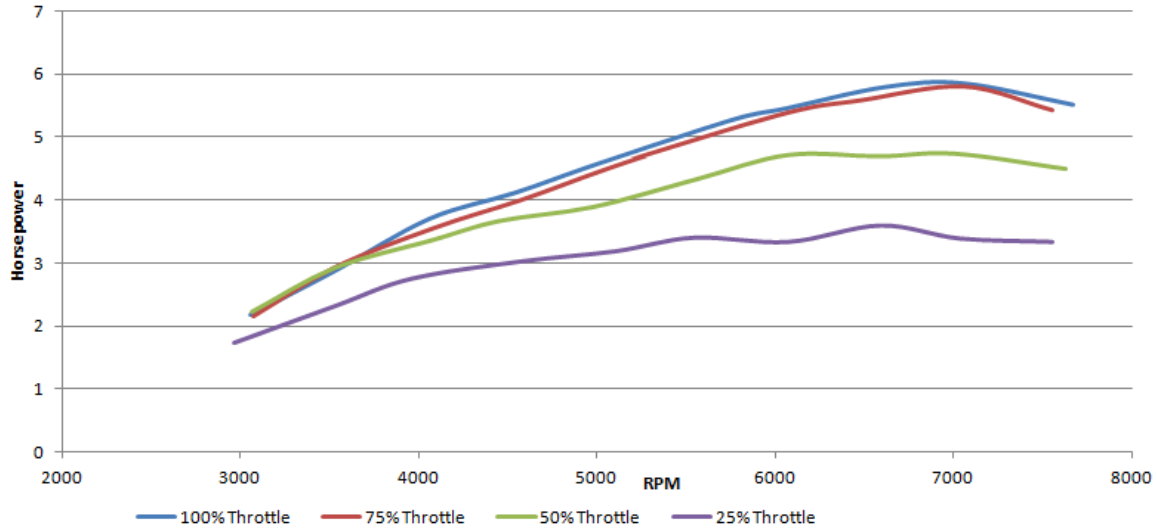
Figure 54: 100%, 75%, 50%, and 25% throttle position power output at SLS conditions

The BSFC for the most part hovers closer to 1.0 lb/(hp-hr) when testing for partial throttle performance. This could be due to many factors including scavenging efficiency, trapping efficiency changes, and the values used in the fuel mapping tables. More time could be spent tuning the partial throttle portion of the tables in order to maximize fuel efficiency at these throttle settings to an optimal AFR that might not be 13.1. The data in Figure 55 does show that the 25% throttle position does use about 15% less fuel than the 100% throttle positions while producing 66% of the maximum power available at 100% throttle. The BSFC data is useful when comparing propeller performance maps for best cruise endurance.
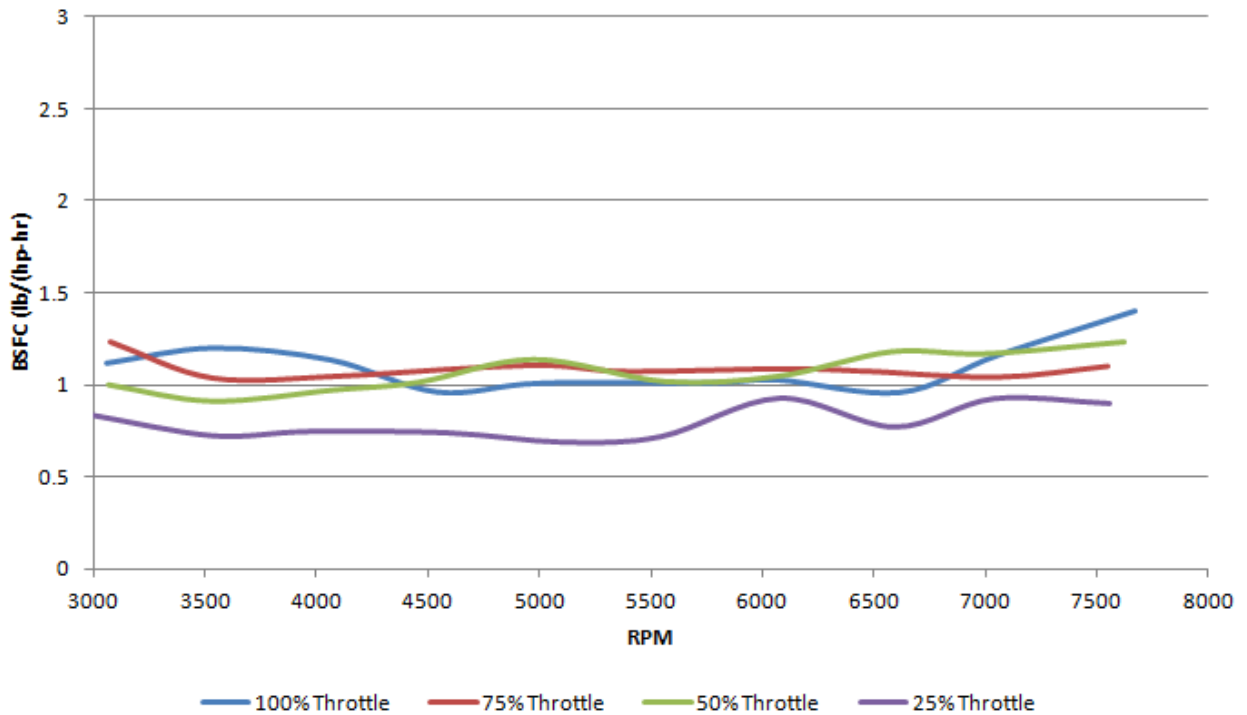
Figure 55: BSFC for 100%, 75%, 50%, and 25% throttle positions at SLS

IV.4.5 Establishing Optimum AFR for best BSFC and BMEP

The last study investigates BSFC and BEMP as a function of changes in AFR. Blair stated in his book that generally speaking beast BSFC occurs at around an AFR of 15.1 and peak BMEP at an AFR of 12.2 (7). The investigation for the Brison is shown in Figure 56 and Figure 57. The data shows that the Brison behaves as Blair describes where peak BMEP occurs at around an AFR of 11.8 while BSFC continued to fall as AFR reached 17. Higher AFRs were not studied as COVs begin to increase beyond a reliable figure and the usable power the engine makes begins to dwindle.
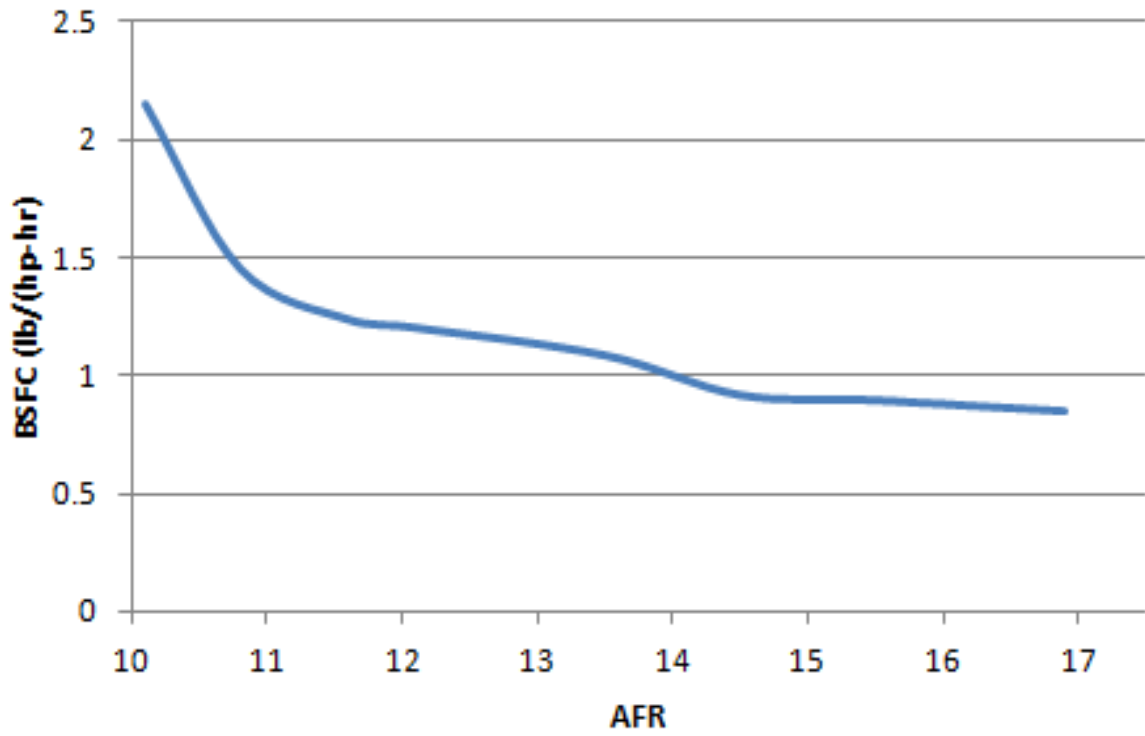
Figure 56:   BSFC test data when changing AFR at 4,000 RPM SLS
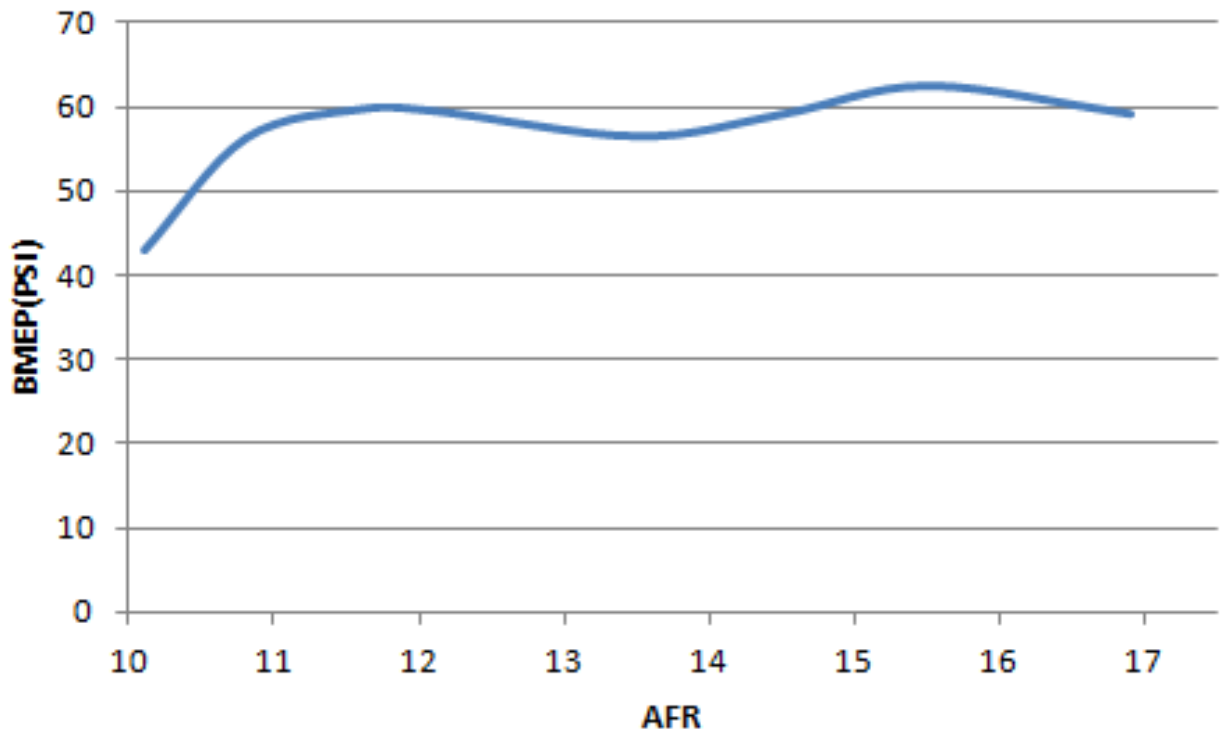
Figure 57: BMEP values for changing AFR at 4,000 RPM SLS

IV.4.6 Utilizing Engine Performance Metrics to Establish Potential Propellers

One of the benefits of having engine performance data that outlines BSFC, available torque, and available power is the data can be paired with published propeller performance data to help chose the right propeller for a given aircraft. Performance data for COTS propellers was established by Baranski et al (28) at the Air Force Research Laboratory Propulsion Directorate in order to assist in downselecting appropriate propellers for Group I and Group II RPA engines.

Before a propeller is selected for the Brison 5.8, several assumptions are required since a specific aircraft is not available for analysis. Table 10 shows the assumptions used in the propeller selection analysis and represent comparable performance of aircraft that would use this size of engine.

Table 10: Assumed Aircraft Values for Propeller Selection

Performance Characteristic	Engineering Assessment
L/D_{max}	8
Aircraft Weight	50 lb_f
Best Cruise Speed	30 mph
Cruise Altitude	5,000 feet
Cruise Density	2.0482 x10^{-3} (lb sec^2)/ft^4

Using the above assumed flight conditions, the best cruise scenario was the first filtering criteria for this aircraft. The reason best cruise is used is due to the primary nature of an RPA's mission of this size. Most RPAs of this size are used for reconnaissance and therefore maximizing their cruise endurance is the most important mission for propeller selection. Steady unaccelerated level flight (SLUF) is the first

assumption used to determine the total drag the aircraft will see. Using this assumption

along with the L/D_{max} and aircraft weight, a total drag is calculated to be 6.25 lb$_f$. From

here, the drag of the aircraft is known and therefore the thrust required from the propeller

is known.

The next piece of information to establish is the cruise condition of the aircraft

engine. In the best cruise case, the lowest BSFC is requested of the engine and this point

is established in Table 11 and derived from this research. It is important to take in the

uncertainty in the data collected on the engine as well as what was collected for the

propellers. Baranski's uncertainty analysis pointed out a 3.9% error and this will be

taken into account in the most conservative manor for both the engine and propeller (28).

Table 11: Best Cruise Engine Characteristics

Performance Characteristic	Value
Engine RPM	4,000 RPM
HP	3.03 hp (+/- 0.02)
Torque	3.90 ft-lb$_f$ (+/- 0.02)
BSFC	0.9373 lb/(hp-hr) (+/- 0.088)
Throttle Position	25%

When selecting propellers, the available thrust at 4,000 RPM was checked to see

if the propeller produced 6.25 lb$_f$ of thrust plus the 3.9% error. If a propeller did not meet

this specification, it was not selected. If the propeller produced an adequate amount of

thrust, the power and torque required to create that thrust was compared with the Brison

performance characteristics. If the engine was able to provide the necessary power, the

propeller was selected as a possible solution for the best cruise scenario.

The next scenario to consider is rate of climb (ROC). Since a ROC requirement

was not established for this aircraft, it will be assumed that all of the cruise propellers

will produce an adequate ROC for the RPA. ROC is calculated by applying a simple energy balance to the RPA. The rate of change of energy height (z_e) can be derived as a function of thrust (T), drag (D), velocity (V), and RPA weight (W), shown in Equation 17. The drag is the calculated drag from the SLUF analysis at cruise, thrust is available thrust from the propeller, velocity is cruise velocity, and the weight is the approximated weight of the RPA (28).

$$ROC = \frac{d_{ze}}{dt} = \frac{(T-D)}{W}V \qquad (17)$$

The energy height (z_e) represents the sum of instantaneous potential and kinetic energies for the RPA. Thus the maximum ROC for constant speed flight would occur where excess thrust is used exclusively to increase altitude. The maximum ROC for the Brison is established at peak power and these values for the engine are given in Table 12 along with the calculated ROC. The 6,000 RPM operating point was selected because it provides maximum peak power. Engine operation at higher RPM actually produces less power and increases BSFC which are not good operating characteristics. When downselecting propellers for ROC, if the propeller at 6,000 RPM required more power or torque than the engine was capable, it was not selected.

Table 12: Rate of climb (ROC) engine performance characteristics

Performance Characteristic	Value
Engine RPM	6,000 RPM
HP	4.64 hp (+/- 0.032)
Torque	4.08 ft-lb$_f$ (+/- 0.032)
BSFC	1.143 lb/(hp-hr) (+/- 0.022)
Throttle Position	100%

The final propellers selected provide enough thrust for best cruise conditions while also allowing producing the maximum thrust given the Brison's engine performance at 6,000 RPM. Table 13 shows the final selected potential propellers.

Table 13: Selected Propellers for Brison 5.8 at 30mph (28)

Manufacturer	Prop Dia (in)	Prop Pitch (in)	Thrust (lbf) @ 6,000 RPM	Thrust (lbf) @ 4,000 RPM	ROC (ft/min)
APC	22	10	19.95	7.48	723.10
Biela	23	8	21.47	7.18	803.53
Biela	24	8	26.28	9.08	1057.62
Biela	24	12	25.79	11.83	1031.89
Mejzlik_CF	22	12	22.50	8.39	858.03

V. Conclusions and Recommendations

V.1   Problem Statement and Objectives

Increasing reliability of a small two-stroke internal combustion engine for dynamically changing altitudes is the primary purpose of this research. Small RPA manufacturers are required to source engines for these aircraft using substandard or often missing altitude performance data. Aircraft manufacturers are challenged to generate these new aircraft with a fast acquisition schedule to meet the demands of the American military. The pool of available power plants for the Group 1 and Group 2 sized aircraft (<50 lbs) is small and a majority of the sourced engines are designed for use within 1,000 AGL.

Adapting COTS engines for use in a military aircraft puts extreme demands on an engine that it was never designed to meet. These engines are produced to be light and affordable in order to make the RC hobby attractive to more people or to make lawn equipment more affordable for users. Those goals do not always correlate to the best engine performance. Since engine manufacturers consider cost a more important factor than engine performance at high altitudes, limited test data is generated for these engines as performing these tests would increase the costs per engine unit (29). The reasons cost is so important to these engine manufacturers has to do with the original purposes behind many of these engines. Originally, many of these engines found their homes powering yard equipment or hobbyist radio controlled aircraft. In all of these cases, sustainable engine performance with dynamically changing altitudes was never a consideration in

their designs. The performance characteristics of these engines are largely unknown to the RPA manufacturers and the United States Air Force.

The primary goals of this research were to investigate the performance of the Brison 5.8 in^3 single cylinder two stroke spark ignition crankcase scavenged engine at altitude. The primary research goals were to:

1. Upgrade the test facility so it is capable of taking reliable test data

2. Run the Brison 5.8 as it comes from the manufacturer to create baseline performance maps for the engine at SLS, 5,000 feet, and 10,000 feet.

3. Convert the Brison 5.8 to throttle body fuel injection and test the engine at SLS, 5,000 feet, and 10,000 feet to see if performance gains were met

4. Map the final engine at 100%, 75%, 50%, and 25% throttle settings in order to size an appropriate prop for the Brison 5.8.

5. Investigate what AFR provides best BSFC and maximum power.

V.2   Results

The first tests involved testing the engine with its supplied carburetor. Tests were completed from 3,000-7,500 rpm at altitudes of sea level (750 feet at Dayton, OH), 5,000 ft, and 10,000 ft MSL. The test results show that if the operator adjusts the fuel needles on the carburetor 1/8th of a turn for each 5,000 feet in altitude, the engine can achieve a maximum performance with about a 10% decrease in available torque across the rpm band. This trend matches similar claims by Taylor. If the engine is not tuned for the specific operating condition, the performance of the engine becomes unpredictable and unreliable. Large power variations will exist due to the over fueling condition. High rpm

operation of the engine mitigates the power loss somewhat, but the low speed performance suffers by as much as 75% less power. To mitigate this effect with the carburetor, the operators will need training on how to tune the engine as well as instruction to not take the engine at altitudes greater than 5,000 feet above where the aircraft takes off thus limiting the operational map of the aircraft.

The primary motivation for adding throttle body injection to the Brison was to investigate a solution that removes the operator from the tuning process while trying to regain the performance losses at altitude. Adjustments to the carburetor are small and the research shows from Schmick et al. (19) that even a 1/8th of a turn of the needle screws off of an optimal tune can cause a 10% reduction in engine performance. A $1/8^{th}$ maladjustment is a very small amount to be off and in the field, adjustments that are off by more than ¼ turn are expected. More substantial losses could be experienced for further screw adjustments. The fuel injection data presented in this paper shows the addition of a more precise fuel metering system, consistent atomization of fuel, and standardized automated adjustments to air-to-fuel ratios increases the engine's performance in all operating conditions without user intervention.

V.3   Conclusions

The major advantages of the TBI system installed on the Brison are:

1. **Significant performance increases at flight altitudes**

   TBI increased engine performance at 10,000 feet by up to 91% depending on engine RPM operating condition. All of the performance losses that the stock SLS tuned carburetor experienced due to poor fuel metering at 5,000 and 10,000

feet are corrected using fuel injection. Now the aircraft can reliably take off at any location and properly lean the mixture at higher altitudes without the risk of the engine dying from being too rich or surging in flight when too lean. This means less aircraft accidents or system failures in the field.

2. **Removal of the operator from tuning operation**

The user no longer is required to make carburetor adjustments for different takeoff conditions. Adjusting the carburetor for high altitude flight is not possible in the stock configuration because you cannot take off in a lean condition, but now with fuel injection, no modification is required. This means that the user no longer needs training to make carburetor adjustments, does not need to take the time to adjust the carburetor in the field, and no longer needs to worry if their carburetor adjustments are correct. The fuel injector combined with the engine computer allow for consistent and repeatable engine performance regardless of takeoff or flying location.

3. **Consistent BSFC over operating regime increases flight endurance**

Consistent BSFC between 1-1.2 lb/(hp-hr) across 3,000-7,000 RPM. Previously with the carburetor, a BSFC of 1.0 lb/(hp-hr) was only met at the 6,500 RPM operating point at SLS. This means that if the aircraft is actually flown at 5,000 feet using 4.5 HP, the BSFC of the carburetor is closer to 2 lb/(hp-hr). If you assume a half gallon fuel tank, this makes for a 23 minute flight time. The same flight conditions using the TBI system would yield a 42 minute flight time. Potentially doubling the flight time of an aircraft is a huge advantage to the user of the system.

4. **Engine starting process much easier**

Ease of starting is difficult to quantify. The engine either starts or it doe not and depending on the implementation of the engine, this can be a higher priority achievement. Previously with the carburetor, the engine would have to be choked and un-choked repeatedly sometimes in order for the engine to start. If the engine was choked too long, the engine would flood and the spark plug would have to be dried off before trying again. All of these problems are exacerbated in cold conditions (<40°F). The TBI system includes starting tables that allow for the fuel system to correct for ambient air temperatures allowing for much more reliable starts regardless of the environment of the engine.

5. **Decreased Combustion Variation**

The Brison's COVs for BMEP are 35% lower by average for the 5,000 foot 100% throttle operating location. The actual average COV for the TBI at this location is 14% with the lowest COV being 8.76% at 5,000 RPM. The Brison had its lowest COVs at 5,000 RPM across the board, but the TBI kept the COVs lower which shows more repeatable combustion events. Repeatable combustion events allow for smoother engine operation and reliable engine power.

6. **Open Loop Fuel Injection Programming Preferred**

Testing observations showed that although closed loop fuel injection is useful for the automobile industry, its use in the aerospace industry for a small two-stroke engine is not beneficial. The gradual changes that closed loop control makes to keep stoichiometric AFRs are not beneficial to an aircraft that could change its ambient pressure quickly depending on its flight altitude. An automobile is never

going to go from 10,000 feet to sea level in a period of minutes and therefore the closed loop control does not negatively impact performance. However, for the aircraft, the closed loop control can lean the mixture too far at altitude and does not correct itself quick enough to be ready for a landing scenario.

The addition of fuel injection does have some drawbacks that need to be addressed when building an RPA. The TBI system adds additional weight and complication to the engine. The addition of the ECU, wiring harness, pressurized fuel system, and throttle body are somewhat offset by the removal of the carburetor. The O_2 sensor is not needed for operation as it is only used for tuning process since the system should be operated in open loop configuration. As well, the reliance on a fuel injection system requires a more robust power source on the aircraft. It is assumed that there already is an available power source on these RPAs since their primary mission uses electronic sensors that already need electricity, but the amount of stored power might need increasing.

Every modification or inclusion of extra systems in an RPA has its downsides, but in the case of adding TBI to the Brison 5.8, the benefits outweigh the disadvantages. TBI allowed for the recovery of up to 91% of the lost power at altitude due to poor carburetor tuning while removing the user from the burden of maintaining proper carburetor tuning is a significant improvement to the system. The Brison 5.8 is now a "turn-key" engine in any of the operating conditions tested and would now be considered extremely easy to operate compared to the carbureted system supplied by the manufacturer. Outside of increasing reliability, RPA manufacturers now have engine performance data for both the carbureted and fuel injected Brison 5.8 systems and this can be used to properly size the

142

engine for an aircraft while selecting the most appropriate propeller design for their respective aircraft. Properly selecting a fuel injection system and propeller for the aircraft can significantly increase mission capability and when combined with the increase in reliability, these modifications can make the Brison 5.8 a much better solution for a future aircraft.

V.4   Future Work and Recommendations

The mobile test facility worked well throughout the data collection for this research. The test facility is now on its second iteration and now operates in a manner that collects reliable data while provided reliable service to the operator. Although that is the case, there are a few pieces of equipment that need attention in order to further the research requirements of AFRL/RZTC. The list includes:

1. Transition the test facility to its new location in Building 71 H-Bay. The new testing location will allow for more time to be spent making modifications to the stand as well as collecting data because the test location no longer requires the currently level of scheduling and time sharing that 5 Stand requires

2. Upgrade the engine air inlet supply system to an intake manifold system that allows the engine manifold pressure to stay closer to constant. The current system was meant for the carburetor and will need to be resized for the fuel injection system. While resizing, a manifold that is pliable (instead of rigid stainless steel) should be considered. A system that works on a constant pressure model versus a constant volume model might allow for easier starting and more reliable operation of the engine during RPM transitions. Separating the intake flow from the flow brought in from the supercharger will allow temperature research.

3. Once the inlet design is complete and offering reliable engine operation, the LN_2 system on the test facility needs to have all of the manual valves replaced with actuated values controlled through LabVIEW. This is a requirement because there are enough pieces of hardware to monitor on the stand already and having to manually adjust LN_2 flow-rates is too substantial of an increase in operator work load.

4. Temperature effects research should be completed to determine how decreasing ambient pressure affects the performance of a two-stroke engine. Unlike a small four stroke engine which loses volumetric efficiency due to heat loss through the cylinder walls, a two stroke might not see as substantial decrease because a two stroke's crankcase pumping efficiency increases with decreases of temperature. If the increase of pumping efficiency combined with increased air density due to the colder air temperatures outweigh the negative effects of the heat loss through the cylinder cooling fins, the prospects for using a two-stroke in cold flying condition might actually make them a better selection than small four-stroke engines.

Outside of the previous research goals, there are a few other avenues of research that could be addressed in order to further the knowledge of how the Brison 5.8 performs. The first item includes research to better understand the effects of pumping losses in the crankcase. A pressure transducer should be outfitted into the crankcase to monitor crankcase pressure as environmental variables are adjusted. It might be found that as engine temperature increases, crankcase pumping efficiency decreases enough to show a

measureable pressure drop. This pressure drop could be plotted against engine performance to see if the pressure significantly changes engine performance.

Another way to decrease fuel consumption of a two-stroke is to optimize the scavenging and exhaust port systems. Reducing the amount of air/fuel mixture that escapes the cylinder while the exhaust port is open would decrease the fuel consumption and increase the power output of the engine. Simply tuning the exhaust to the primary cruise RPM using the exhaust pressure waves to reduce short circuiting might provide a significant increase in cruise endurance.

This research primarily looked at fuel systems in order to increase RPA reliability, but one of the primary causes of failures for the test facility were due to the vibration from the engine. Future research should look into more advanced ways to mitigate the vibration problems without adding heavy flywheels and fluid filled dampers. Studying the amount of vibration the engine produces at different engine RPMs and engine loads would be useful for determining where the engine should operate in an RPA. An engine RPM that induces significantly more vibration than other RPMs should be avoided for sustained operation. Finally, decreasing the amount of vibration will allow bolts to stay in place, keep bolts from breaking, and reduce the probability of electrical connects failing allowing for a significantly more reliable system.

Bibliography

1. United States Air Force Unmanned Aircraft Systems Flight Plan 2009-2047, Headquarters, United States Air Force, Washington DC, 18 May 2009.

2. Groenewegen, J. R. The Performance and Emissions Characteristics of Heavy Fuels in a Small, Spark Ignition Engine. UD Thesis. University of Dayton, Dayton, OH December 2011.

3. Weatherington, Dyke, Unmanned Aircraft Systems Roadmap, 2005-2030, Deputy, UAV Planning Task Force, OUSD(AT&L) 2005.

4. Rozenkranc, M., & Ernst, J. Tactical UAV Engines Integration in IAI. AIAA 2003-6534. 2nd AIAA Unmanned Unlimited Systems Technologies and Operations, San Diego, CA, 2003.

5. Schmick, P. (2011). Effect of Atmospheric Pressure and Temperature on a Small Spark Ignition Internal Combustion Engines' Performance. AFIT Thesis. AFIT/GAE/ENY/11-M28 Air Force Institute of Technology, Wright Patterson AFB, OH.

6. Haywood, John B., Internal Combustion Engine Fundamentals; McGraw-Hill, Inc., 1988.

7. Blair, Gordon. P. Design and Simulation of Two-Stroke Engines. Society of Automotive Engineers Inc., Warrendale, PA 1996.

8. Marine Engineering. "Scavenging in Diesel Engines". 2010. http://www.marineengineeringonline.com/scavenging_in_diesel_engines.htm.

9. "Carburetor: Mixing the Gas Vapor with Air to Make Combustion." 2009. http://hdabob.com/the-vehicle/fuel-injection/carburetor/.

10. "A Basic Bosch Fuel Injector Diagram to Show Injector Components." 2009. http://www.injectorrx.com/cutaway.html.

11. Attard, W. (2008). Small Engine Performance Limits -- Turbocharging Combustion or Design. PhD Dissertation. The University of Melbourne, Melbourne, Victoria.

12. Zhao, F., Lai, M., & Harrington, D. Automotive Spark-Ignited Direct-Injection Gasoline Engines. Progress in Energy and Combustion Science, Vol. 25, No. 5, 1999.

13. Grasas-Alsina, C., Freixa, E., Esteban, P., & Masso, J. "Low-Pressure Discontinuous Gasoline Injection in Two-Stroke Engines", 860168. SAE Technical Paper Series, Detroit Michigan, 1986.

14. Harari, R., Sher, E., "The Effect of Ambient Pressure on the Performance Map of a Two-Stroke SI Engine", 930503, SAE International Congress & Exposition, Detroit, MI, Pg 115-123, 01 March 1993.

15. Shin, Y., Chang, S.H., Koo, S.O., <u>Performance Test and Simulation of a Reciprocating Engine for Long Endurance Miniature Unmanned Aerial Vehicles</u>, Proceedings of Institution of Mechanical Engineers Vol. 219, Part D: Journal of Automobile Engineering, Pg 573-581, 6 Oct 2004.

16. Taylor, C. F. <u>The Internal-Combustion Engine in Theory and </u>Practice. (2nd ed). The MIT Press. Cambridge, MA, 1985.

17. Watanabe, I., Kuroda, H., "Effect of Atmospheric Temperature on the Power Output of a Two-Stroke Cycle Crankcase Compression Gasoline Engine", 810295, SAE International Congress and Exposition, Detroit, MI, 23-27 February 1981.

18. Turns, S. R. <u>An Introduction to Combustion</u>. (2nd ed). New York: McGraw-Hill, Inc., 1996.

19. Schmick, P., Crosbie, S., Polanka, M., Litke, P., & Hoke, J. (2011). <u>Development of a Small Internal Combustion Engine Altitude Test Chamber.</u> Joint Propulsion Conference, San Diego, CA, 2011.

20. Magtrol Inc. (2010). "Magtrol Model DSP6001 High Speed Programmable Dynamometer Controller User Manual." Unpublished manuscript.

21. Lovejoy Inc. (2011*). "Curved Jaw Couplings." Unpublished manuscript. http://www.lovejoy-inc.com/products/curved-jaw-couplings.aspx.

22. Cinnmaster, "Brison Engines Owner's Manual," 2006.

23. SAE Gasoline Fuel Injection Committee, "Low Pressure Gasoline Fuel Injector," Surface Vehicle Recommended Practice, No. J1832, 2001

24. "Small Engine EFI Conversion Kits Installation Manual." Vol. 1.5.7. Ecotrons. 2011.

25. "SE-EFI Tuning Guide." Vol 2.3. Ecotrons. 2011.

26. "ALM-ECU Integration Guide." Vol. 1.0. Ecotrons. 2011.

27. Kline, S.J., McClintock, F.A., <u>Describing Uncertainties in Single-Sample Experiments</u>, Mechanical Engineering, pg 3-8, Jan 1953.

28. Baranski, J., Fernelius, M., Hoke, J., Wilson, C., & Litke, P. Characterization of Propeller Performance and Engine Mission Matching for Small Remotely Piloted Aircraft. Joint Propulsion Conference 2011, San Diego, CA, 2011.

29. Crosbie, S., Polanka, M., Litke, P., & Hoke, J.   Increasing Reliability of a Small 2-Stroke Internal Combustion Engine for Dynamically Changing Altitudes. 50th AIAA Aerospace Sciences Meeting, Nashville, TN, 2012.

30. Menon, S., Moulton, N., & Cadou, C. Development of a Dynamometer for Measuring Small Internal-Combustion Engine Performance. Journal of Propulsion and Power, Vol. 23(1), pp 194. 2007.

31. Walter, T., Brechbuhl, S., Gossweiler, C., Schnepf, M., & Wolfer, P. (2004). Pressure Indicating with Measurement Spark Plugs on a DI-Gasoline Engine -- State of Technology. 920-333e09.04) Kistler Instrumente, Germany. 2004.

Vita

Captain Steven Christopher Crosbie was born on March AFB, California and graduated salutatorian from Floresville High School in May of 2003. After high school, he was selected for undergraduate studies at the United States Air Force Academy in Colorado Springs, Colorado. He graduated from the Air Force Academy with a Bachelor of Science in Mechanical Engineering and was commissioned into the United States Air Force in May of 2007.

Steven's first assignment was with the 586th Flight Test Squadron, 46th Test Group, Holloman AFB, New Mexico. At Holloman, he was an advanced programs flight test engineer where he was the primary test engineer on several radar and missile upgrade programs. Following this assignment, he was selected for enrollment at the Graduate School of Engineering and Management at the Air Force Institute of Technology in August of 2010, seeking a degree in Aeronautical Engineering. Upon graduation he will return to the Air Force as an advanced programs flight test engineer in Las Vegas, Nevada.

Appendix A: Carbureted Operating Procedures

SMALL ENGINE ALTITUDE TEST STAND

STAND SETUP AND INSPECTION

1. ___ ___ ___ **Verify** fire extinguisher is mounted within reach of test stand and fully charged.

2. ___ ___ ___ **Inspect** engine and thrust stand connections/wiring/plumbing/bolts for damage, excessive wear, loose bolts, and proper installation.

3. ___ ___ ___ **Inspect** couplings for damage or excessive wear and proper installation and alignment.

4. ___ ___ ___ **Fill** fuel tank to test level.

5. ___ ___ ___ Turn **ON** main 115VAC power supply bar.

6. ___ ___ ___ Turn **ON** 480VAC wall power switch.

7. ___ ___ ___ Turn **ON** test computer and monitor computer.

8. ___ ___ ___ Verify/Turn **ON** exhaust fans in control room.

9. ___ ___ ___ Verify/Turn **ON** main water supply valve in control room.

10. ___ ___ ___ **Verify/Connect** air supply line to test stand.

11. ___ ___ ___ Turn **ON** air supply main isolation valve and set pressure to 70 psi.

12. ___ ___ ___ **Verify/Connect** inlet and outlet water supply lines.

13. ___ ___ ___ **DON** cryogenic PPE if test matrix requires LN_2 usage.

14. ___ ___ ___ **Verify/Connect** that LN_2 coolant hose is connected and secured.

15. ___ ___ ___ **Verify/Close** fuel drain valve.

16. ___ ___ ___ **Ensure** guards and windows are in place and secure.

17. ___ ___ ___ **Start** Small Engine Altitude Main program.

TEST STAND STARTUP

1. ___ ___ ___ Turn **ON** oil pump.

2. ___ ___ ___ Turn **ON** dynamometer controller and verify maximum RPM set point (3000 RPM)

3. ___ ___ ___ **CLOSE** inner test cell door and display "Test In Progress" sign.

4. ___ ___ ___ **OPEN** roll-up door to allow for adequate ventilation.

5. ___ ___ ___ **OPEN** Dynamometer cooling water supply valve.

6. ___ ___ ___ Turn brake to **ON** from dynamometer controller.

7. ___ ___ ___ Turn **ON** ignition power.

8. ___ ___ ___ **Verify/Open** fuel tank isolation hand valve.

9. ___ ___ ___ **Set** choke to desired level.

10. ___ ___ ___ **Set** throttle to starting position to roughly 25%

11. ___ ___ ___ **Open** Fuel Valve 1 and Fuel Valve 2.

12. ___ ___ ___ **Verify/Close** Coolant Valve 1 and Coolant Valve 2.

13. ___ ___ ___ **Clear** non-testing personnel from test cell.

14. ___ ___ ___ **Set** Control Valve 1, Control Valve 2, and Manual Bypass Valve to desired position.

15. ___ ___ ___ Set Air Valve 1 **OPEN/CLOSE** as applicable for test matrix.

*CAUTION: Do **NOT** perform next step until oil pressure reaches ~35 psig.*

16. ___ ___ ___ Turn **ON** Compressor and set desired speed.

*CAUTION: If compressor oil temperature exceeds 200 ˚F perform **Test Shutdown***

***Procedure**.*

17. ___ ___ ___ **Adjust** Control Valve 1 and Control Valve 2 for desired pressure.

NOTE: Control Valve 1 is % Open, Control Valve 2 is % Closed.

18. ___ ___ ___ **OPEN** LN_2 Supply Tank Valve.

19. ___ ___ ___ **Adjust** Coolant Valve 1 and Coolant Valve 2 for desired temperature.

*CAUTION: If O_2 or CO alarm indicates YELLOW condition begin **Test Shutdown procedure**.*

*WARNING: IF O_2 or CO alarm indicates RED condition perform **Emergency Shutdown Procedure** and leave Test Cell Immediately!!*

GENERAL STAND TEST PROCEDURE

1. ___ ___ ___   **Set** Dynamometer speed set point to 3000 rpm.

2. ___ ___ ___   Momentarily turn **ON** starter switch.

3. ___ ___ ___   **Adjust** dynamometer speed set point to desired value in 500 rpm increments. If using the inlet manifold, rpm increments need to be 20RPM at a time in order to adjust airflow to match engine demands

4. ___ ___ ___   **Adjust** throttle/mixture controls to achieve stable operation.

5. ___ ___ ___   Turn **ON** Write Data once set point reached.

6. ___ ___ ___   Turn **OFF** Write Data after 10 seconds.

7. ___ ___ ___   Repeat steps 3 through 6 to complete applicable test matrix.

TEST SHUTDOWN PROCEDURE

1. ___ ___ ___   Turn **OFF** ignition power.

2. ___ ___ ___   **CLOSE** Control Valve 1 by setting slider bar to 0.

3. ___ ___ ___   **CLOSE** LN_2 Supply Tank Valve.

4. ___ ___ ___   **CLOSE** Fuel Valve 1 and Fuel Valve 2.

5. ___ ___ ___   **OPEN** Control Valve 2 by setting slider bar to 0.

6. ___ ___ ___   **STOP** compressor operation.

7. ___ ___ ___   **CLOSE** dynamometer coolant supply valve.

8. ___ ___ ___   Turn **OFF** brake from dynamometer controller.

9. ___ ___ ___   Turn **OFF** oil pump.

FINAL SHUTDOWN PROCEDURE

1. ___ ___ ___   **CLOSE** manual fuel shut off valve.

2. ___ ___ ___   Turn **OFF** 480VAC wall power switch.

3. ___ ___ ___   **CLOSE** roll-up door.

4. ___ ___ ___   **OPEN** inner test cell door and remove "Test In Progress" sign.

5. ___ ___ ___   Turn **OFF** dynamometer controller.

6. ___ ___ ___   **CLOSE** air supply isolation valve.

7. ___ ___ ___   **CLOSE** Small Engine Altitude Main program.

8. ___ ___ ___   Turn **OFF** Computer and Monitor.

9. ___ ___ ___   Turn **OFF** 115VAC power supply bar.

EMERGENCY SHUTDOWN PROCEDURE

10. ___ ___ ___   **PRESS** Emergency shutdown button.

11. ___ ___ ___   **Verify** that reset light goes **OFF.**

12. ___ ___ ___   **LEAVE** test cell immediately.

13. ___ ___ ___   **Notify** appropriate emergency response personnel as needed.

14. ___ ___ ___   **Notify** responsibly facility manager.

15. ___ ___ ___   After given the all clear perform **Test Shutdown** and **Final Shutdown Procedures**.

Appendix B: Altitude Chamber Pass Through Wire Connections

pass through 1		Top	
wire number			
1	Throttle		
2	Throttle		
3	Throttle		*All Pass through Wires labeled with Wire number
4	Ignition Pwr		*All ECU wires labeled with name of wire
5	Ignition Pwr		
6	Spk Timing		
7	Intake Air Temp Signal		
8	Lambda Wire 2		
9	Engine Temperature (ECT) Signal		
10	Injector Voltage		
11	Injector Ground (Ing1)		
12	Lambda Wire 6		
pass through 2		Bottom	
wire number			
1	Manifold Pressure Signal		
2	Lambda Wire 1		
3	Sensor Voltage Supply (12V)		
4	Lambda Wire 4		
5	Empty		
6	Lambda Wire 3		
7	Throttle Position Sensor Signal		
8	Inlet Pressure		
9	Inlet Pressure		
10	Inlet Pressure		
11	Lambda Wire 5		
12	Sensor Ground		

Appendix C: Engine Computer Wire Connector Pin Identifications

Plug 1				
1	Manifold Pressure			
2	Sensor Voltage			
3	Throttle Position Sensor Signal			*Plugs are wired same outside and inside chamber
4	Engine Temperature Signal			*Plugs are labeled with their respective numbers
5	Intake Air Temperature Signal			
6	Injector Voltage (VING)			
7	Injector Ground (ING1)			
8	Sensor Ground			
9	*Empty*			
10	*Empty*			
11	*Empty*			
12	*Empty*			
Plug 2				
1	Lambda Wire 1			
2	Lambda Wire 2			
3	Lambda Wire 3			
4	Lambda Wire 4			
5	Lambda Wire 5			
6	Lambda Wire 6			
7	*Empty*			
8	*Empty*			
9	*Empty*			
10	*Empty*			
11	*Empty*			
12	*Empty*			

Appendix D: TBI Equipped Operating Procedures

SMALL ENGINE ALTITUDE TEST STAND

STAND SETUP AND INSPECTION

18. ___ ___ ___   **Verify** fire extinguisher is mounted within reach of test stand and fully charged.

19. ___ ___ ___   **Inspect** engine and thrust stand connections/wiring/plumbing/bolts for damage, excessive wear, loose bolts, and proper installation. Pay close attention to the engine head and mounting bolts.

20. ___ ___ ___   **Inspect** couplings for damage or excessive wear and proper installation and alignment. Pay close attention to spider wear/deformation. If deformed, replacement is warranted

21. ___ ___ ___   **Fill** fuel tank to test level. No more than 2 gallons at a time.

22. ___ ___ ___   Turn **ON** main 115VAC power supply bar.

23. ___ ___ ___   Turn **ON** 480VAC wall power switch.

24. ___ ___ ___   Turn **ON** test computer and monitor computer.

25. ___ ___ ___   Verify/Turn **ON** exhaust fans in control room.

26. ___ ___ ___   Verify/Turn **ON** main water supply valve in control room.

27. ___ ___ ___   **Verify/Connect** air supply line to test stand.

28. ___ ___ ___   Turn **ON** air supply main isolation valve and set pressure to 70 psi. (Blue valve located on the right under the red control valves)

29. ___ ___ ___   **Verify/Connect** inlet and outlet water supply lines.

30. ___ ___ ___   **DON** cryogenic PPE if test matrix requires LN_2 usage.

31. ___ ___ ___   **Verify/Connect** that LN_2 coolant hose is connected and secured.

32. ___ ___ ___   **Verify/Close** fuel drain valve. (Red Handle)

33. ___ ___ ___   **Ensure** guards and windows are in place and secure.

34. ___ ___ ___   **Start** Small Engine Altitude Main program. (LabVIEW VI)

TEST STAND STARTUP

20. ___ ___ ___   Turn **ON** oil pump/oil cooler.

21. ___ ___ ___   Turn **ON** dynamometer controller and verify maximum RPM set point set to 2500 RPM. A lower RPM can be run with the TIB setup.

22. ___ ___ ___ **CLOSE** inner test cell door and display "Test In Progress" sign.

23. ___ ___ ___ **OPEN** roll-up door to allow for adequate ventilation. Only about 6 inches is really needed for this.

24. ___ ___ ___ **OPEN** Dynamometer cooling water supply valve. (Blue handle under starter)

25. ___ ___ ___ Turn brake to **ON** from dynamometer controller.

26. ___ ___ ___ Turn **ON** ignition power.

27. ___ ___ ___ Turn **ON** ECU power (should hear a relay click when this is powered on)

28. ___ ___ ___ **Verify/Open** fuel tank isolation hand valve. (Blue valve under fuel tank)

29. ___ ___ ___ **Open** Fuel Valve 1 (Should hear the air system actuate when this is opened)

30. ___ ___ ___ Turn **ON** 12V power for fuel pump. Fuel pump is not in the LabVIEW VI, but instead turn on the manual switch located on the 12VDC power supply next to the battery

31. ___ ___ ___ **Set** throttle to starting position.

32. ___ ___ ___ **Verify/Close** Coolant Valve 1 and Coolant Valve 2.

33. ___ ___ ___ **Clear** non-testing personnel from test cell.

34. ___ ___ ___ **Set** Control Valve 1, Control Valve 2, and Manual Bypass Valve to desired position.

35. ___ ___ ___ Set Air Valve 1 **OPEN/CLOSE** as applicable for test matrix.

36. ___ ___ ___ **Open** coupler cooling valve to desired flow rate (> ½ open). (Green valve)

*CAUTION: Do **NOT** perform next step until oil pressure reaches ~35 psig.*

37. ___ ___ ___ Turn **ON** Compressor and set desired speed. When running SLS conditions, 50% is really maximum achievable without over current situation. This reads is PSIA on the output pressure transducer. If running altitude conditions, set the compressor to 50%, then close the Hand Valve 1. After closing the valve, increase the compressor speed until 16psia is reached at the compressor output. Once that is reached, open the compressor map and look at stall lines to verify where the compressor is operating. Then slowly close the second control valve while

increasing compressor RPM to reach desired altitude. Lowest pressure possible is 8.2psia in the chamber

*CAUTION: If compressor oil temperature exceeds 200 ℉ perform **Test Shutdown Procedure**.*

38. ___ ___ ___ **Adjust** Control Valve 1 and Control Valve 2 for desired pressure.

        NOTE: Control Valve 1 is % Open, Control Valve 2 is % Closed.

39. ___ ___ ___ **OPEN** LN$_2$ Supply Tank Valve.
40. ___ ___ ___ **Adjust** Coolant Valve 1 and Coolant Valve 2 for desired temperature. (these are the yellow LN$_2$ manual control valves)

*CAUTION: If O$_2$ or CO alarm indicates YELLOW condition begin **Test Shutdown** procedure.*

*WARNING: IF O$_2$ or CO alarm indicates RED condition perform **Emergency Shutdown Procedure** and leave Test Cell Immediately!!*

GENERAL STAND TEST PROCEDURE

8. ___ ___ ___ **Set** Dynamometer speed set point to 2500 rpm.
9. ___ ___ ___ Momentarily turn **ON** starter switch.

10. ___ ___ ___ Once engine is running, turn **ON** Lambda sensor. Sensor takes 20 seconds to warm up before readings will read on the white ALM box located above the computer

11. ___ ___ ___ **Adjust** dynamometer speed set point to desired value in 100 rpm increments. If using intake metering system, 20 rpm increments are needed while adjusting for engine airflow demands.

12. ___ ___ ___ **Adjust** throttle/mixture controls and control valve 1 to achieve stable operation.

13. ___ ___ ___ Turn **ON** Write Data once set point reached.

14. ___ ___ ___ Turn **OFF** Write Data after 10 seconds.

15. ___ ___ ___ Repeat steps 3 through 6 to complete applicable test matrix.

TEST SHUTDOWN PROCEDURE

10. ___ ___ ___ Turn **OFF** ignition power. (shuts down engine)

11. ___ ___ ___ Turn **OFF** ECU power

12. ___ ___ ___ Turn **OFF** Lambda sensor power

13. ___ ___ ___ **CLOSE** Control Valve 1 by setting slider bar to 0.

14. ___ ___ ___ **CLOSE** LN$_2$ Supply Tank Valve.

15. ___ ___ ___ Turn **OFF** 12V fuel pump power

16. ___ ___ ___ **CLOSE** Fuel Valve 1

17. ___ ___ ___ **OPEN** Control Valve 2 by setting slider bar to 0. (Note: If running low altitude pressures with high RPM compressor operation, gradually open control valve and lower compressor RPM at the same time to avoid compressor over-current failure.)

18. ___ ___ ___ **STOP** compressor operation.

19. ___ ___ ___ **CLOSE** dynamometer coolant supply valve.

20. ___ ___ ___ Turn **OFF** brake from dynamometer controller.

21. ___ ___ ___ Turn **OFF** oil pump/oil cooler.

FINAL SHUTDOWN PROCEDURE

16. ___ ___ ___ **CLOSE** manual fuel shut off valve.

17. ___ ___ ___ Turn **OFF** 480VAC wall power switch.

18. ___ ___ ___ **CLOSE** roll-up door.

19. ___ ___ ___ **OPEN** inner test cell door and remove "Test In Progress" sign.

20. ___ ___ ___ Turn **OFF** dynamometer controller.

21. ___ ___ ___ **CLOSE** air supply isolation valve.

22. ___ ___ ___ **STOP** and **CLOSE** Small Engine Altitude Main program.

23. ___ ___ ___ Turn **OFF** Computer and Monitor.

24. ___ ___ ___ Turn **OFF** 115VAC power supply bar.

EMERGENCY SHUTDOWN PROCEDURE

25. ___ ___ ___ **PRESS** Emergency shutdown button.

26. ___ ___ ___ **Verify** that reset light goes **OFF.**

27. ___ ___ ___ **LEAVE** test cell immediately.

28. ___ ___ ___ **Notify** appropriate emergency response personnel as needed.

29. ___ ___ ___ **Notify** responsibly facility manager.

30. ___ ___ ___ After given the all clear perform **Test Shutdown** and **Final Shutdown Procedures**.

Appendix E: Matlab Code for Averaging Test Data

```matlab
clear all

% ls command lists all files in the current directory, be sure that the
% m-file is in the directory that has all the excel files that need
reduced.
filenames = ls
% logic to determine the number of files in the directory to determine
% length of for loop.
tot_files = size(filenames)
num_of_files = tot_files(1,1)


% for loop goes through each of the files in the directory
for file = 1:num_of_files
    % filename variable is a complete string of a file in the directory
    filename = filenames(file,:);
    % xls_file is a returned value from the findstr command (the value
of
    % xls_file is the position in the string of the '.xls' criteria so
if
    % any value is returned the file has a .xls extension or there is
an
    % unfortunate naming error.
    xls_file = findstr(filename,'.xls');

    % if xls_file variable greater than zero the code continues with
the
    % xls file and reads the data into matlab.
    if xls_file > 0
        xls_filename = filename
        strip = size(xls_filename)
        strip = strip(1,2)
        strip_xls = strip - 5
        xls_stripped = xls_filename( 1 : strip_xls )

        % xlsread of a given file in the syntax written will return all
the
        % data in the given sheet name (in this case 'sheet1') and in
        % seperately returns the textual headers.
        [Data Headers] = xlsread(xls_filename, xls_stripped);
        % Data size is needed to know the number of data points that
were
        % recorded for a given test run.
        Data_size = size(Data);
        % the number of columns should stay at 52 for the given data
        % recording setup.
        num_columns = Data_size(1,2);
        % num_rows is the exact number of data points that were
recorded at
        % 33Hz.
        num_rows = Data_size(1,1);

        % mean(1) is the first column which is elapsed time since we
don't
```

```matlab
        % average this the last row value is taken for total elapsed
time.
        mean_value(1) = Data(num_rows,1);

        % For loop calculates the mean for each column as well as the
        % standard deviation
        for i = 2:num_columns
            mean_value(i) = sum(Data(:,i))/num_rows;

            % Standard Deviation = sqrt{sum[(value-mean)^2]/(N-1)}
            % where j represents the row and i represents the column.
            for j = 1:num_rows
                diff(j) = (Data(j,i)- mean_value(i))^2;
            end
                summation(i) = sum(diff);
                std_dev(i) = sqrt(summation(i) / (num_rows - 1));
        end

        % Computations can be made using the average values. Be sure
that
        % the variables you are using correctly correspond to the
values in
        % the mean_value() array. Once you have calculated your desired
        % value, error analysis can be done and output to the excel
file.
        % When writing to the excel file be sure to label the
calculated
        % value in the 'A column' in excel and then plug the value or
error
        % bar into the 'B column'. i.e.
        % 'xlswrite(xls_filename,name_calculated_value,'avg','A5')'
        % 'xlswrite(xls_filename,name_calculated_value_err,'avg','A6')
        % 'xlswrite(xls_filename,calculated_value,'avg','B5')
        % 'xlswrite(xls_filename,calculated_value_err,'avg','B6')

        % logic needed to input labels into the excel sheet
        x = {'Mean'};
        y = {xls_filename};
        s = {'Std_Dev'}

        % write statements write to the file currently being evaluated
        % (xls_filename). Variable names are placed on a new sheet that
is
        % named 'avg'
        xlswrite(xls_filename, y,'avg','A1')
        xlswrite(xls_filename, x,'avg','A2')
        xlswrite(xls_filename, s,'avg','A3')
        xlswrite(xls_filename, Headers,'avg','B1')
        xlswrite(xls_filename, mean_value ,'avg','B2')
        xlswrite(xls_filename, std_dev, 'avg','B3')
    end
end
```

1. REPORT DATE *(DD-MM-YYYY)* 24-03-2012	**2. REPORT TYPE** Master's Thesis	**3. DATES COVERED** *(From – To)* August 2010 – March 2012

4. TITLE AND SUBTITLE INCREASING RELIABILITY OF A SMALL 2-STROKE INTERNAL COMBUSTION ENGINE FOR DYNAMICALLY CHANGING ALTITUDES	**5a. CONTRACT NUMBER**
	5b. GRANT NUMBER
	5c. PROGRAM ELEMENT NUMBER

6. AUTHOR(S) Crosbie, Steven C., Captain, USAF	**5d. PROJECT NUMBER**
	5e. TASK NUMBER
	5f. WORK UNIT NUMBER

7. PERFORMING ORGANIZATION NAMES(S) AND ADDRESS(S)
    Air Force Institute of Technology
    Graduate School of Engineering and Management (AFIT/EN)
    2950 Hobson Way, Building 640
    WPAFB OH 45433-8865
	8. PERFORMING ORGANIZATION REPORT NUMBER
	
	    AFIT/GAE/ENY/12-M08

9. SPONSORING/MONITORING AGENCY NAME(S) AND ADDRESS(ES) Air Force Research Lab, Propulsion Directorate, Turbine Combustion Branch, 1790 Loop Road, Wright Patterson AFB, OH, Paul Litke, DSN 785-1673, paul.litke@wpafb.af.mil	**10. SPONSOR/MONITOR'S ACRONYM(S)** AFRL/RZTC, SERL
	11. SPONSOR/MONITOR'S REPORT NUMBER(S)

12. DISTRIBUTION/AVAILABILITY STATEMENT   APPROVED FOR PUBLIC RELEASE; DISTRIBUTION UNLIMITED.

13. SUPPLEMENTARY NOTES The views expressed in this thesis are those of the author and do not reflect the official policy or position of the United States Air Force, Department of Defense, or the United States Government. This material is declared a work of the U.S. Government and is not subject to copyright protection in the United States.

14. ABSTRACT Remotely Piloted Aircraft (RPA) typically utilize commercial internal combustion engines (ICE) as their power sources. These engines are designed to run at sea level, but these aircraft are often pressed into service at higher altitudes where the performance characteristics deteriorate. A Brison 95cc two-stroke engine's performance characteristics at altitude are investigated using a test facility that can measure these characteristics over a range of pressures and temperatures. With its stock carburetor at sea level static (SLS) conditions, the engine makes 5.5 peak hp and brake specific fuel consumption (BSFC) ranged from 1.2-4.0 lb/(hp-hr). At 10,000 ft conditions, the peak hp drops 40% while off peak hp conditions can see a drop of over 90%. As well, the carburetor makes operating at high altitudes unreliable. In order to increase reliability, a throttle body fuel injection (TBI) system was installed on the engine. The fuel injection system matched carburetor peak power at SLS conditions while increasing power by as much as 90% at low RPM and high altitude operating conditions. BSFC is decreased to a consistent 1.0 to 1.2 lb/(hp-hr) across all operating conditions. Lastly both reliability at high altitude and startup reliability are increased with the TBI system while eliminating the need for the tuning by the end user.

15. SUBJECT TERMS   Spark Ignition, Internal Combustion Engine, Altitude, BSFC, BMEP, Two-stroke, Fuel Injection

16. SECURITY CLASSIFICATION OF:			**17. LIMITATION OF ABSTRACT**	**18. NUMBER OF PAGES**	**19a. NAME OF RESPONSIBLE PERSON** Marc Polanka, PhD.
a. REPORT	**b. ABSTRACT**	**c. THIS PAGE**	**UU**	166	**19b. TELEPHONE NUMBER** *(Include area code)* (937) 255-6565, ext 4174 (marc.polanka@afit.edu)
U	U	U			